UNCERTAINTY MANAGEMENT IN PROGNOSIS OF ELECTRIC VEHICLE ENERGY SYSTEM

A Dissertation
Presented to
The Academic Faculty

by

Hwanjune Cho

In Partial Fulfillment
of the Requirements for the Degree
Doctor of Philosophy in the
School of Electrical and Computer Engineering

Georgia Institute of Technology

December 2018

UNCERTAINTY MANAGEMENT IN PROGNOSIS OF ELECTRIC VEHICLE ENERGY SYSTEM

Approved by:

Dr. George Vachtsevanos, Advisor
School of Electrical and Computer Engineering
Georgia Institute of Technology

Dr. Gregory David Durgin
School of Electrical and Computer Engineering
Georgia Institute of Technology

Dr. Gisele Bennett
School of Electrical and Computer Engineering
Georgia Institute of Technology

Dr. Seung-Kyum Choi
George W. Woodruff School of Mechanical Engineering
Georgia Institute of Technology

Dr. Patricio Antonio Vela
School of Electrical and Computer Engineering
Georgia Institute of Technology

Date Approved: November 07, 2018

To my family, parents, and parents in law.

ACKNOWLEDGEMENTS

Although this study is the result of my personal experience and ambition to achieve my scientific curiosity, I am supported by all the people I have met, who have provided academic and personal helps in connection with this study. I would like to express my heartfelt gratitude to Dr. George Vachtsevanos for taking me under his guidance and support for the programs related to this body of work. He has not only supported me academically towards the successful completion of this study but also has mentored me into becoming a good engineer. I would like to thank Dr. Gisele Bennett, Dr. Patricio Antonio Vela, Dr. Gregory David Durgin, and Dr. Seung-Kyum Choi, the distinguished members of my committee for their time, invaluable advice, effort they have taken to review, and provide me with their guidance. I also would like to acknowledge the Georgia Institute of Technology specifically the department of Electrical and Computer Engineering for initial support. Last but not the least, I would like to extend my sincere gratitude to my family for their constant encouragement, support and unconditional love. I acknowledge to my parents, Mr. Myungche Cho and Mrs. Eunsook Kim, and parents in law, Mr. Moohyun Park and Mrs. Youngmi Kim, have support for my personal and academic success. I would like to thank my wife Jieun Park, for her support and being part of this journey. I also would like to thank my son Daniel and daughter Olivia, for making me smile and motivating my life.

TABLE OF CONTENTS

LIST OF TABLES

LIST OF FIGURES

LIST OF SYMBOLS AND ABBREVIATIONS

ARMA	Autoregressive Moving Average
ARNN	Adaptive Recurrent Neural Network
AVDPIP	Air Vehicle Diagnostics and Prognostics Improvement Program
BEV	(pure) Battery Electric Vehicles
DMS	battery management system
BPNN	Back Propagation Neural Networks
CBM	Condition-Based Maintenance
CDF	Cumulative Distribution Function
CI	Confidence Interval
CIS	Confidence Interval Sensitivity
CM	Corrective Maintenance
CPNN	confidence prediction neural networks
DC	Direct Current
DD	Data-Driven
DOD	Depth of discharge
DWNN	dynamic wavelet neural networks
ECM	Equivalent Circuit Model
ECU	Engine Control Unit
EKF	Extended Kalman filter
EOL	End of Life
EV	Electrical Vehicle
EVES	Electric Vehicle Energy System

FCEV	Fuel Cell Electric Vehicles
FFNN	feed forward neural networks
FORM	First-Order Reliability Methods
FPMB	First-Principle Model-Based
GP	Gaussian Process
GPFR	Gaussian Process Functional Regression
HEV	Hybrid Electric Vehicles
HB	Health-Based
HMM	Hidden Markov Model
HUMS	Health and Usage Monitoring System
ICE	Internal Combustion Engine
IID	Independent and Identically Distributed
IS	Importance Sampling
IOS	International Organization for Standardization
PDF	Probability Density Function
RNN	recurrent neural networks
SMC	Sequential Monte Carlo
Li-ion	Lithium Ion
MCMC	Markov Chain Monte Carlo
MPP	Most Probable Point
NN	Neural Network
OCV	open circuit voltage
OFAT	One Factor at a Time
PdM	Predictive Maintenance
PF	Particle Filter

PHEV	Plug-in Hybrid Electric Vehicles
PHM	Prognostics and Health Management
PM	Preventive Maintenance
RCM	Reliability Centered Maintenance
RM	Reactive Maintenance
RMB	Reliability Model-Based
RUL	Remaining Useful Life
SEI	solid electrolyte interface
STD	standard deviation
SIS	Sequential Important Sampling
SOC	State of Charge
SOH	State of Health
SORM	Second-Order Reliability Methods
STD	Standard deviation
TDNN	time delay neural networks
UB	Usage-Based
UKF	Unscented Kalman Filter

SUMMARY

The body of work described here seeks to understand uncertainties that are inherent in the system prognosis procedure, to represent and propagate them, and to manage or shrink uncertainty distribution bounds under long-term and usage-based prognosis for accurate and precise results. Uncertainty is an inherent attribute of prognostic technologies, in which we estimate the End-Of-Life (EOL) and Remaining-Useful-Life (RUL) of a failing component or system, with the time evolution of the incipient failure increasing the uncertainty bounds as the fault horizon also increases. These increased uncertainty bounds may result in maintenance failure and system life reduction. In the given testbed case, the life of the electric vehicle energy system is not measurable. It is only estimated, thereby increasing the importance of uncertainty management. Furthermore, the more complex the system, the greater the impact of uncertainty on the prognosis procedure over time. Therefore, methods are needed to handle this uncertainty appropriately in order to improve the accuracy and precision of prognosis via shrinking the uncertainty bounds.

To this end, this thesis introduces novel methodologies for the RUL prognosis, that is data-driven, model-based, and hybrid methods. It introduces next two important classifications for prognostic technologies, i.e. usage-based and health-based prognosis. At this point, each uncertainty method has its own uncertainty bound properties that depend on the system or prognosis conditions. Therefore, an understanding of prognosis methods and finding optimized uncertainty methods for a given condition is the basis of uncertainty management procedures. In this thesis, Gaussian process regression, neural networks,

Kalman filtering, particle filtering, and Gaussian process functional regression are used to derive the RUL prediction.

Next, this thesis discusses proposed uncertainty management methods, and suggests an innovative way to reliably estimate the life of a given system subjected to disturbances and various usage patterns. The enabling technologies build upon a three-tiered architecture that aims to shrink EOL/RUL bounds: uncertainty representation, uncertainty propagation, and uncertainty management. The first step, uncertainty representation, is addressed via identification, characterization, and classification of the uncertainty sources that are inherent in the system and prognosis procedure. In the next step, uncertainty propagation, estimates of the propagation of each uncertainty source are derived using the gradient vector from the most probable point technique and a short- and long-term prognosis bounds ratio is derived using a source relation dependency approach. An uncertainty tree and a relation equation are formulated to assess the flow of the uncertainty in the system and model. In the last step, uncertainty management, sensitivity analysis methods are used to weigh the impact of each uncertainty source while feedback and hyperparameter loops are adopted to update the uncertainty tree. Finally, the most important uncertainty sources are retained that have an impact on the state model and the prognosis process.

The expected results and contributions of the study will provide a framework for uncertainty management tasked to shrink uncertainty bounds; they will also suggest a general and systematic listing of uncertainty sources for a given engineering system, derive more precise and accurate predictions based on three prediction methods, and assist to arrive at a true assessment of the current health state of complex engineering systems.

Additionally, the electric vehicle energy system is used as the testbed, along with a baring crack case study. These examples are used to illustrate the efficacy and easy applicability of the proposed methodology.

CHAPTER 1. INTRODUCTION

1.1 Overview and Statement of the Problem

The adage “Γ Ν Ω Θ Ι Σ Α Υ Τ Ο Ν (in English: Know thyself)” is traditionally ascribed to ancient Greece. According to the Greek writer Pausanias, the aphorism was inscribed in the pronaos of the temple of Apollo at Delphi [104]. Legend tells us that in ancient Greece, philosophers, statesmen and law-givers gathered together in Delphi and encapsulated their wisdom in this phrase [105]. The phrase is commonly used to emphasize the importance of knowing your authentic state [106] and it was adopted later by the famed Greek philosophers Aeschylus, Socrates, and Plato. Similar wisdom is found in ancient Chinese texts: “知彼知己，百戰百勝” (In English: “Know yourself and you will fight without danger in battles). This is a Chinese idiom that was derived from the ancient book, “孙子兵法”(“The Art of War”), written in the 5th century BC [107].

As these famous dictums emphasize, irrespective of time and place, understanding one’s own states such as character, limitations, strengths, and weaknesses is always important [110]. The importance of knowing states is not only for humans; it applies to engineering systems as well. The systems are always subjected to incipient fault or failure conditions. In addition, their performance degrades as a function of time, reaching a limit state beyond which the system must be repaired, re-engineered or maintained appropriately. These degradations or failures of engineering systems may also give harmful results to humans, directly or indirectly. Examples range from oil pipe leaks, to building or bridge collapses, to airplane engine failure crash cases. Therefore, estimating current

engineering system states is important. Fortunately, engineering systems are less complex than human beings [108] and do not typically require an entire lifetime of self-examination. However, there are many factors, such as functional coupling complexity, processing power increase, and product miniaturization, that contribute to the complexities of engineering systems. For these reasons, the importance of state estimation is growing.

The classical methods of system state estimations are based on scheduled maintenance practices, in which the system components are maintained, whether such maintenance is required or not. It is preferable if such costly practices are based on an exact assessment of the current health of the system. Life extension, availability, and cost benefits are derived if one is able to predict the system's health status and take appropriate action only when needed. Research about system lifespan extension starts with the maintenance cycle. The maintenance cycle began with the concept of dead and fix, such as reactive maintenance (RM) or unplanned corrective maintenance (CM). Later, research topics progressed to preventive maintenance (PM) which was developed and executed based on a predefined schedule or an accessible condition called Condition-Based Maintenance (CBM). Essentially, maintenance tendencies have switched from dead and fix to predict-prevent. With current advances in technology, researchers are able to improve maintenance support systems that enhance reliability and availability of significant engineering assets, while dropping overall costs through predictive and prognostic strategies. This latest maintenance stage is called Prognosis and Health Management (PHM).

In this thesis, a novel framework for the prognosis of engineering system remaining useful life (RUL) is introduced to suggest an innovative way to reliably estimate the life of

a given system from various characteristics. There is a need to explore state-of-the-art prognosis strategies such as usage-based/health-based strategies and model-based/data-driven strategies, as well as to acknowledge the existence of uncertainty during these procedures. Uncertainty is inherent in systems, because in the real world systems rarely, if ever, exist under ideal circumstances. This uncertainty also increases with the complexity of the system. The emphasis of this research is to represent uncertainties of prognosis procedures for a given system and to determine how they propagate, followed by a discussion of how to manage these uncertainties. The efficacy of the suggested research will be demonstrated through the evaluation of a lithium-ion (Li-ion) battery system in an electric vehicle (EV).

1.2 Motivation

There are many prediction methods, which in general can be grouped into three categories: data-driven methods, model-based methods, and hybrid methods. Data-driven prognostics use regularly-monitored data without any consideration of physical modeling to identify the characteristics of the current state and future behavior of a system [10]. Model-based prognosis considers a system's underlying physical understanding and thus incorporates a mathematical expression of the system into the estimation of RUL [15]. The hybrid method incorporates positive features of both the data-driven and model-based prediction methods; it is also called the surrogate method. Prediction results can be shown through statistical expressions such as probability distribution graphs; however, it is almost impossible to perfectly and accurately predict the operating and environmental conditions under which an engineering system functions. Therefore, it is necessary to acknowledge the presence of uncertainty in the prognosis of a system. At this point, observation and research are needed to 1) analyze and identify uncertainties of systems, and 2) infer and

control the increase in uncertainty within systems, rather than the uncertainties that come juxtaposed with the system. When the proportion of uncertainties in the system is fairly small, there is a common misconception that the effect of uncertainty can be considered in the later stages of the analysis after the fundamental and deterministic problem has been solved. However, the more complex the system, the greater the impact of uncertainty. Therefore, it is important to account for uncertainty throughout the analysis, design, testing, and operation of a system. For example, if a battery in the tractive system of an electric vehicle, or EV, is very sensitive to various influences, then researchers must investigate uncertainties and their effects on RUL estimation of battery life degradation in the EV system. Furthermore, such an electric plane requires more efficient and accurate battery life prediction by battery limitation, and even though it has a much simpler power system than an EV, an uncertainty mitigation algorithm in prognosis must be investigated and evaluated.

This thesis presents several approaches that can be used to shrink uncertainty bounds that result from long-term and usage-based prognosis procedures. This goal, shrunk uncertainty bounds, represents more accurate and precise prognosis results. The main algorithm for these approaches was developed through uncertainty representation, uncertainty propagation, and uncertainty management steps; however, it has minor differences that depend on prediction methods and application data states. The principal contributions of these works are the following.

- Novel methodologies of prognoses of remaining useful life in usage-based conditions. Results of model-based methods such as the particle filter method and the Markov Chain Monte Carlo Method have high accuracy and low precision, whereas results of data-driven methods such as the Gaussian Process Method and the Neural Network

Method have high precision and low accuracy under long-term and usage-based conditions.

- A general framework of characterization, representation, and classification of sources of uncertainty in the system. The general uncertainty management procedure of the prognostics system is frequently discussed from the representation, propagation, and management points of view. However, there are various interpretations of each procedure's terms and orders depending on the writer, so clarification here is helpful.
- The introduction and comparison of methodologies to estimate the propagation or impact ranking of uncertainty sources in the system. Generally, Monte Carlo simulation methods, probabilistic fuzzy approach, interval analysis, first- and second-order reliability methods (FORM; SORM), evidence approach methods, regression technique polynomial chaos expansions, and most probable point (MPP) methods are used for uncertainty propagation methods. Among these methods, some are not suitable for all types of uncertainty source handling, and some are difficult to classify in terms of the impact of sources. The rest of the methods have less accurate propagation; however, they have other positive aspects. Among the pros and cons of these methodologies, this thesis helps the reader to select the best methods for a given application via a thorough comparison.
- More accurate model-based methods results are shown via the uncertainty management procedure. The model-based methods have high accuracy and less precision, usually because the physical model is expected to catch most of the behavior or states via an outline of the model plot. However, the uncertainty management procedure has higher numbers of uncertainty sources than data-driven methods. It also affects uncertainty

bounds on prediction points. For this reason, it has lower precision than data-driven methods. However, it can be improved via uncertainty management methods and results also show that the uncertainty bounds are shrunk.

- Data-driven methods, upgraded by adding a physical model, are introduced, with improved accuracy and precision results shown via adapted uncertainty handling methods. General Data-Driven (DD) methods only consider relationships between each data point, so the property of high accuracy does not always hold true when an early phase prognosis is performed. In other words, DD methods do not catch later-occurring behavior in the system. Accuracy can be improved by adding a physical model to DD methods. However, in doing so, many additional uncertainty sources are added. At this point, expanded uncertainty bounds can be reduced by uncertainty management, thereby providing more accurate and precise results.
- The validation of the proposed framework in two case studies. The approaches presented in this thesis can be validated using an 18650 li-ion battery, usually used in determining electric vehicle life degradation data, and also used in bearing crack growth data. Both data results indicated shrunk uncertainty bounds. Furthermore, this author's suggested approaches also are adaptable for comparison with other uncertainty management methods for validation.

1.3 Organization

This thesis will cover a brief review of the literature. Then, in Chapters 2 and 3, the author will discuss technical approaches for handling uncertainty in the prognosis procedure. Next, the author will introduce the three/four major sections of this thesis. The first major section will discuss prognosis strategies in Chapter 4. This chapter handles

prognosis; prognosis methodologies such as model-based prognosis; data-driven prognosis; and surrogate approaches such as the hybrid method. It also covers major techniques used in each method such as the Particle filter, the Gaussian process regression, and the Gaussian process functional regression. The second major section treats strategies of uncertainty in Chapter 5. This chapter introduces an overall understanding and appreciation of uncertainty, and methods for increasing prognosis performance using uncertainty handling via uncertainty representation, propagation, and management procedures. Chapter 6 shows how these methodologies work on electric vehicle energy systems (EVES) cases. The last major section, in Chapter 7, shows another performance verification using a different application from the EVES case. Finally, Matlab codes and references are included at the end of this thesis.

CHAPTER 2. BACKGROUND STUDY

2.1 Background

Much has happened in engineering since the Industrial Revolution a couple hundred years ago; however, the most dramatic changes have occurred in the past century. During this period, maintenance management has evolved tremendously from reactive

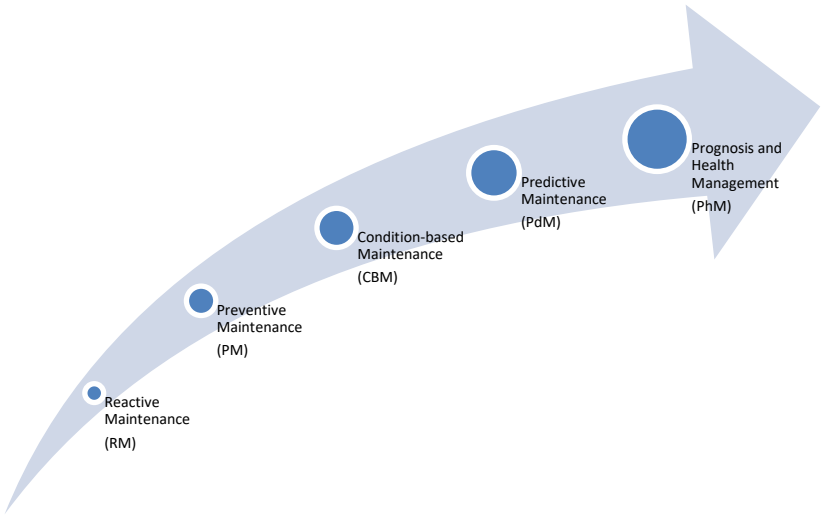

Figure 2.1 Uncertainty bounds example on prognostics approach

maintenance (RM) to prognosis and health management (PHM) as Figure 2.1 indicates. In particular, maintenance was promoted in the 1950's with the rebuilding of industry after World War II [1]. The rapid development of system failure-detecting in the 1970's led to the growth in popularity of predictive methods [2]. At the left bottom of Figure 2.1, Reactive Maintenance (RM) indicates maintenance

action applied on a failure machine. Smith and Hinchcliffe (2003) mention that the task of RM is to restore functional capabilities of failed systems, so this type of maintenance is also called corrective or unplanned maintenance [111]. There is no action required to maintain the component until it reaches end of life, so RM may provide economic benefits

due to a low investment cost. However, as Sullivan et al. (2010) mention, RM may increase costs due to unplanned equipment downtime, increased labor costs if overtime is needed, possible secondary damage from equipment failure, and insufficient use of staff resources [112]. The next type of maintenance depicted in the above figure, Preventive Maintenance (PM), can be defined as an implementation that is based on a certain schedule intended to prevent the failure of a component or of the system. Therefore, scheduled adjustments, replacement of components, repairs, calibration, and lubricants are part of this strategy, the goal of which is to avoid unexpected failures during the operation cycle [113]. PM has an increased component life cycle, is cost-effective in many capital-intensive processes, and its flexibility allows for the adjustment of maintenance periodicity. However, it may suffer from being labor intensive, with potential for incidental damage in conducting unnecessary maintenance, with catastrophic failure still likely to occur [112].

Predictive maintenance (PdM) is the next shift in the trend depicted in Figure 2.1. PdM, as its name suggests, predictively handles actual conditions instead of schedule pre-setting, as PM did. Sullivan et al. (2010) defined the detection of system or component degradation, then elimination or control, allowing for casual stressors, prior to any significant disaster in the system's physical state. PdM has many more advantages than RM or PM. It decreases process downtime, decreases cost of labor and/or parts, increases product quality, and improves the component operational cycle. However, this maintenance methodology may incur increased investment in diagnostic skills or staff training, therefore being more difficult to justify for management [112]. Indicative of the developing nature of diagnostic engineering, PdM methods have become more varied. At the end, PdM can be classified into reliability-centered maintenance (RCM) and condition-based maintenance (CBM). RCM only considers the important equipment in the system. It recognizes that safety and major repair cost issues outweigh the cost of components.t A higher probability to withstand failure or life degradation exists. Therefore, RCM methods evaluate system

components to best mate the two and result in a higher reliability and cost-effectiveness [112]. In contrast, CBM focuses more on monitoring the entirety of the parts in the system. In other words, this methodology involves a process for monitoring the operating characteristics of a system; changing the monitoring can be used to predict failures or abnormal degradations. CBM methods are better than other methods for real-time maintenance resources and for avoiding unnecessary maintenance. Therefore, this method can adapt to more varied systems than can the RCM methods. CBM became the predominant maintenance strategy implemented in production systems. However, the more complex the system, the less rapid the processing speeds of CBM methods [3].

With increases in system complexities over the years, it has become essential to develop more rapid and accurate forecasting methodology; additionally, online monitoring and prognosis became more important. At this point, state-of-the-art research on maintenance strategy, prognostics, and health management (PHM), was introduced. The PHM method focuses on understanding, detecting, and tracking failure, then predicting the remaining useful life of the system or components. In other words, PHM includes a set of technologies that link studies of failed mechanisms to system lifecycle management, degradation tracking mechanisms, and predictions on the remaining useful life of components and systems. This is the most useful maintenance method in terms of helping to reduce labor costs, reducing unnecessary or unplanned activities, and increasing proactivity. This thesis is based on the PHM method to predict components and system life degradation.

2.2 Literature Review

Academic research in three distinct areas is reviewed in this section: 1) The general prognosis of engineering systems that covers theoretical and technical approaches; 2) The uncertainty of prognostics in the engineering system; and 3) State-of-the-art-research about the tractive/energy system of the electric vehicle.

2.2.1 Prognosis of engineering system

In the field of engineering and in this thesis, prognostics is defined as the prediction of the remaining useful life in a system [7]. Prognosis algorithms can be categorized into health-based and usage-based prognostics, which refer to differing theoretical approaches. The former refers to the detection, isolation, and assessment of a fault or incipient failure condition. In contrast, usage-based prognostics algorithms refer to a long-term prediction of the health of a system subjected to internal and external condition factors without any consideration of incipient failure modes or the existence of fault detection [4]. As an example, the aircraft industry is very sensitive to matters of maintenance. For instance, R. Patrick (2009), of Impact Technologies LLC, suggests increasing prognostic system effectiveness of the health and usage monitoring system (HUMS) in the YH-60 helicopter [8]. Patrick's team approached the improvement of the helicopter CBM system performance and implemented prognostics as a part of the Air Vehicle Diagnostics and Prognostics Improvement Program (AVDPIP). The team also utilized the general characteristics of both categories of prognostics in their research on air vehicle diagnostics and prognostic improvement programs [5].

Methods of prognosis can also be classified into two categories, these being data-driven and model-based prognostics. Data-driven prognostics use regularly-monitored data without any consideration of physical modeling to identify the characteristics of the current state and future behavior of a system. The advantage of this method is that it is relatively simple to implement and the speed of estimation is both fast and inexpensive when compared to other approaches. It also helps to gain an understanding of the tendencies of physical systems through large data sets without the need for a physical system.

Mathematical regression approaches, neural fuzzy, relevance vector machines, support vector machines, Markov Chain, Gaussian process regression, Dempster-Shafer regression, neural network, and other computational methods have provided alternative tools for data-driven prognoses [10]. As examples, D. Brown (2009) introduced a data-driven methodology for the Electro Mechanical Actuator that takes advantage of online and real-time estimation of RUL [12]. J. Liu (2010) presented a developed adaptive recurrent neural network (ARNN), which is constructed based on the optimized recursive Levenberg-Marquardt method mixed with the adaptive/recurrent neural network for RUL prediction of lithium-ion batteries [13]. There are also some other methods cited in K. Javed (2011) on data-driven prognostics improvements by assessing the predictability of features when selecting them for bearing cases [14]. M. Rigamonti (2016) proposed using differential evolution for the optimization of the Echo State Network, which is a relatively new type of Recurrent Neural Network for RUL prediction of a turbofan engine working under variable conditions [11]. While the data-driven methodology does not utilize physical cause-and-effect relationships, it does require a substantial lifecycle of data. Furthermore, the dependency on the quality of data is high, so it may have wider confidence intervals than other methods.

Model-based prognosis considers a system's underlying physical understanding and thus incorporates a mathematical expression of the system into the estimation of RUL. Therefore, the main advantage of model-based prognostics is to achieve a higher accuracy estimation due to the incorporation of the physical understanding of the model by directly monitoring it [15]. Models can be used to account for differences in design between various systems, and are computationally efficient to implement [7]. Paris' law, Forman's law,

Bayesian methods, nonlinear least squares, the Karman filter, autoregressive moving averages, the Monte Carlo simulation, particle filters, and other states or methods have provided alternative tools for model-based prognosis. This method is used in various areas such as the mechanical, electrical, aerospace, and automotive industries. J.C. Newman (1992) developed a conventional computing platform for initiation and propagation of common crack configurations in structural components [16]. J. Luo (2008) suggested the model-based prognostic process for a suspension system under nominal and degraded conditions with an interacting multiple model [15]. M. Daigle and S. Sankararaman (2013) described first-order reliability-based methods for battery prediction [17].

Furthermore, as time goes by, these theoretical boundaries of model-based and data-driven are blurred and becoming more complex. Therefore, it is necessary to further refine the application with methods that are more appropriate. G. Vachtsevanos (2006) presents many approaches for prognostics, such as PHM in control, fault diagnosis and prognosis, and performance metrics in unmanned aerial vehicle systems [100]. M. Orchard (2007) developed a model-based approach of a particle filter, for on-line fault diagnosis and prognosis [102] and presents outer feedback correction loops for on-line model parameter adjustments [103]. D. Edwards presents sets of uncertainty measurements to quantify the impact on prognostic algorithms [101].

2.2.2 Uncertainty in prognosis procedure

The general meaning of ‘uncertainty’ can be defined as the things that are only known imprecisely or not known exactly [56]; the inability to determine the exact state of the system [57]; reflecting potential outcome distributions [58]; and so on. Historically, the

concept of uncertainty has long been associated with civilizations starting with the early Egyptians and Greeks of the 4th century BC; however, the definition has persisted almost unchanged until the 20th century, and only recently has the contribution of uncertainty to engineering systems been analysed [55]. Uncertainty is also inherent in the engineering system; therefore, uncertainty should be considered carefully to design and maintain a more accurate and effective engineering system. In classical philosophy, uncertainties have been classified into two groups, aleatory uncertainty and epistemic uncertainty [52, 53]. Aleatory uncertainty comes from inherently uncertain natural phenomena. It is also variably referred to as irreducible uncertainty, objective uncertainty, and stochastic uncertainty. In other words, when a fault in a system forces an outage, aleatory uncertainty is the most considerable uncertainty in the system. Epistemic uncertainty, on the other hand, comes from a lack of knowledge. It is also called subjective uncertainty and state-of-knowledge uncertainty [54]. A usage-based system prognosis case, epistemic uncertainty is the most considerable uncertainty the researcher commonly encounters. These uncertainty classifications have become more complex with the passage of time than their counterparts in many uncertainty-related research fields, including economics, geometrical engineering, mechanical engineering, electrical engineering, system engineering, structure engineering, management science, uncertainty analysis, and risk analysis [55]. The goal of these wide ranges of research is to find out more accurate and precise results by mitigating, managing, or modeling uncertainty [59~66]. For example, Girish et al. (2013) show improved results by modeling the uncertainty in Gaussian Process model reference adaptive control [87], and H.A. Kingravi et al. (2012) use capturing the uncertainty for a connection between kernel methods using reproducing kernel Hilbert space theory [88].

Furthermore, there is more uncertainty in the state prediction and/or prognosis case than in the general estimation case [74] There are numerous studies that have dealt with uncertainty management methods in prognosis [67~73]. The general uncertainty management procedure of the prognostics system is generally discussed from the representation, propagation, and management points of view. Different sources also describe the procedure of the prognostics system as identification, quantification, propagation, and analysis [75]; or quantification, representation, and management [76]. Though the interpretations of the term vary, the procedural outlines are similar. This paper will now define representation, propagation, and management steps for uncertainty management procedures for the system life degradation prognosis.

2.2.2.1 Uncertainty representation (add more paper reviews)

Uncertainty representation, identifying and characterizing a source of uncertainty in the system, is the first step in prognostics uncertainty management [75]. Merrick J.R et al. (2003) describe four steps of input and output uncertainty representation in a Bayesian framework [78]. The representation step can also be broken down into the uncertainty identification and qualification of certain mathematical formulas, described below [79].

2.2.2.2 Uncertainty propagation (add more paper reviews)

A general case of uncertainty propagation can be derived via a mathematical function such as the Monte Carlo Simulation for prognostics [80] or the improved Monte Carlo algorithm [79]. J.R. Celaya (2012) defined that this step can be guided by the choice of modeling and simulation frameworks of common theories such as classical set theory, probability theory, fuzzy set theory, fuzzy measure theory, and rough set theory [74].

Orchard (2008) and Saha (2009) mentioned that representation of uncertainty is dominated by probabilistic measures in the prognosis and health management domain when simulation has a sufficient statistical database [73,85]. Wang suggested using the Dempster Shafer theory for occasions when data is incomplete or scarce [84]. These mathematical approaches work well for simple systems or on a single uncertainty case such as a measurement error or a parameter uncertainty. However, a real-world engineering system has more complex relations than those for which these methods are suited. Therefore, this paper suggests a new approach for finding the percentage of each growth in the whole, rather than observing the growth of the elements over time.

2.2.2.3 Uncertainty management

There are numerous publications about 'uncertainty management' [51,58,60,63,69,73,77,81,83]. However, many articles do not directly show a mathematical approach for management. Often, they omit management terms instead of quantification or propagation, or they suggest management methods without sufficient mathematical support. The suggested management stage in this thesis starts with the relationship between sensitivity analysis and uncertainty analysis [82], and the method of local or global sensitivity analysis, which can be used to aid uncertainty reduction and management [83]. Chapter 2 will discuss suggested management in more detail.

2.2.3 Uncertainty management of energy system degradation for electric vehicles

The biggest issue of the EV, or electric vehicle, is that the energy storage system degradation is much shorter than others. Although it has more benefits than the inter-combustion engine (ICE), the EV system's battery degradation holds its popularity.

Therefore, a significant amount of research remains to be done. Battery degradation consists of calendar aging [89] and cycle aging [90]. These degradations cannot be measured directly, so the role of estimation techniques for SOC and SOH with uncertainty handling becomes more important. First of all, the battery has various modeling approaches, such as the equivalent circuit model [91], the NCA model, the simple model [92], the first/second/third order RC model [93], the electrochemical model [94], the electrochemical impedance spectroscopy model [95], and more. In addition, by using the prognostic technique as mentioned in the previous section, battery life degradation can also be predicted [9,23,96] and uncertainty management becomes an important issue to shrink the uncertainty bounds. The following section is devoted to this topic and discusses suggested shrinking distribution bounds on the prognostics technique.

CHAPTER 3. TECHNICAL APPROACH

The previous section describes a brief overview of engineering system life degradation, prognoses of degradation, and prognoses of remaining useful life (RUL) estimation. It also explained briefly that there is an inherent uncertainty in the system and that this uncertainty increases in the prognosis process. This next section briefly introduces the suggested approach of uncertainty management for engineering system RUL prediction via three steps of uncertainty representation, propagation, and management for accurate and precision prognosis results. Detailed about suggested methods are treated in Chapters 4 and 5.

3.1 Strategy of the design and analysis of uncertainty in prognostics

Prognostic algorithms must account for inherent uncertainty in the system, which cannot be eliminated. It would be possible to effectively predict the engineering system state in an ideal scenario, but uncertainty becomes more blurry and complex in practice. Furthermore, it is necessary to account for uncertainty beginning with the initial stages of system development through the whole system process, including design, build, and modification, rather than misunderstanding that the effect of the uncertainty can be included at the later stages of the analysis. Using a three-step strategy, this section will examine the design and analysis of the uncertainty algorithm to accurately account for the effect of uncertainty in prognostics under the long-term and usage-based prognosis cases. The steps are as follows: (1) Uncertainty Representation; (2) Uncertainty Propagation; and (3) Uncertainty Management. The goal of this three-step strategy is to shrink the uncertainty bounds. Figure 3.1 illustrates the suggested algorithm. It shows that a long-

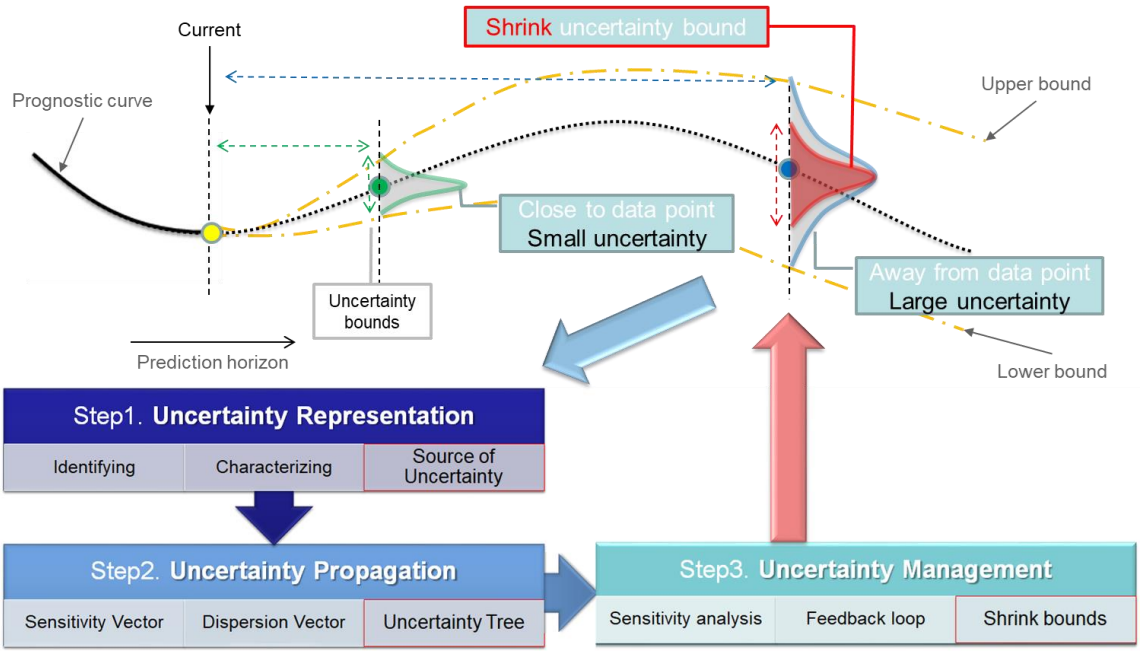

Figure 3.1 Illustration of suggested algorithm to shrink uncertainty bound

term prediction period prognosis distribution has wider uncertainty bounds than a short-term prognosis distribution and depicts suggested methods for shrinking the bounds for precise and accurate results.

3.2 Uncertainty Representation

The first step to shrinking distribution bounds on the prognostics technique is an "uncertainty representation." This step is guided by the recognition that there are many different uncertainties (Δ) in the system and prediction procedures. Therefore, the task of the uncertainty representation stage is to identify and characterize these uncertainties first, then classify each source as much as possible. Generally, the sources of uncertainty in the RUL prediction can be classified into three main sources: physical uncertainty, data uncertainty, and model uncertainty [97], as shown in Figure 3.2.

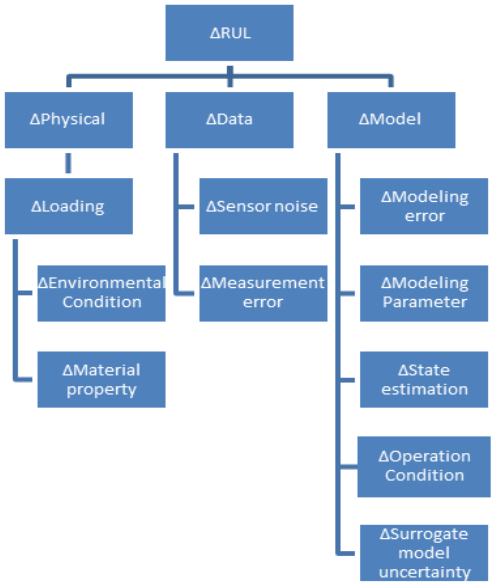

Figure 3.2 Taxonomy of the general sources of uncertainty in RUL prediction

Physical uncertainty (Δphysical) refers to the inborn variation of the physical system. The uncertainty or fluctuations can appear in the form of uncontrollable variations in the external environment, instruments, test procedures, observers, and so on. They are usually modeled as random phenomenon characterized by their probability distributions and require large amounts of information [26]. The physical variability in the loading (Δload), environmental condition (Δe.c.) and operation condition of load (Δo.c.) are considered during this proposed research. The variability in other physical properties is insignificant, so it is not considered to be human error or physical measurement error.

Another type of uncertainty is *data uncertainty (Δdata)*. Acquired data can contain outliers, have errors, or simply have missing data. In addition, the probability distributions of some technical properties of energy systems are inferred using data from laboratory experiments [27]. The measurement error (Δm.e.), sensor noise (Δs.n.) and sparse noise (Δsparce) are considered for the source of Δdata.

Model uncertainty (Δmodel) refers to the difference between the true variable and the predicted variable that can neither be measured accurately nor already be known, and comprises several parts such as modeling error (Δm.e.), model parameter (Δm.p), state estimation (Δs.e.), operation condition (Δo.c.), and surrogate model uncertainty (Δs.u.). In addition, the state model cannot be perfect, because system phenomena cannot be expressed completely by equations and numbers, so the prognosis must account for the model uncertainty. Any remaining uncertainty in the system during prognostics is called *unclassified uncertainty* (Δunclassified). This paper assumes that the uncertainty source has an insignificant effect on the prognostics, neglectable during procedure, and without regard to dependent or independent sources.

3.3 Uncertainty Propagation

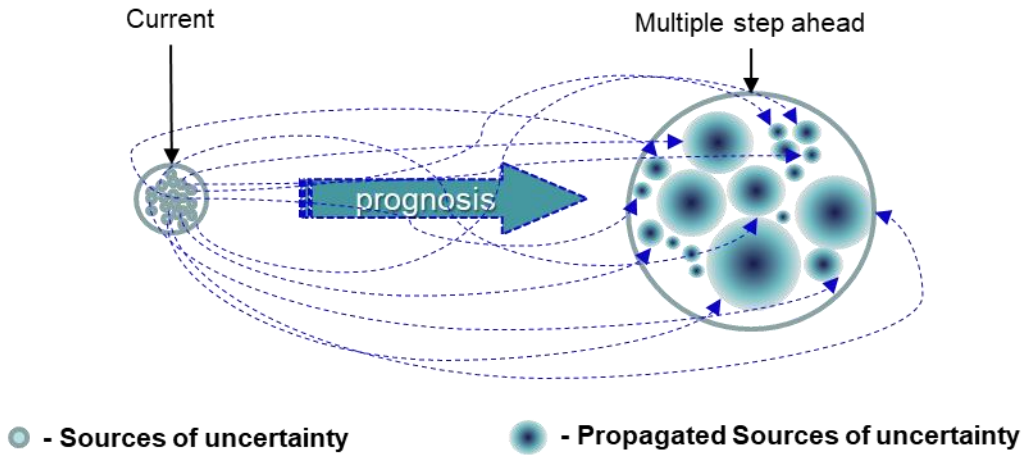

Figure 3.3 Illustrate the propagated source of uncertainty

Identified and classified sources of uncertainty from the previous steps are propagated throughout the prognostics procedure. In addition to such an RUL prediction case, general prognostics methodologies such as data-driven, model-based, and hybrid methods show different results of RUL estimation from what these three methods consider

at the propagation step. After that, the ideal propagated uncertainty can be estimated from the ratio of increased uncertainty (the gap of output and input uncertainty) and original uncertainty. At this point, as mentioned in the literature review, the Monte Carlo method and improved Monte Carlo methods such as SRSM and SFEM can be used for this estimation. However, these methods are only good for the single or source of uncertainty calculation, and it is impossible to figure out all mathematical uncertainty source propagations using these methods in the RUL prediction. This thesis suggests using the most probable point (MPP) method at this propagation stage. The performance of this method alone is not optimal because the accuracy is lower than average. However, when combined with the uncertainty tree method, the effect is brilliant. The most probable point method classifies each propagation during transformation via gradient vector. After that, using this gradient vector, the researcher can classify the source of uncertainty into the uncertainty tree and can express the result with the sensitivity and dispersion vector. Using the concept of the uncertainty tree [28], one can estimate total propagated uncertainty by using the ratio or size of each propagated source of uncertainty with an uncertainty relation equation. It is also beneficial to determine how sources of uncertainty occupy spaces in the propagated uncertainty distribution through a sensitivity and effectiveness vector from the visualized tree. The uncertainty tree shows a graphical/hierarchical structure to assess the flow of uncertainty in prognostic computational models. Essentially, it is a graphical depiction of the variable dependencies employing sensitivity analysis tools in uncertainty analysis [28]. Figure 3.4 shows an example of the uncertainty tree with the uncertainty relation expression.

Propagated uncertainty can be written as:

$$\Delta A = \sqrt{\left[\left(\frac{\partial A}{\partial B_A}\frac{\partial B}{\partial E_B}\Delta E_B\right)^2 + \left(\frac{\partial A}{\partial B_A}\frac{\partial B}{\partial F_B}\Delta F_B\right)^2 + \left(\frac{\partial A}{\partial C_A}\Delta C_A\right)^2 + \left(\frac{\partial A}{\partial D_A}\Delta D_A\right)^2\right]}$$

Furthermore, each branch shows the mathematical relationship between each source of uncertainty. These relationships are shown in the uncertainty relationship equation as f_A and f_B in figure 3.4. After this second propagation step, propagated uncertainty in the

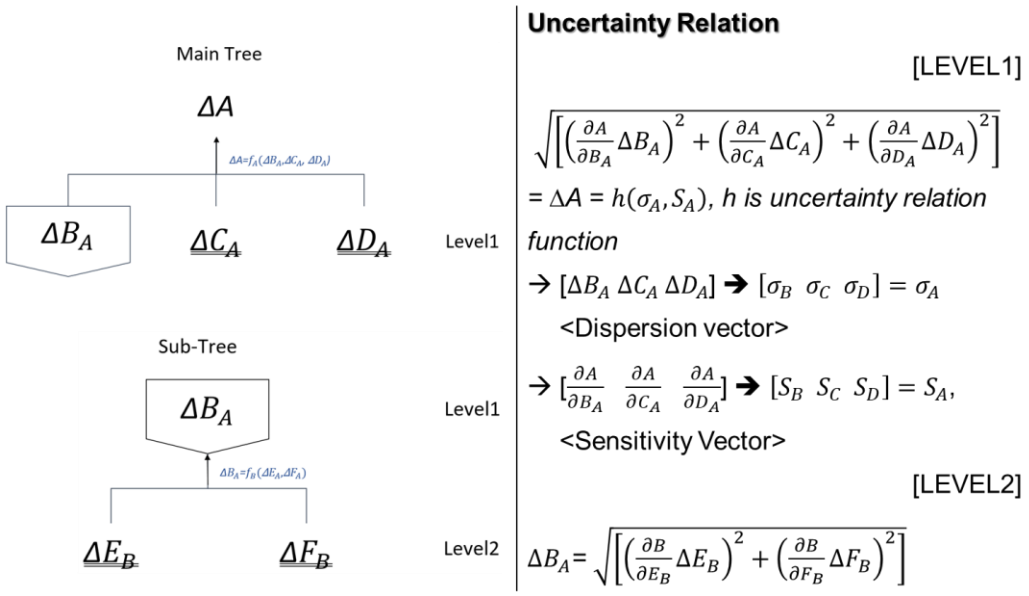

Figure 3.4 Basic Uncertainty Tree with expression of uncertainty relations

system can be expressed with a dispersion and sensitivity vector on the uncertainty relation equation, and each uncertainty relation also can be shown by the uncertainty tree. Furthermore, this propagated uncertainty algorithm and two vectors will help to shrink the uncertainty bounds in the next step.

3.4 Uncertainty Management

The last step of the suggested method for shrinking the uncertainty bound distribution on RUL prognosis is the uncertainty management step. The uncertainty management has

two feedback loops, the inner loop and outer loop. From the previous step, the dispersion vector and sensitivity vector can be estimated via the most probable point and uncertainty tree approaches. After that, each dispersion vector shows how those sources of uncertainty occupy space on top of the desired uncertainty. Sensitivity vectors show how each source of uncertainty is sensitive to the prediction point, and they help to estimate propagation sensitivity via sensitivity analysis. As the final step, the system can be understood via a source impactor that shows the ranking of the contribution factors in the source of uncertainty, by using the dispersion vector and sensitivity analysis. Repeat this contribution factor configuration, then update to the uncertainty tree. This is referred to as the updated uncertainty tree, or inner loop, at the third stage, the management step. Figure 3.5 illustrates

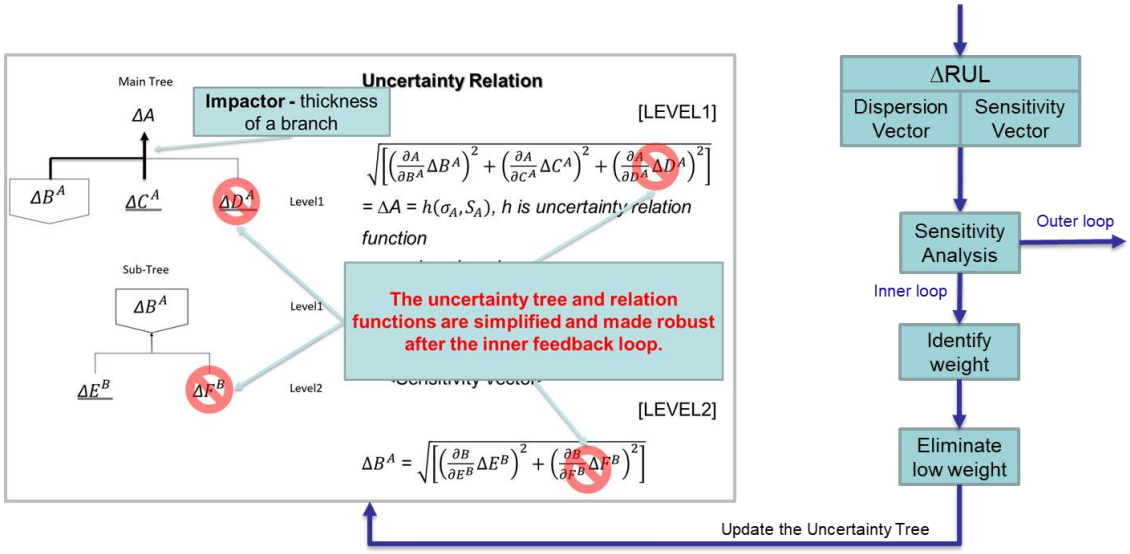

Figure 3.5 Uncertainty management stage illustration

this concept visually.

The second feedback loop begins from the updated uncertainty tree. From this updated tree, sources of uncertainty can be expressed via the percentage of impact. Then, use the impactor source percentage in the prognosis parameter, which is generally set to

zero during the prognosis method. These steps do not provide the exact propagated source of uncertainty during prognosis, but they focus on major factors of impact and neglect less important factors during the procedure. The result of this third stage of uncertainty handling during prognosis is shrunk uncertainty bounds at the end of the procedure.

To summarize, using this methodology, the researcher can accomplish a shrinking uncertainty distribution bound by disregarding tiny contribution sources of uncertainty and managing high contribution sources of uncertainty. The researcher is advised to process important uncertainty sources more carefully, by collecting more data or changing the prognostics method. The next chapter will dive deeper into a discussion of such concepts as system degradation, propagation, and uncertainty handling that this chapter briefly covered. After that, the electric vehicle energy system case study and the bearing crack case study are both discussed for thesis verification.

CHAPTER 4. PROGNOSIS MECHANICS

This chapter introduces the various prognosis methods for the end-of-life prediction of the engineering system, comparing advantages and disadvantages under the given operational and observational conditions, and combined for better prediction results. Next, this chapter shows the prediction results obtained in a given battery life degradation case. This chapter's structure is the following: Section 4.1 briefly introduces prognosis. Section 4.2 introduces a general description of model-based prognosis such as Particle Filter (PF) and linear regressions. Section 4.3 provides a general description of data-driven methods such as the Neural Network (NN) method and the Gaussian Process Regression (GPR) method. Section 4.4 presents a surrogate method, also known as the hybrid method. This section particularly emphasizes the Gaussian Process Functional Regression (GPFR) method.

4.1 System Life Degradation

Engineering systems do not maintain their performance from their initial conditions permanently, because all stresses gradually accumulate and result in damage to the system. The damage also gradually accumulates, leading to system fault. The ageing of the engineering system under the normal usage condition also occurs naturally. When system faults and natural deterioration continue, the system will either reach soft failure at a pre-specified threshold, or hard failure when it ceases to function entirely. This procedure is called a system life degradation. Figure 4.1 illustrates these two general types of degradation [128]. The life, or performance, degradation cannot be avoided because it inherently exists in every engineering system, with different degradation ratios to its time frame. Generally, $t_0$is the initial condition time and $t_f$is the failure time. The cause of

degradation can vary greatly. It could be a mechanical issue, a chemical issue, an electrochemical issue, an electro-chem-mechanical issue, a thermal issue, a usage condition, a health condition, an environmental condition, and so on. The classification of degradation varies with each of the above causes. It can be classified by degradation speed, term of the time frame, degradation reason and factors, or methodological approaches.

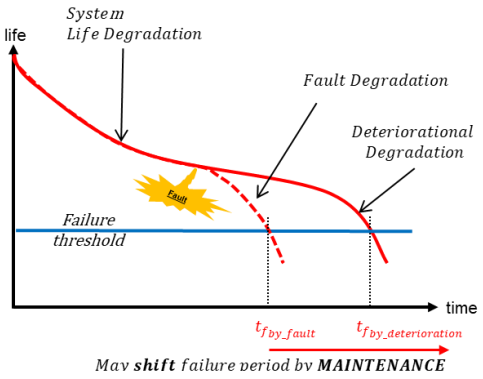

Figure 4.1 Example of the engineering system life degradation

Therefore, the degradation can be classified as on-line performance degradation and off-line performance degradation, mutant degradation and gradual degradation, cycle-based degradation and calendar-based degradation, and so on.

Modeling and simulation are the main approaches to estimating life degradation, because modeling follows the degradation process path and judges system health condition performance via simulation. The system degradation process modeling can generally be divided into two categories. One modeling methods in this category focuses on physical-based models and captures several degradation models that derive from physical changes. X. Ni (2014) shows one example of degradation modeling under discrete time through this approach. This method set t is time, ∇x is a damage or physical deterioration, and both initial conditions are set to zero. Cumulative damage and distribution is then shown as the following:

$$t_i;\ i = 0,1,2,\cdots,n,\cdots,f; t_0 = 0$$

$$\{\nabla x_i;\ i = 0,1,2,\cdots,n,\cdots,f;\nabla x_0 = 0\}$$

Assuming the variable ∇x is independent and identically distributed (IID) and that it is also independent from t, then the cumulative damage x_c is:

$$x_c = \sum_{j=1}^{m}\left(\sum_{i=1}^{f}\nabla x_i\right)$$

where m is the number of physical damage factors. Next, the cumulative damage distribution can be calculated via the Poisson Process, $P(f = n) = \frac{(\lambda t)^n}{n!}e^{-\lambda t}$ as is shown below:

$$F_c(x) = P(x_c \le x) = \sum_{n=1} P\left(\sum_{i=1}^{f}\nabla x_i \le x\right)\frac{(\lambda t)^n}{n!}e^{-\lambda t}$$

This approach is frequently used in bearing wear, oil pipelines, and gas pipeline corrosion. Ideally, this method could handle every degradation mechanism; however, it is not perfect under complicated empirical conditions. First of all, the mathematical equations increase in complexity as the number of degradation mechanisms increase. Therefore, this method's effectiveness is limited to handling just one or two degradation mechanisms. The other modeling methods focus on statistical models and fitted them to measured data. They may also change or update statistical models to reduce errors between the model and the data, expressing the current state via a probability distribution function (p.d.f). Furthermore, the statistical model may also include a physical model as a surrogate method before handling the full state of the engineering system. This thesis, as mentioned, uses the statistical degradation prediction model. The goal is to find and track system degradation

so as to extend the system's performance and life via maintenance. Details about this method and maintenance are presented in Chapter 5.

4.2 About Prognostics

As briefly mentioned in a previous section, PHM can be divided into two parts, P (prognosis), and HM (health and management). According to the International Organization for Standardization (ISO), "Prognostics refers to a prediction / forecasting / extrapolation process by modeling fault progression, based on current state assessment and future operating conditions" and "Health Management refers to a decision-making capability to intelligently perform maintenance and logistics activities on the basis of diagnostics / prognostics information" [114]. Therefore, PHM focuses on determining the operating state of components or of the system, predictive action that includes estimating the remaining useful life of the system, and determining appropriate actions for maintenance based on diagnosis and prognosis. PHM consists of diagnostics and prognostics for system health management, and this results in hugely positive effects, such as extending the system cycle, safety improvements, reliability improvements, increases in quality and productivity, and a reduction in maintenance time, labor, and costs. Therefore, PHM has become a rising solution in many engineering fields nowadays.

G. Vachtsevanos suggests seven modules for an integrated approach to PHM system design as Figure 4.2 depicts. This configuration shows that feedback loops, complete data collection,

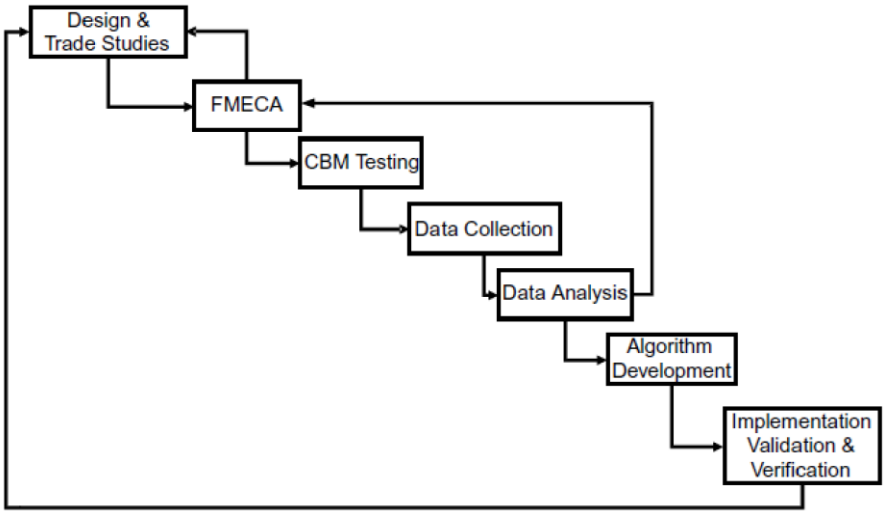

Figure 4.2 An integrated approach to PHM design (from G. Vachtsevanos)

and complete data analysis steps are essential for failure diagnosis and prognosis development [100]. PHM can be broken down into seven functional layers: data acquisition, data manipulation, health assessment, diagnostics, prognostics, decision support, and human interface [115]. The data acquisition layer generally refers to the module that provides system access to, and monitoring of, data. The data manipulation layer performs data filtering, denoising, feature extraction, and classification, along with specialized extraction algorithms. The health assessment layer detects any degredation or abnormal state in the health of monitored components, systems, and subsystems. The diagnostic layer detects and identifies failures. The prognostics layer projects the current health state into the future and estimates the RUL of the system or components, taking a confidence interval into consideration. The decision support layer generates recommendations related to maintenance action and modification of the objective profile. The last layer, the human interface layer, displays alerts and status updates, such as health assessments and prognosis assessments of the different layers. Among these layers,

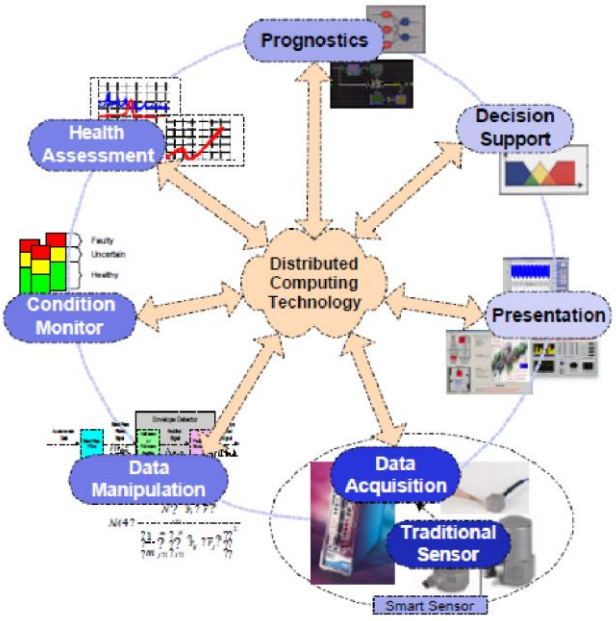

Figure 4.3 The seven-layered ISO - PHM architecture (from G. Vachtsevanos)

prognosis layers and RUL prediction are the keys to maintaining and extending the engineering components or system life via PHM. To summarize, better RUL prediction can result in more accurate and precise maintenance, followed by logistic cost decrease, unnecessary maintenance decrease, and increases in reliability and safety.

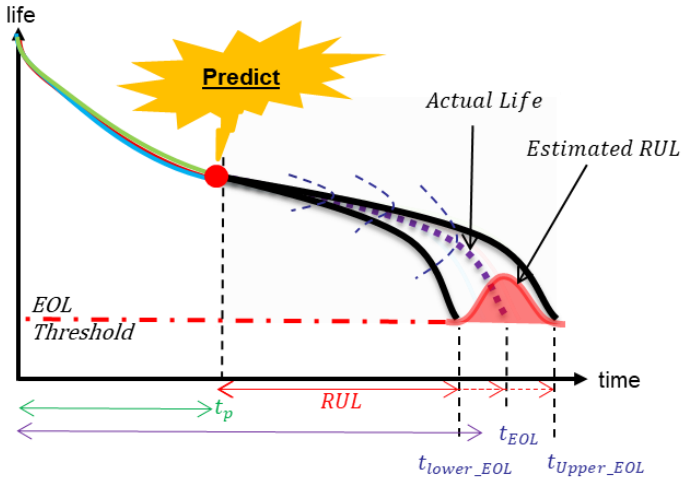

Figure 4.4. Illustration of prognosis and RUL prediction

The prognosis is based on an analysis of failure modes, detection of the current state, aging, fault conditions, and correlation of degradation symptoms with a goal of increasing them. As previously mentioned, an illustration of RUL prediction as the goal of prognostics is given in Figure 4.4. This configuration consists of actual life, prediction time t_p, end-of-life (EOL) time t_{EOL}, estimated RUL, threshold, and current time t_c. In such cases, life degradation starts right after the initial state. As discussed, it always exists in a system, but the most users do not notice the degradation right after the initial state due to its low degradation ratio. This ratio is shown in the nonlinear graph in Figure 4.4. Threshold refers to the suggested timing for changing the component or maintenance schedule. It is also referred to as the EOL threshold of the component or system. The prediction time (t_p) is regarded as the current time (t_c), or vice versa because the assumption of such a prognostic case is that prediction behavior performs at the current point. Actual EOL (t_{AOL}) refers to actual values of system/component life status and estimated or predicted t_{AOL} is referred to as end-of-life (EOL) time (t_{EOL}). The goal of system state prediction is to find the t_{EOL} that is in a similar position to t_{AOL} under the same threshold. Therefore, the result of system/component EOL is expressed in probabilistic terms, such as a probability distribution and/or a graph after the prediction is performed. In other words, t_{EOL} shows the potential possibilities for t_{AOL} to exist at the threshold.

Most traditional prediction techniques deliver a single point [116]. However, it is impossible to use such techniques for an empirical system, because system and/or environmental conditions are never ideal and it is not possible to handle whole conditions mathematically. Furthermore, even under ideal conditions simple point prediction is impossible for complex and uncertain systems. Therefore, single point prediction is not

adequate to state prognostics or decision makings [117]. In such cases, the value of end-of-life (EOL) time (t_{EOL}) is estimated into lower limit EOL time (t_{lower_EOL}) and upper limit EOL time (t_{upper_EOL}). These are the upper and lower limits of the confidence interval (CI), with 98%, 95%, 90%, and 80% confidence.

The remaining useful life (RUL) estimation, which is the remaining time to maintenance from the present time, is also estimated as a probabilistic term because it comes from the result of EOL prediction and present time. The simplified general RUL can be defined by Eq. (4.1):

$$RUL = t_{EOL} - t_P \tag{4.1}$$

It is also expressed as $RUL(t_P) = t_{EOL}(t_P) - t_P$, because the predicted t_{EOL} and RUL are updated when new data arrives at each time point. Previous expressions fixed the time point at t_P on Eq. (4.1). RUL is also the same as t_{EOL}. Just as EOL has lower and upper bounds, RUL prediction also has lower and upper bounds. The lower bound of RUL is the replacement or maintenance time under PHM. The gaps between these bounds are also referred to as RUL bounds or RUL uncertainty bounds. The difference between them will

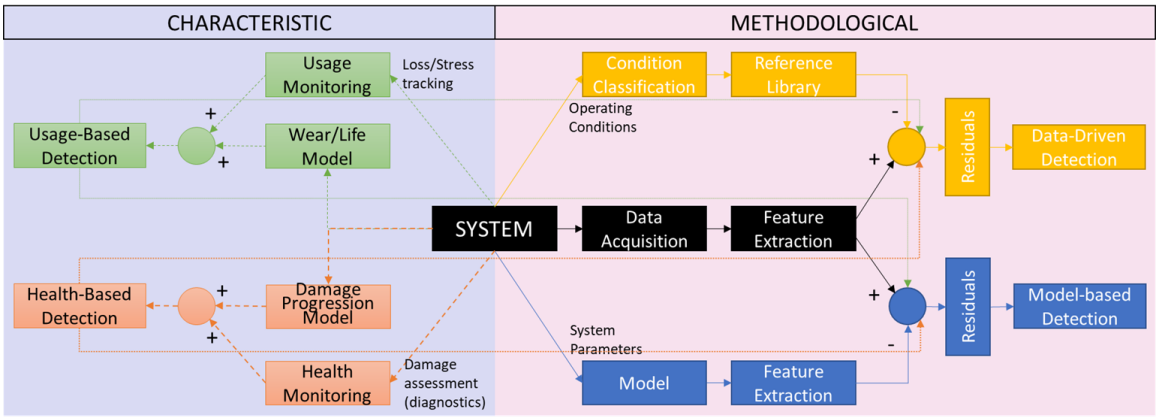

Figure 4.5 Prognosis classification

be explained in more depth in Chapter 5, along with uncertainty explanations. In general, prognostics methods to estimate EOL and RUL predictions can be categorized into characteristics classification and methodological classification as Figure 4.5 indicates. The former, characteristic classification, is categorized into two activity levels: a usage-based (UB) prognosis and a health-based (HB) prognosis. The UB prognosis considers the past, present, and future usage of the system to predict the RUL of the system. The UB prognosis is also subjected to external and internal stresses during the whole performance period, so it is used for long-term prediction. This method does not suppose the fault mode on the system cycle. In contrast, the health-based prognostics always suppose the fault mode because the HB prognosis predicts the RUL of the failing system. The HB prognosis detects and isolates a fault when the fault condition has been detected, and assesses its severity. The HB prognosis fits well to the online and real time prognoses of the system via a diagnosis that keeps monitoring and updating the system and data. After deciding between the HB and UB prognoses for a given project, the researcher must choose the prognosis method. Methodological categories can be classified into three categories: model-based, data-driven, and hybrid approaches. Physical models illustrate the differences between

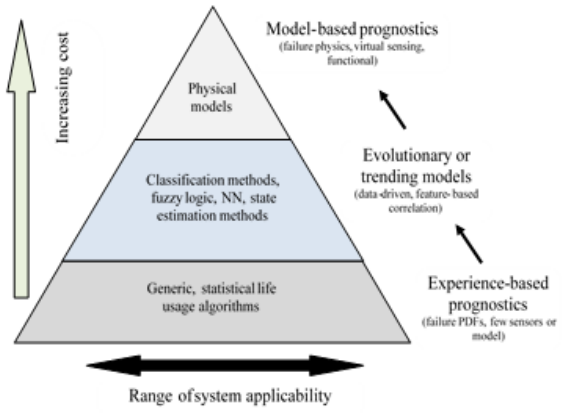

Figure 4.6 A Taxonomy of Prognostic Approaches from K. Goebel

these approaches, depicting the evolution of damage or degradation, field operating conditions, and required amount of life degradation data. K. Goebel and G. Vachtsevanos describe the range of these methods as a function of the range of system applicability and cost, shown in Figure 4.6. The pyramid in the figure starts with the experience-based prognostic as the base, the widest range of applicability. In the experience-based approach, prognostics are based on the evaluation of a stochastic deterioration function or a fiability function, thereby covering most statistical terms of prognostics [120]. Subsequently, cost increases and the range of applicability narrows as the pyramid migrates from data-driven prognostics to model-based prognostics at the top. These approaches will be discussed in more detail in the following sections.

4.3 Model-Based Methods

4.3.1 Basic Principles of Model-Based Prognostics

As briefly mentioned in the literature review, the model-based approaches for prognostics consider a system's underlying physical understanding, such as mechanical, electrical, chemical, and thermal processes, and then incorporate a mathematical expression of the system into the estimation of RUL. Model-based methods may be classified into the first-principle model-based (FPMB) and reliability model-based (RMB) methods as described by Enrico Zio, 2012. FPMB approaches use a mathematical model derived from first principles to describe the degradation process leading to the failure for the prognosis procedure. The author mentions that if this approach is applicable, it leads to the most accurate prediction results but the first principle model definition is the hardest step in the process. In addition, it is impossible to find a first principle model for complex

or real systems. RMB approaches estimate the average equipment life under average usage, then use traditional reliability models to estimate the system failure behavior or prediction of system RUL. This method includes the environmental stresses and conditions under average usages, so prediction is more flexible than in the FPMB approaches. However, this approach may require sufficient representative data, especially reliable equipment life degradation data, which is quite difficult to come by.

J. Luo et al. (2012) suggest a block diagram of model-based prognostics as shown in Figure 4.7 [122]. This diagram consists of six blocks: (1) Identify system or degradation model; (2) Calculate simulation under load condition; (3) Prognostic modeling; (4) Feature estimation; (5) Track and measure the model; and (6) Predict RUL. There are also other diagrammatic suggestions for model-based prognostics from authors M. Diagle [123], A. Dawn [124] and L. Honglei [125]. Differences exist in the details of each researcher's the diagrams, because their models are different and filtering/state space choices to obtain the model parameters or RUL are also different. However, the outlines of these various diagrams are similar in that they focus on identifying model parameters, then predict future

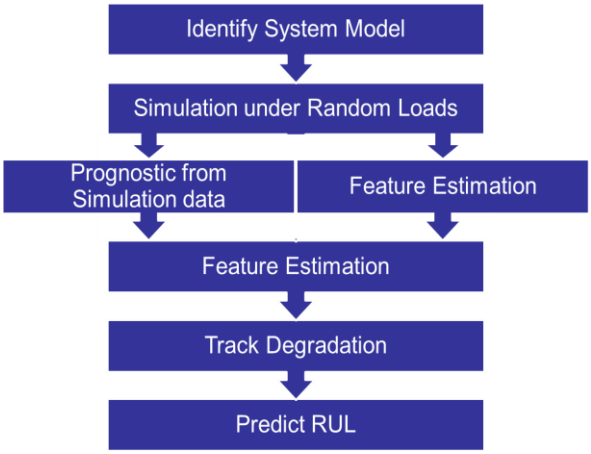

Figure 4.7 Model-based prognostic process diagram from J.Luo

behaviour via consistent parameter updating. Therefore, this method has such high reliability and robust prediction that it has become very popular for a number of applications in aerospace, the automotive industry, power generation, artificial intelligence, transportation, and heavy industry. In addition, autoregressive moving-average (ARMA) techniques, Bayesian filtering algorithms, and empirically-based methods are also included in the model-based prognostic schemes. Furthermore, there are a variety of methods raging from Bayesian estimation to artificial intelligence tools to estimate model parameters. Common approaches include the Kalman filter (KF), the Extended Kalman filter (EKF), the Unscented Kalman Filter (UKF), the particle filter (PF), stochastic autoregressive models, the Markov chain Monte Carlo (MCMC) method, the Weibull model, and nonlinear least square methods. This thesis will only handle the Particle Filter for model-based prognostic methods.

4.3.2 Hidden Markov Models

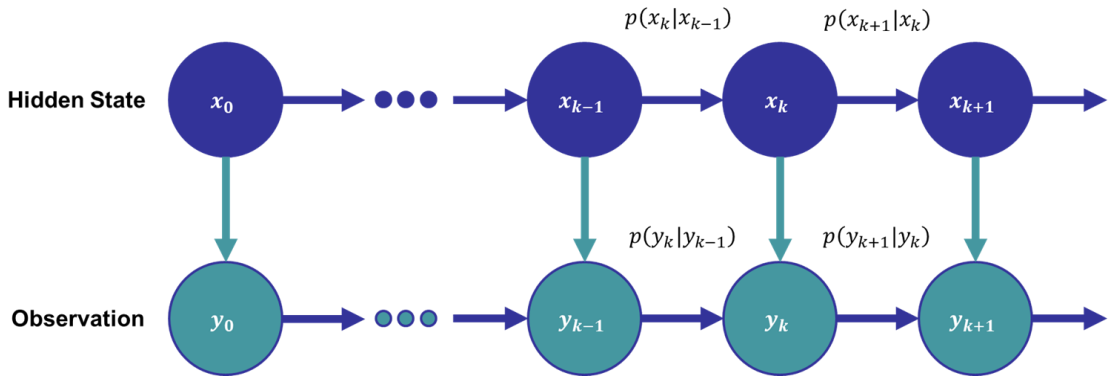

Figure 4.8 Representation of Hidden Markov Models (HMM) as graphical model

The mathematical modeling of the model-based prognosis starts from the understanding of two state models, the first two of which are the State-Space Model and the Hidden Markov Model (HMM). Both models are based on Bayesian analysis and they have a similar feature

in that they express unobserved states or physical models of the system in terms of numerical and mathematical representations. According to L. Fahrmeir et al. (2001), both state models have been used in the context of time series or longitudinal data $\{y_t\}$; but the observation model of the state space model for y_t is given by a single state, whereas the observation model of HMM uses the sequence of states. In this subchapter, only the general HMM are introduced with some detail; the State-Space Model with uncertainty will be expanded upon in Chapter 5 as part of the explanation for handling uncertainty.

The fundamental idea of HMM is illustrated in Figure 4.8. It is expressed by the variables $x_0, x_1, \cdots, x_{k-1}, x_k, x_{k+1}$ that represent the states on the top nodes, and the variables $y_0, y_1, \cdots, y_{k-1}, y_k, y_{k+1}$ that represent observations or evidence on the bottom nodes. Each vertical discrete slice represents time steps. In HMM, state models are hidden or non-observable but they can be modeled with the Markov process. The goal of HMM is to estimate the state model by providing all observations up to the current point, then also estimating future states via past and current state inferences. This method has three probability distributions: (1) The transition model, denoted as$p(x_k|x_{k-1})$, only depends on the previous state means, initial state distribution $p(x_0)$, and observation model $p(y_k|x_k)$. With these probability distributions, the posterior distribution can be expressed as follows:

$$p(x_0, x_1, \dots, x_{k-1}, x_k) = p(x_0) \prod_{t=1}^{k} p(x_k|x_{k-1}) p(x_k)$$

$$p(x_k, y_{k-1}, y_{k-1}, \dots) = p(x_k)$$

$$p(x_0, x_1, \dots, x_{k-1}, x_k|y_0, y_1, \dots, y_{k-1}, y_k) = p(x_0)p(y_k|x_0) \prod_{t=1}^{k} p(x_k|x_{k-1}) p(x_k)$$

At this point, posterior distribution can be solved using Bayes' rule for conditional probability and non-linear filtering as follows:

$$p(x_0, \dots, x_k | y_0, \dots, y_k) = \frac{p(x_0, \dots, x_k, y_0, \dots, y_k)}{p(y_0, y_1, \dots, y_{k-1}, y_k)} = \frac{p(y_0, \dots, y_k | x_0, \dots, x_k) p(x_0, \dots, x_k)}{p(y_0, \dots, y_k)}$$

$$p(x_0, x_1, \dots, x_{k-1}, x_k, y_0, y_1, \dots, y_{k-1}, y_k) = p(x_0, x_1, \dots, x_{k-1}, y_0, y_1, \dots, y_{k-1}) p(x_k | x_{k-1}) p(x_k)$$

$$p(y_0, y_1, \dots, y_{k-1}, y_k) = \int p(y_0, \dots, y_k | x_0, \dots, x_k) p(x_0, \dots, x_k) dx_0 \dots, dx_k$$

$$p(y_0, y_1, \dots, y_{k-1}, y_k | x_0, x_1, \dots, x_{k-1}, x_k) = \prod_h^k p(x_h)$$

$$p(x_0, x_1, \dots, x_{k-1}, x_k) = p(x_0) \prod_h^k p(x_{h-1})$$

Filtering, smoothing, and predicting tasks are used to determine $p(x_k | y_0, \dots, y_n)$, which depends on the position of the time slot t. Smoothing is the estimation of $p(x_0, \dots, x_k | y_0, \dots, y_k)$; as observations arrive, filtering is the estimation of $p(x_k | y_0, \dots, y_k)$. Finally, the formal solution of $p(x_0, \dots, x_k | y_0, \dots, y_k)$ is the following:

$$p(x_0, x_1, \dots, x_{k-1}, x_k | y_0, y_1, \dots, y_{k-1}, y_k) = \frac{p(x_0, x_1, \dots, x_{k-1}, y_0, y_1, \dots, y_{k-1}) p(x_k | x_{k-1}) p(x_k)}{p(y_n | y_1, \dots, y_{k-1})}$$

$$p(x_k | y_0, \dots, y_{k-1}) \rightarrow [updating\ step]: p(x_k | y_0, \dots, y_k) = \frac{p(x_k) p(x_k | y_0, \dots, y_{k-1})}{p(y_n | y_1, \dots, y_{k-1})}$$

$$p(x_k|y_0, \dots, y_{k-1}) \rightarrow [prediction\ step]: p(x_k|y_0, y_1, \dots, y_{k-1})$$
$$= \int p(x_k|y_0, y_1, \dots, y_{k-1}) p(x_{k-1}|y_0, y_1, \dots, y_{k-1}) dx_{k-1}$$

To achieve prognostics, update the prediction step in the Bayesian inference. Then, use the nonlinear filtering equation above in Sequential Important Sampling (SIS) or Important Sampling (SI) methods with resampling. This combination is referred to as Sequential Monte Carlo methods (SMC).

4.3.3 Particle Filters

PF is an emerging popular method for physical-based prognostics with a wide range of applications in science and engineering. It fundamentally uses sequential importance sampling and Bayesian Theory. Bayesian state estimation calculates a posterior probability density function (PDF) from prior observation in the system state. At this point, the parameters of the posterior and prior PDFs of the PF method are represented by random samples and referred to as particles, hence the name "particle filtering". PF is also referred to as Sequential Monte Carlo (SMC) Methods because the posterior and prior parameters change sequentially. In other words, the posterior from the current step shifts to the prior on the next step. The parameters are also updated by multiplying them with the likelihood from the updated measurement. This is the main difference between the Sequential Monte Carlo Method and the classical Monte-Carlo Method. The required number of samples to perform filtering will be reduced by likelihood multiplication or necessary precision. Therefore, PF is faster and more efficient than the classical Monte Carlo Method, and it also covers complex systems, because it can handle non-linear and non-gaussian cases. In

addition, PF can perform long-term prediction in multiple steps if the calculation of the future state is extended.

Importance sampling (IS), mentioned at the end of previous subchapter, uses importance density and weighting to model density as follows:

$$\pi_k(x_0, \dots, x_k) = \frac{w_n(x_0, \dots, x_k) q_n}{Z_n}$$

$\pi_k(x_0, \dots, x_k)$ is model density. It is combined with weight and importance such that $w_k(x_0, \dots, x_k)$ is weight, $q_k(x_0, \dots, x_k)$ is importance, and z_k is a normalization factor. After that, the model density can then be estimated as:

$$\hat{\pi}_k(x_0, \dots, x_k) = \sum_{i=1}^{N} \left(\frac{w_n\left(X_0^i, \dots, X_k^i\right)}{\sum_{j=1}^{N} w_n\left(X_0^j, \dots, X_k^j\right)} \right) \left(\delta_{\left(X_0^i, \dots, X_k^i\right)}(x_0, \dots, x_k) \right)$$

For the SIS case, select the importance distribution first such that $q_k(x_0, \dots, x_k) = q_{k-1}(x_0, \dots, x_{k-1}) q_k(x_0, \dots, x_k)$ and the original distribution initial probability sample is $q_0(x_0)$. Then pick *(i)* from the conditional probabilities for subsequent steps such as $q_k\left(x_k | x_0^i, \dots, x_{k-1}^i\right)$. Note that these estimated variances also increase as n is increased, so a resampling step is required. Resampling generates the sample again from the newly created approximation distributions to reduce increased variance on SIS. At this step, each sample is associated with a number of offspring samples to estimate the already estimated distributions. Figure 4.9 will help to understand this PF algorithm.

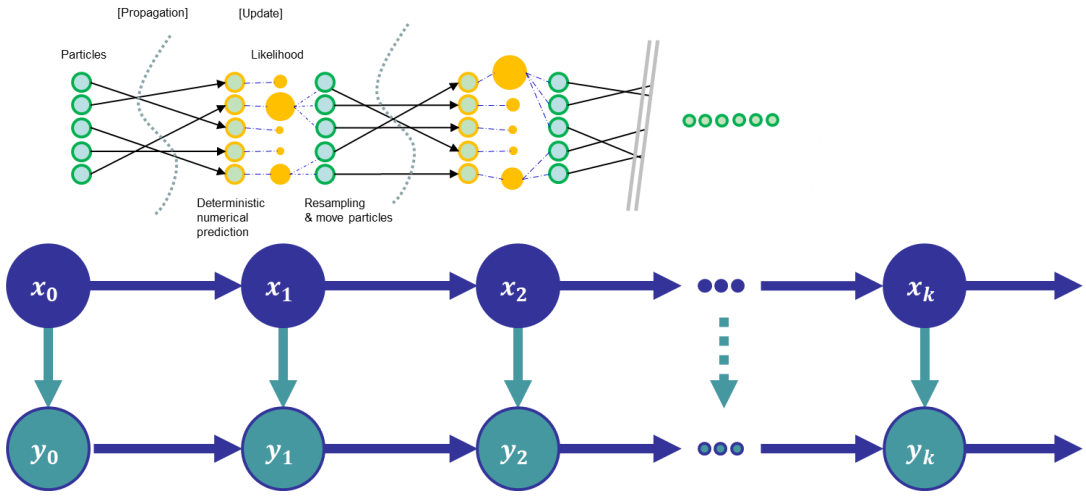

Figure 4.9 Illustration of PF/SMC algorithm

4.4 Data-Driven Methods

The model-based prognostics methods introduced in the previous subchapter are popular and powerful tools for predicting system state or life degradation. However, they are limited in that these models can only be used when physical models or system life degradation descriptions are available. Even when well-defined physical models are used, there may be drawbacks such as mis-parameterization, parameter instability, mis-calibration, and high computational time required [133]. In sum, these drawbacks tend to generate more uncertainty and increasing the uncertainty bounds. Furthermore, in some cases involving complex systems, it is almost impossible to derive a system state model or physical process. In such cases, it is possible to set up a surrogate system model via assumption of certain forms for the dynamic model first, and then use the observed inputs and outputs of the system to determine the model parameters needed [100]. This is a fundamental concept of data driven prognosis methods, based on having little physical meaning of the system.

4.4.1 Basic Principles of Data-Driven Prognostics

Data-Driven Prognosis Methods define the relationship between system state variables directly from monitored system operating data. They usually rely on knowledge-based, signal processing, and statistical methodologies to extract the hidden information in the measurements. That may require much observed data from similar systems to make reliable prognostics without the physical models, since measured data can be major sources for deep understanding of system degradation behavior in applications. Therefore, even if the physical meaning of the system was not included in this method, the pattern of system degradation can be found from trends within measured data. Those trends can then be used for estimating the current degradation state and predicting the future system remaining useful life. This data can now be referred to as training data. The next step is to evaluate the predicted performance or difference between the current data and historical degradation using a testing data set. Validation data set is also similar as training and testing data set, that means another training data set act as testing dataset and checking performance validation. T. Wang et al. (2008) explained four steps (operating regime partitioning, sensor selection, performance assessment, and model identification) of training data and three steps (signal transformation, distance evaluation, and RUL estimation) of testing data [134].

The Data-Driven Approach's methodologies rely upon the statistical and learning approaches from pattern recognition in computational intelligence and machine learning. Therefore, as mentioned in the literature review, popular techniques include NN, Fuzzy Rule-based, tree-based methods, evolution computational methods, support vector machines, relevance vector machines, least square regression, wiener process, and gaussian

process regression. Among these techniques, the Gaussian Process is used for the data-driven methods in this thesis.

4.4.2 Gaussian Process Regression (GPR)

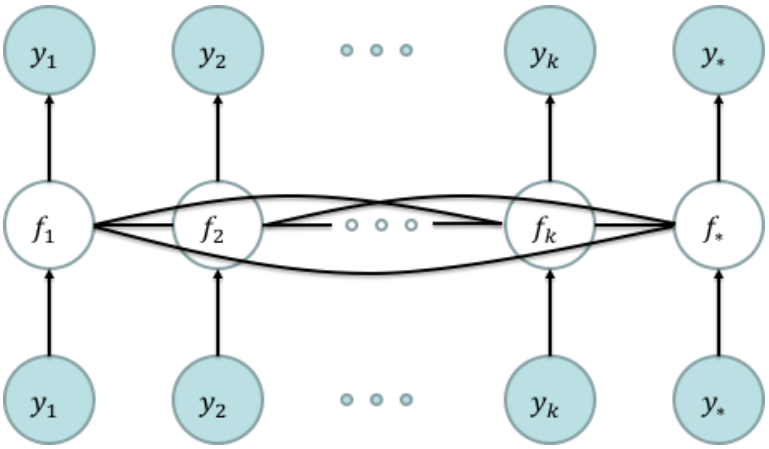

Figure 4.10 Gaussian Process Regression Concept illustration

Figure 4.10 illustrates the concept of the Gaussian Process. The Gaussian Process (GP) is a framework for a global black-box and non-parametric regression method based on Bayesian inference. It uses the empirical data in the absence of the specific system model structure to estimate the most probable output algorithm as one of the data-driven methods. According to Dr. Melo's explanation about GP, A Gaussian Process is a collection of random variables, any finite number of which have joint Gaussian distribution that is fully specified by a covariance matrix and a mean vector. Therefore, the Gaussian Process is also a stochastic process that is completely specified by its mean function $\mu(x)$ and positive definite covariance function $k(x, x')$:

$$f(x) \sim GP\big(\mu(x), k(x, x')\big);$$

$$\mu(x) = E\big(f(x)\big);\ k(x, x') = E\big[\big(f(x) - \mu(x)\big)\big(f(x') - \mu(x')\big)\big];$$

Formally, the stochastic process $f(x)$ is a Gaussian Process and its value at a discrete and finite number of points $\{f(x^1), \dots, f(x^n)\}$ can be seen as part of the normal distribution:

$$f(x^1), \dots, f(x^n) \sim N(0, k(x, x'))$$

In most cases, it is commonly assumed that the mean function, $\mu(x)$, is zero, because there is no prior knowledge about the mean function and linear combination of the random variable with the normal distribution to support this assumption. In contrast, the covariance function, $k(x, x')$, should reflect prior knowledge, such as smoothness or continuity, about the underlying function; therefore its role is important. A popular choice of the covariance function is the squared exponential as follows:

$$Cov(f, f') = k(x, x') = \sigma_f^2 \; exp \; exp \left[\frac{-(x - x')^2}{2l^2} \right];$$

Where l and σ_f are hyperparameters of covariance function and σ_f^2 is the maximum allowable covariance, that should cover a broad range on the y-axis. If the exponential function is zero inside when the function $f(x)$ is almost correlated with $f(x')$ or $x \approx x'$, then $k(x, x') = \sigma_f^2$ and the covariance function approaches this maximum allowance. On the other hand, if x and x' are far away, $k(x, x')$ is zero and each x and x' are not visible [136]. At the end of this equation, the output is a normal distribution based in terms of mean and variance. The mean represents the most likely output and the variance represents the confidence of measurement.

The prediction stage is slightly different from previous methods. Given a set of data and prior GP and $f(x)$ with the mean and covariance function, the prediction stage aims to

predictively distribute the function $f_*(x)$ at the new input, x_*. The typical prediction methods are given with some observations $\{y_1, \dots, y_k\}$ and certain time instances $\{x_1, \dots, x_k\}$, and they estimate new observations on a new time instance at $k+1$. However, GP sets an input vector $X = \{x_1, \dots, x_k\}$ as training, and a test points vector X_*, composed of all points. In this process, system models are very flexible because they aren't fixed by physical models and the GP chooses the best choice in every case. Therefore, the GP always handles additional noise (Gaussian noise is assumed) and is denoted by the following observation:

$$y = f(x) + N(0, \sigma_n^2)$$

This equation is also classified into the global function output, $f(x)$, and the local departure, $N(0, \sigma_n^2)$. The global function handles the alternative system model and its parameter via regression. Local departure handles error between the global function and measured data as noise. This noise folds into $k(x, x')$ by the following equation with the Kronecker delta function $\sigma_n^2 \delta(x, x')$:

$$Cov(f, f') = k(x, x') = \sigma_f^2 \; exp \; exp \left[\frac{-(x - x')^2}{2l^2}\right] + \sigma_n^2 \delta(x, x')$$

$$K = \begin{bmatrix} k(x_1, x_1) & \cdots & k(x_1, x_n) \\ \vdots & \vdots & \vdots \\ k(x_n, x_1) & \cdots & k(x_n, x_n) \end{bmatrix}$$

$$\begin{pmatrix} y \\ f' \end{pmatrix} = (0 \quad (K))$$

Once prior distribution is set up from this redefined covariance function, it can be used in posterior distribution as follows:

$$f_*(x) \sim GP(f', cov(f'));$$

$$f_* = E[f_*] = \frac{k(x, x')}{(k(x, x') + \sigma_n^2 I)} y$$

$$cov(f_*) = k(x', x') - \frac{k(x, x')}{(k(x', x) + \sigma_n^2 I)}$$

4.4.3 Neural Network Methods

The NNs are a family of models inspired by biological neural networks that do not have direct storage space in the brain. The brain then stores them in a way that changes the connections of nerve neurons. At this point, neurons only receive signals coming from other nerve cells and serve to send out their signals [30]. The Neural Network Models operate upon a similar principle. A Neural Network is a network that connects a small element called a node, corresponding to the nerve cells in the brain. The neural connections of the most vital nerve cells of the brain represent the connection weights of nodes. Figure 4.11.a represents graphical simple nodes on NN where $x_1, x_{1,} x_3$ are inputs, $w_1, w_{1,} w_3$ are weights of input, b is bias, and y is output. Output y is $y = \rho(wx + b)$ where $x = [x_1, x_{1,} x_3]^T$, $w = \left[w_1, w_{1,} w_3\right]$, and ρ is the activation function. NN then connects to simple nodes as a network, shown in Figure 4.12.b. NN have various architecture such an artificial neural networks (ANN), back propagation neural networks (BPNN), confidence prediction neural networks (CPNN), dynamic wavelet neural networks (DWNN), feed forward neural networks

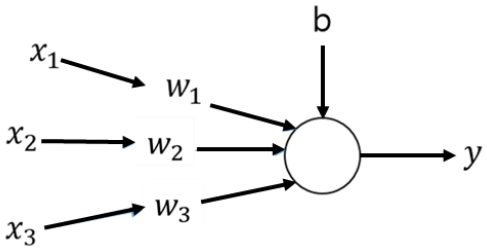

Figure 4.12.a. Simple node of NN

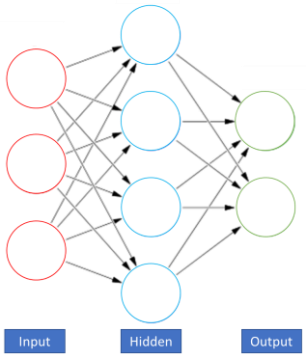

Figure 4.12.b. Network of NN

(FFNN), recurrent neural networks (RNN), time delay neural networks (TDNN), and so on; however, this paper only considers ANN.

4.5 Hybrid Methods

Data-Driven Methods are also popular and powerful tools for predicting system state or life degradation on complex systems at low cost. However, they have some drawbacks such as mis-parameterization, parameter instability, mis-calibration, and high computational effort and time required. Even if huge data are ready for prognosis, if training data and testing data have a big gap, the prognosis result will not be accurate and precise. In other words, data-driven methods are not also perfect for prognosis as dependent of system, operating, or environmental condition. Therefore, there is no single prognosis method that covers any engineering system. The methods covered in this chapter have their own identical techniques to estimate current system states and predict the remaining useful life of the components or system. Accuracy and precision results could be high or low depending on the situation if using just one method. Therefore, researchers have tried to use fusion approaches as hybrid methods that combine data-driven and model-based methods to improve the prognosis performance. Examples include averaging combinations

between model-based and data-driven method prognosis results [137], replacing the system model in the model-based method by using data-driven methods [138], and using data-driven methods using model-based methods [139].

4.5.1 Gaussian Process Functional Regression (GPFR)

Dr. Shi JQ et al. (2007) introduced Gaussian Process Functional Regression (GPFR) modeling methods for batch data to improve performance of multiple step-ahead prediction with Gaussian Process Regression [140]. This method keeps comparing and updating the mean function and covariance function of the basic Gaussian Process Method continuously. In most cases, the Gaussian Process commonly assumes that the mean function, $\mu(x)$, is zero because there is no prior knowledge about the mean function, and the linear combination of random variables with normal distribution also supports this assumption. However, certain methods of the mean, $\mu(x)$, suggest optimizing the mean function via training data sets or physical state models that come from similar model-based methods in the GPFR method. This is why the GPFR model could have improved results on long-term based prognoses. The GPFR model is defined as follows:

$$y = \mu(t) + \tau(x) + N(0, \sigma_n^2)$$

$$\tau(x) \sim GP\big(0, k(x, x'|\theta)\big)$$

$$\mu(t) = \mu'\beta(t)$$

Then y can be decomposed by

$$y = \mu'\beta(t) + \sum_j \phi(x)\, \mathcal{N}(0, \lambda) + \mathcal{N}(0, \sigma_n^2)$$

Where $\phi(x)$ is eigenfunction for covariance function of $k(\cdot,\cdot)$. At the end, prior and posterior distribution of GPFR are as follows:

$$\begin{pmatrix} y \\ f' \end{pmatrix} = \begin{pmatrix} u \\ u_* \end{pmatrix} \begin{pmatrix} k(x,x') + \sigma_n^2 & k(x,x') \\ k(x,x')^T & k(x',x') \end{pmatrix}$$

$$f_*(x) \sim GP(f', cov(f'));$$

$$f_* = E[f_*] = \mu(x) + \frac{k(x,x')}{(k(x,x') + \sigma_n^2 I)}(y - \mu)$$

$$cov(f_*) = k(x',x') - \frac{k(x,x')}{(k(x',x) + \sigma_n^2 I)}$$

CHAPTER 5. UNCERTAITNY HANDLING IN PROGNOSIS

The previous section introduced the overall properties of prognosis and its technical methods. Prognosis deals with predicting the future state of a system. Prediction is always blurred by uncertainty, due to a lack of information, unexpected incidents, and so on. Uncertainty is a key factor in prognosis to which close attention must be paid, in order to maximize the accuracy and precision of results. This chapter will introduce the overall properties of uncertainty, including sources of uncertainty and their effects in the system, propagation estimation of uncertainty, and how to achieve more accurate and precise prognostics by mitigating uncertainty.

5.1 About Uncertainty

The Cambridge Dictionary defines uncertainty as “a situation in which something is not known, or something that is not known or certain”[141]. Ironically, the actual meaning of uncertainty is uncertain; therefore, numerous definitions for uncertainty exist in the literature. Uncertainties arise from various factors, including inaccuracy, imprecision, vagueness, lack of knowledge or data, randomness, and ignorance. Some sources of uncertainty are measurable, whereas others are not; some sources are manageable and others are not, and so on. In addition, certainty in a real-world system is vastly less than uncertainty in the same system. Therefore, the literature shows numerous attempts to research uncertainty reduction in both real world and engineering systems.

Different researchers categorize uncertainty differently. Yen et al. (1971) categorized uncertainty into objective uncertainty, that which is associated with random processes, and

subjective uncertainty, or that which is related to imprecision [142]. Burges et al. (1975) classified uncertainty into Type I and Type II errors; the former of which is related to the use of an inadequate model with proper parameters, and the latter of which is related to the implementation of inadequate parameters with proper model [143]. Klir et al. (1987) categorized uncertainty into ambiguity, which is associated with one-to-many relations (situations in which the choice between two or more alternatives is left unspecified), and vagueness, which is associated with a difficulty in making sharp distinctions [144].

Among these various uncertainty categories, the most popular classification distinguishes between aleatory uncertainty and epistemic uncertainty [145, 146]. Aleatory uncertainty derives from the inherently uncertain nature and variability of basic information. Therefore, it is referred to as irreducible uncertainty, objective uncertainty, and stochastic uncertainty. When a system experiences a forced outage due to a fault, aleatory uncertainty is the most considerable uncertainty in the system. Epistemic uncertainty, on the other hand, results from imperfect knowledge. It is also called reducible uncertainty, subjective uncertainty, and state-of-knowledge uncertainty [54]. Since the majority of this thesis focuses on knowledge-based propagation and uncertainty handling, the epistemic category is most relevant here.

Given the information above, how should we resolve uncertainty in engineering systems? Researchers have developed many approaches, including mathematical approaches such as uncertainty modeling, uncertainty analysis, the importance of uncertainty, the effects of uncertainty in the system, propagation of uncertainty, risk management of uncertainty, and more. New theories currently trending are imprecise

probability theory [147], interval analysis [148, 149], evidence theory [150, 151], possibility theory [152, 153], and fuzzy set theory [154, 155].

5.2 Significance of Uncertainty in Prognostics

Prognostics attempts to predict the future state of the engineering system, which is invariably clouded by uncertainty. Uncertainty plays a significant role in prognosis; while prognosis predicts the system state, uncertainty propagates and reducing accuracy. Furthermore, the longer the prognosis performance time, the more potential for the outcome to become even more blurred, because the quantity of the uncertainty source increases proportionately and propagates uncertainty. This is the reason why long-term prognosis involves more significant uncertainty than short-term prognosis. As a clarifying point, in the literature, long-term prognosis also refers to multiple-step-ahead prognosis and short-term prognosis refers to one-step-ahead prognosis. In this thesis, the author assumes that the short-term prognosis has less than 10% segment of the whole degradation period, and the long-term prognosis has greater than 50% segment of the entire degradation period.In this thesis, long-term prognosis indicates that the prognostics procedure is performed anytime from right after the initial time, to the system half life period.

5.3 State-space and RUL modeling with uncertainty

Generally, a mathematical approach of system uncertainty management or RUL prediction starts from describing state spaces. In the prognosis mechanism introduction, in Chapter 4, the Hidden Markov Models were introduced. These models have a function similar to that of the state space model. Both models are based on Bayesian analysis and they have a similar feature in that they express the unobserved state of the system in terms

of numerical and mathematical representation. However, the state-space model can describe both: the hidden state of the equipment and the uncertain relationship of the states. In addition, it considers both the uncertain relationships between the latent degradation condition and the indirect degradation indicators, as well as the asset latent degradation processes. The state space model provides a comprehensive approach to RUL estimation and to the degradation process [19, 20, 21, 22].

The following mathematical representations indicate the system with nonlinear, time-variant, continuous time state-space representation:

$$\dot{x(t)} \triangleq f\big(t, x(t), \theta(t), u(t), v(t)\big),$$

$$y(t) \triangleq h\big(t,\ x(t), \theta(t), u(t), n(t)\big),$$

Where $x(t) \in \mathbb{R}^{N_x}$ is the state vector, t is the continuous time variable, $\theta(t) \in \mathbb{R}^{N_\theta}$ is the unknown parameter vector, $\mathrm{y(t)} \in \mathbb{R}^{N_y}$ is the output vector, $u(t) \in \mathbb{R}^{N_u}$ is the input vector, $v(t) \in \mathbb{R}^{N_v}$ is the process noise vector, and f is the state equation, $f\colon \mathbb{R}^{N_x} \times \mathbb{R}^{N_\theta} \times \mathbb{R}^{N_u} \times \mathbb{R}^{N_v} \to \mathbb{R}^{N_x}$, $n(t) \in \mathbb{R}^{N_n}$ is the measurement noise vector, h is the output vector, and $h\colon \mathbb{R}^{N_x} \times \mathbb{R}^{N_\theta} \times \mathbb{R}^{N_u} \times \mathbb{R}^{N_n} \to \mathbb{R}^{N_y}$. Furthermore, the energy available in the system at any moment is represented by:

$$\varepsilon(t) \triangleq \vartheta\big(t,\ x(t), \theta(t), y(t)\big),$$

Where $\varepsilon(t) \in \mathbb{R}^{N_\varepsilon}$ is the energy available at the time t, ϑ is the mapped function between system stages[23], and $\vartheta\colon \mathbb{R}^{N_x} \times \mathbb{R}^{N_\theta} \times \mathbb{R}^{N_y} \to \mathbb{R}^{N_\varepsilon}$. From the system state mode, the EOL

at the current time t_c, $EOL(t_c)$ is defined as end of time from current time (t_c) , before which point the system can no longer fulfill its requirement. It is then represented by:

$$EOL(t_c) \triangleq \inf\{t > t_c, Th(t) \in \Gamma\} \, and \, t_c < t < t_{EOL};$$

Where Γ is the failure zone that refers to the set of undesired system states and $Th(t)$ is a threshold function. In the prognosis approach, note that this state space focuses on the predicting the future and the associated uncertainty; the output equation $y(t)$ is not used in the prognosis stage, because output measurements are only available until $t = t_c$ [24] and the state of performance system lies outside the desired region of acceptable states. The desired state is expected through a set of constraints, $S_{desired} \triangleq \{c_i\}_{i=1}^{N_c}$, where c_i is a function c_i: $\mathbb{R}^{N_x} \times \mathbb{R}^{N_\theta} \rightarrow \mathcal{B}$ that maps a given point in the joint space parameter given the current inputs $\big(x(t), \theta(t), u(t)\big)$, to the Boolean domain $B \triangleq [0,1], where$ $c_i\big(x(t), \theta(t), u(t)\big) = 1$ if the state of the performance system lies outside of the desired region, otherwise zero [25]. The RUL is expressed as

$$RUL(t_c) \triangleq EOL(t_c) - t_c$$

From the above expression $RUL(t_c)$, it is clear that RUL depends on the following: (1) present time; (2) present state; (3) parameter; (4) future loading; and (5) process noise. Since these variables are random, $RUL(t_c)$ is also random at any prediction time. The variables $v(t)$ and $u(t)$ are never known exactly on the range $t_c < t < t_{EOL}$, and the system evolution is randomly processed; thus, uncertainty is inherent to the RUL estimation and it cannot be avoided in the prognostics approach. The prediction of RUL is affected by several sources of uncertainty, such as measurement error, modeling error, loading

uncertainty, and so on. It is important to accurately account for these sources of uncertainty during the RUL procedure.

5.4 Mathematical Approaches of Uncertainty

Many researchers express uncertainty through mathematical formulas; this refers to uncertainty quantification. One of the uncertainty quantification methods suggests using different approaches via the aleatory and epistemic uncertainty classifications. This method includes probability-based methods (section 5.4.1), possibility-based methods (section 5.4.2), and evidence theory methods (section 5.4.3). The probability-based methods are widely used for modeling aleatory uncertainty; possibility-based methods are used for modelling epistemic uncertainty; and evidence theory is used to cover both types of uncertainty [156].

Probability theory: This is one of the traditional tools used to express uncertainty. In probability theory, random variables and probability measures are used to represent a magnitude of uncertainty, such that the uncertainty about the occurrence of an event A is represented by a P(A). Let Ω be the sample space that contains all possible outcomes X, so $X \in \Omega$. For a discrete case, $\Omega = (x_1, \cdots, x_n)$. A probability distribution function $d_X(x)$: $\Omega \rightarrow [0,1]$ exists such that $\sum_{X \in \Omega} d_X(x) = 1$. At this point, $d_X(x)$ represents the frequency of observing x after many trials. Similarly, for a continuous case, if $p_X(x)$ represents the frequency density of x, then the probability distribution function $p_X(x)$ exists such that $\int_{X \in \Omega} p_X(x)dx = 1$. For any measurable subset A of Ω called "event", the probability P(A) is:

$$Discrete\ case, P(A) = \sum_{X \in \Omega} d_X(x)$$

$$Continuous\ case, P(A) = \int_{X \in \Omega} p_X(x)dx$$

In this interpretation, the probability is defined as a fraction of the repeated number of times of an event. To take repetitions of the situation as a sample, randomness determines whether or not the event occurs. This process generates a fraction of success, P(A), and this uncertainty is sometimes referred to as aleatory uncertainty [157].

Evidence theory: This also known as Dempster-Shafer theory, proposed by Dempster (1967) and Shafter (1967). It provides a representation for uncertainty of incomplete information [158, 159]. The metrics used to measure uncertainty in this method are plausibility and the belief that is determined from known information for the proposition. In this method, the lower and upper bounds of probability are defined as a range of metrics, instead of precise probability for the proposition. The mathematical structure of evidence theory starts from defining the sample space as:

$$X = \{x: x\ is\ possible\ value\ of\ the\ uncertain\ quantity\}$$

Based on the information available concerning uncertainty quantities, a basic probability assignment can be defined as:

$$m: X \rightarrow [0,1]$$

$$m(E) \geq 0\ for\ E \subset X$$

$$\sum_{E \subset X} m(E) = 1$$

Where evidence theory defines a mass assignment function m. The focal element of the uncertain quantities is subsequently defined as:

$$X = \{E: E \subset X, m(E) > 0\}$$

The belief function, $Bel(E)$ represents the degree of belief that, based on the available evidence, indicates that a given element X belongs to B, as well as to any of subsets of B; therefore, this is the degree of belief in set B. The plausibility function, $Pl(E)$ represents the sum of the sets that intersect with the amount of all evidence that does not rule out the fact that the actual state belongs to B. The fundamental properties of the plausibility and belief functions can be defined as follows:

$$Pl(E) = \sum_{E \cap X \neq 0} m(B)\,; Bel(E) = \sum_{B \subset E} m(B)$$

$$Pl(E) + Pl(\underline{E}) \geq 1;\ Bel(E) + Bel(\underline{E}) \leq 1$$

$$Bel(E) = 1 - Pl(\underline{E});\ Pl(E) = 1 - Bel(\underline{E});$$

In evidence theory, likelihood is assigned to sets, as opposed to probability theory, in which likelihood is assigned to a probability density function [161].

Possibility theory: Classical possibility theory, as introduced by Zadeh in 1978, is based on possibility and necessity measures. The concept starts with a branch of evidence theory that deals with elements $(A_1, \cdots, A_n)$ on the power set $(P(E))$ of the universe of

discourse (Ω) and are connected as $A_1 \subset \cdots \subset A_n \in P(E)$. The plausibility belief functions are represented as a consonant body of evidence with $X, Y \in P(E)$ as follows:

$$Pl(X \cup Y) = \big(Pl(X), Pl(Y)\big); Bel(X \cap Y) = \big(Bel(x), Bel(Y)\big);$$

The consonant plausibility and belief are then referred to as possibility $Pos(\cdot)$ and necessity $Nec(\cdot)$, adapting the basic notion of numerical possibility theory with a possibility distribution (r) that expresses the degree of analysis considering the chance of event occurrence. Therefore, r provides a measure of confidence that is assigned to each element of X, where X is the set of possible values for the uncertain variable x, and subjective knowledge is modeled with the pair (X, r). At this point, $r(x) = 1$ indicates that there is no known information or occurrence and $r(x) = 0$ means that known information completely refutes the occurrence of x. So, every possibility ($Pos(Y)$) and necessity ($Nec(Y)$) is uniquely represented by association with r through the following supremum and infimum:

$$Pos(E) = sup\{r(x): x \in E\}$$

$$Nec(E) = 1 - Pos\big(\underline{E}\big) = inf\{1 - r(x)\}$$

These are brief explanations about well-known uncertainty mathematical approach methods. However, it is difficult to interpret the results from one method to another, since these methods developed from different statistical theories. In addition, as the system becomes more and more complex, the boundaries of epistemic and aleatory uncertainty become more ambiguous, and the appropriate uses for these methods become less defined [161].

5.5 Uncertainty Bounds in Prognosis Metrics

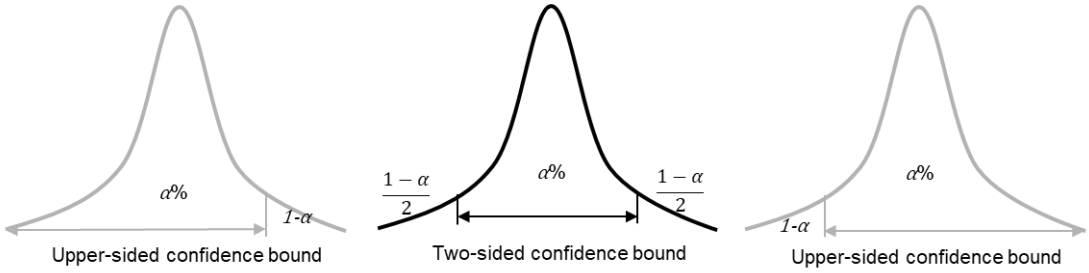

Figure 5.1 Examples of Confidence Interval

In statistics, an estimated range of values is likely to include an unknown parameter (θ) with the population mean (μ) and the sample mean ($\underline{x}$), and the estimated range is calculated from observed data given by the confidence interval (CI). This interval describes the amount of uncertainty associated with a sample estimation of the population parameter. The CI is constructed with a confidence level (α), which is the probability that the interval produced by the method employed includes the true value of the parameter. The confidence level α is expressed as the percentage chance that the unknown parameter is contained within the interval. Common choices of α are 0.99, 0.97, 0.95, and 0.90; these are also used in Matlab. This interval estimation can be classified into either the one-sided confidence bounds or the two-sided confidence bounds shown in Figure 5.1. In addition to these differences, the mathematical approach of CI for an unknown mean and a known standard deviation case, versus an unknown mean and an unknown standard deviation case are shown by the following expressions:

$$Unknown\ \mu\ and\ known\ \sigma\ case, CI = \underline{x} \pm z\frac{\sigma}{\sqrt{n}}$$

$$Unknown\ \mu\ and\ unknown\ \sigma\ case, CI = \underline{x} \pm t\frac{s}{\sqrt{n}}$$

Where z is the upper critical value for the normal distribution on the two-sided bound CI, n is the sample size, and σ is the standard deviation for the upper case when σ is known. t is the upper critical value for the t-distribution with n-1 degrees of freedom on the two-sided bound. The only two-sided confidence bound is used for the uncertainty bounds; it addresses the degree of uncertainty associated with data under a given prognosis process.

5.6 Uncertainty Management for the Long-term Prognosis

This subsection of Chapter 5 is the goal of this thesis. To summarize, as the result of the prognosis, the narrowed range of the uncertainty bounds carries more accurate and precise results. This thesis suggests how the uncertainty bound is shrunk by the methods Chapter 3 suggests. There are three steps of uncertainty management: i. Uncertainty Representation, ii. Uncertainty Propagation, and iii. Uncertainty Management. As

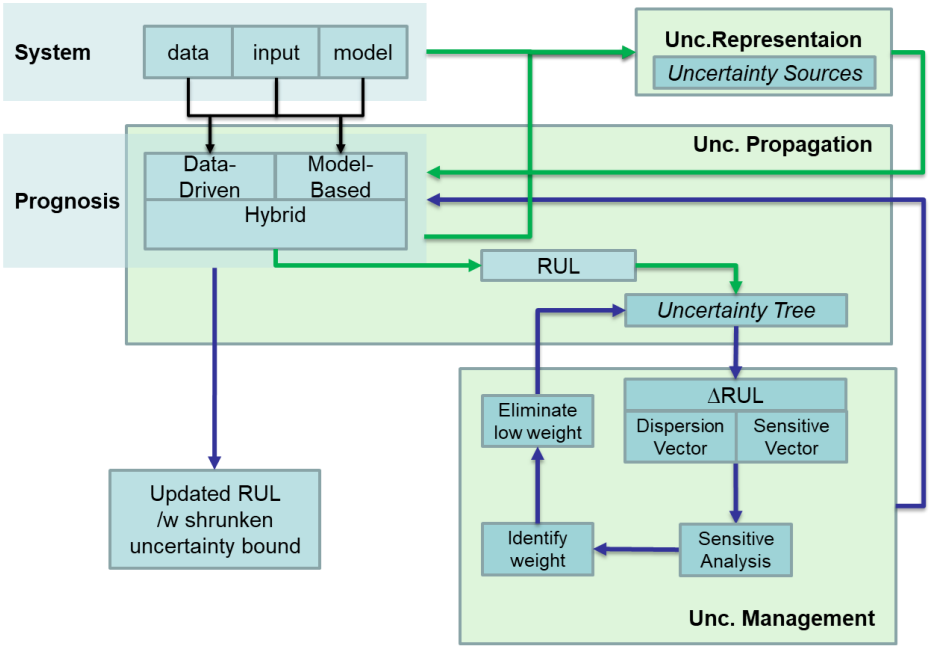

Figure 5.2 Illustration of uncertainty managing metrics in prognosis

mentioned earlier, this thesis does not distinguish between aleatory uncertainty and epistemic uncertainty.

5.6.1 Uncertainty Representation

In the engineering system, uncertainties arise from a variety of sources and at different points during the prognosis process. The first step for shrinking distribution bounds in prognosis is to recognize, characterize, and classify the sources of uncertainty in the system's RUL prognosis procedure. This is referred to as "Uncertainty Representation". At this stage, it is not important to determine the exact mathematical approach for classifying each uncertainty source in prognosis. The reason is that, as a system increases in complexity, such a mathematical approach may become meaningless if the properties of each classification are mixed together. However, there is one trend that becomes clearer over time with regards to prognosis metrics. Prognosis methods (model-based, data-driven, and hybrid methods) are all becoming more methodologically distinct and the usage of hybrid methods also increases with time. Therefore, uncertainty classification at this stage begins with "system/physical uncertainty" at the base, "data uncertainty" as the next layer, and "model uncertainty" as the top layer [97, 162]. Such a taxonomy makes it easy to model where the uncertainty occurs from the system and the prognosis. For example, model-based methods focus more on the model uncertainty layer, and data-driven methods focus more on the data uncertainty layer. Figure 5.3 shows a general illustration of engineering system uncertainty classification in the prognosis. The top three classifications of system/physical uncertainty, data uncertainty, and model uncertainty remain more or less unchanged, but the remainder of the linked branches from these top layers may be added to or skipped

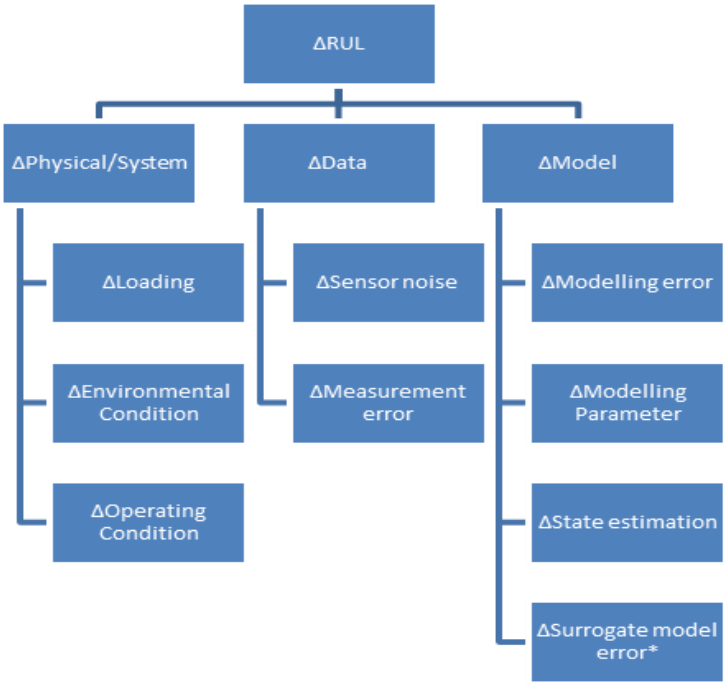

Figure 5.3 Taxonomy of the sources of uncertainty in RUL prediction

over, depending on the system and prediction method. Each source of uncertainty can be described as follows:

Physical uncertainty (Δphysical) refers to the inborn variation of the physical system. Uncertainty or fluctuations can appear in the form of uncontrollable variations in the external environment, instruments, test procedures, observers, and so on. They are usually modeled as random phenomena characterized by probability distributions and they require large amounts of information [26]. The physical variability in the loading (Δload), the environmental condition (Δe.c.) and the operation condition of the load (Δo.c.) is considered during this proposed research. The variability in other physical properties is insignificantly small, and thus is not considered to be human error or physical measurement error.

Another type of uncertainty is data uncertainty (Δdata). Acquired data can contain outliers, errors, or simply have missing data. In addition, the probability distributions of some technical properties of energy systems are inferred using data from laboratory experiments [27]. The measurement error (Δm.e.), sensor noise (Δs.n.) and sparse noise (Δsparse) are the sources of Δdata.

Model uncertainty (Δmodel) refers to the difference between the true variable and the predicted variable that can neither be measured accurately nor already be known, and comprises several parts such as modeling error (Δm.e.), model parameter (Δm.p), state estimation (Δs.e.), operation condition (Δo.c.), and surrogate model uncertainty (Δs.u.). The state model cannot be perfect, because equations and numbers cannot completely explain system phenomena Therefore, the prognosis will have to account for the model uncertainty. Any remaining unidentified or uncategorized uncertainty in the system during prognostics is called *unclassified uncertainty* (Δunclassified). This thesis assumes that the uncertainty source has an insignificant effect on the prognostics, neglectable during procedure, and without regard to dependent or independent sources.

5.6.2 Uncertainty Propagation

Figure 5.4 below illustrates traditional uncertainty propagation, determined by mapping input structures to output structures after using mathematical quantification to classify the uncertainty. Mapping is commonly done by random sampling or analytical methodology, such as using the Monte Carlo simulation methods or the probabilistic fuzzy approach. For this reason, many researchers place this propagation stage right after the

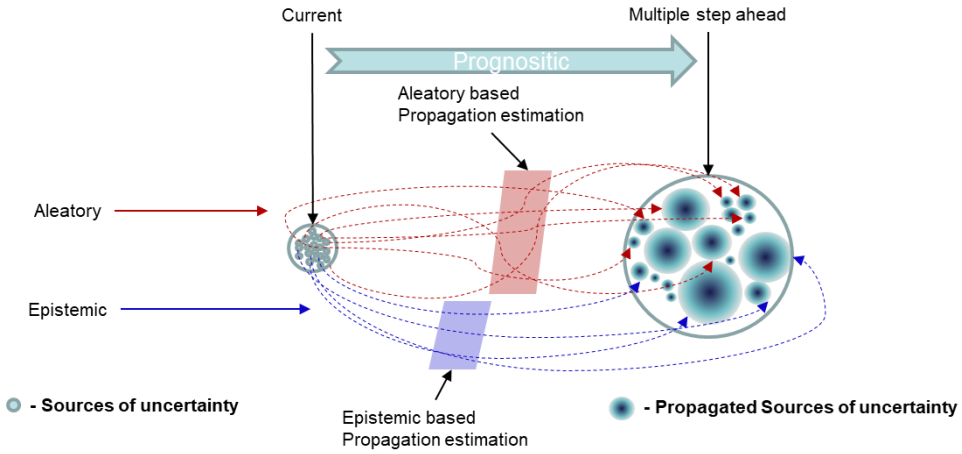

Figure 5.4 Traditional uncertainty propagation

uncertainty quantification step. In past decades, the most common uncertainty propagation considers the mathematical function given by:

$$Y = \gamma(X_1, X_2, \cdots, X_l, X_{l+1}, \cdots, X_m, \cdots, X_n) \tag{5.1}$$

Where X is the input, Y is the output, γ is the mapping model, the source of uncertainty from each input is $f_{X_i}(x_i)$ or $\pi_{X_i}(x_i)$, and all inputs may be expressed with the joint pdf of each source as $f_X(x)$. The n number of variables as inputs to X and $(X_1, X_2, \cdots, X_l)$ are affected purely by epistemic uncertainty and $(X_{l+1}, \cdots, X_m, \cdots, X_n)$ is affected purely by aleatory uncertainty. The epistemic uncertainties can be described by probability distributions as $f_{X_1}(x_1), f_{X_2}(x_2), \cdots, f_{X_l}(x_l)$; aleatory uncertainties, however, are described by possibility distributions as $\pi_{X_1}(x_{l+1}), \cdots, \pi_{X_m}(x_m), \cdots, \pi_{X_n}(x_n)$. The possibility distributions can be described in terms of α-cuts at vertical levels α. In other words, set α to zero for the initial setup, then select the α-cuts $A_\alpha^{x_{l+1}}, \cdots, A_\alpha^{x_m}, \cdots, A_\alpha^{x_n}$ of the possibility distributions $\pi_{X_1}(x_{l+1}), \cdots, \pi_{X_m}(x_m), \cdots, \pi_{X_n}(x_n)$. Next, calculate the smallest and largest values of $\gamma(X_{l+1}, \cdots, X_m, \cdots, X_n)$ as lower and upper limits then when α is 1, and input the

selected distribution to the probability distribution [163]. These total uncertainties on inputs may be expressed in terms of the joint probability density function:

$$f_X(x) = \int \cdots \int f(x_1, \cdots, x_n)\, dx_1, \cdots, dx_n \tag{5.2}$$

The goal of the uncertainty propagation stage is to compute uncertainty in the output of Y, in terms of $f_Y(y)$ or $F_Y(y)$, as either the CDF, or the PDF of output as follows:

$$f_Y(y) = \int f_Y(y|x) f_X(x)\, dx \tag{5.3}$$

$$F_Y(y) = \int_{\gamma(X)<y} f_X(x)\, dx \tag{5.4}$$

The three common methods for solving these equations are 1) sampling-based methods; 2) analytical methods; and 3) surrogate methods. The Monte Carlo and fuzzy methods are

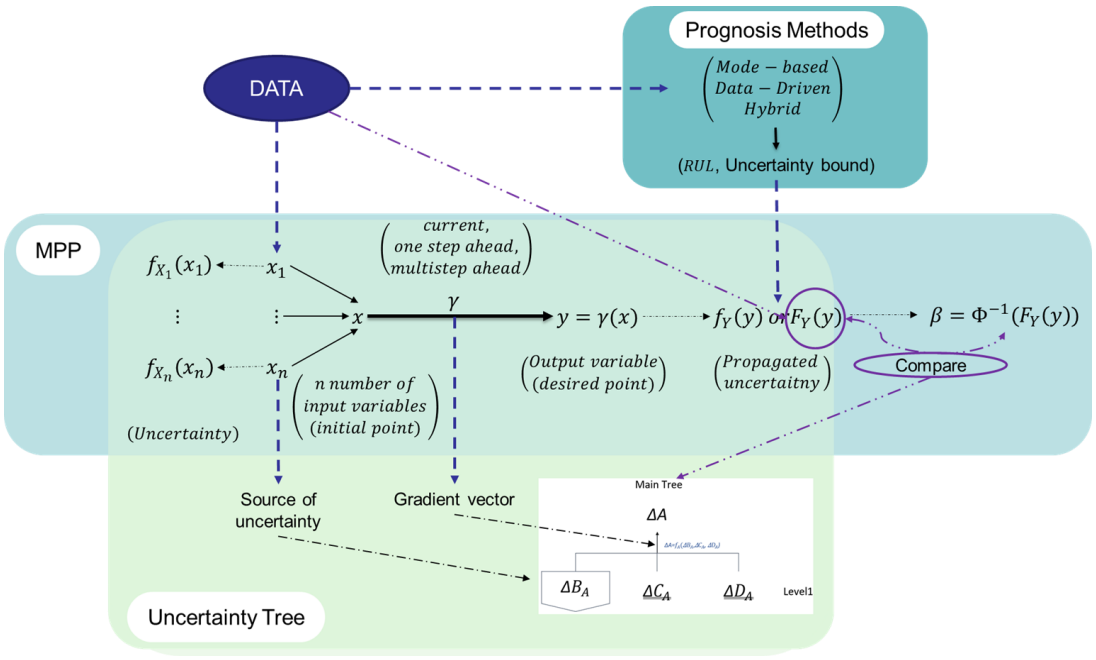

Figure 5.5 Uncertainty propagation stage illustration

sampling-based methods. Interval analysis and the evidence approach belong to the analytical method. Regression, chaos expansion, and the most probable point methods are classified as surrogate methods. The sampling-based method may require several thousand samples. It is time-consuming and costly. The analytical method is not readily suitable to account for all types of uncertainty in prognosis. In addition, both methods are not well-suited to classifying propagated uncertainty sources. Therefore, all sources are considered reducible uncertainty, which affects the input variables $(X_1, \cdots, X_n)$. In addition, the model whose output is the function $Y = \gamma(X_1, X_2, \cdots, X_l, X_{l+1}, \cdots, X_m, \cdots, X_n)$ has n number of uncertainty sources $(\Delta x_1, \cdots, \Delta x_n)$ that can be described by the probability distributions as $f_{X_1}(x_1), \cdots, f_{X_n}(x_n)$ without the possibility distribution handling loop. For common sources of uncertainty from the uncertainty representation step, use input variables $X_1, X_2, \cdots, X_n$. This research utilizes the Most Probable Point (MPP) method for propagation estimation because, although it has less accurate propagation results, it classifies each propagation during transformation via a gradient vector, which, as this thesis will show, will be very useful in the final procedure.

5.6.2.1 Uncertainty Tree

Dr. Jon P. Longtin suggested the uncertainty tree concept in 2002. The uncertainty tree represents a graphical depiction of the variable, with the desired uncertainty at the top of tree. It indicates dependence in handling uncertainty. This is an effective tool to properly account for showing the flow of uncertainty from the input to the output variables via a hierarchical structure in prognostic computational models. This tree grows downward. The most desired uncertainty

source is located at the top of the tree. t Each uncertainty sources upon which the top source depends is listed at descending sublevels, until every branch is eventually terminated. After that, each branch is connected via a functional uncertainty relationship. Figure 5.6 illustrates an example of the uncertainty tree

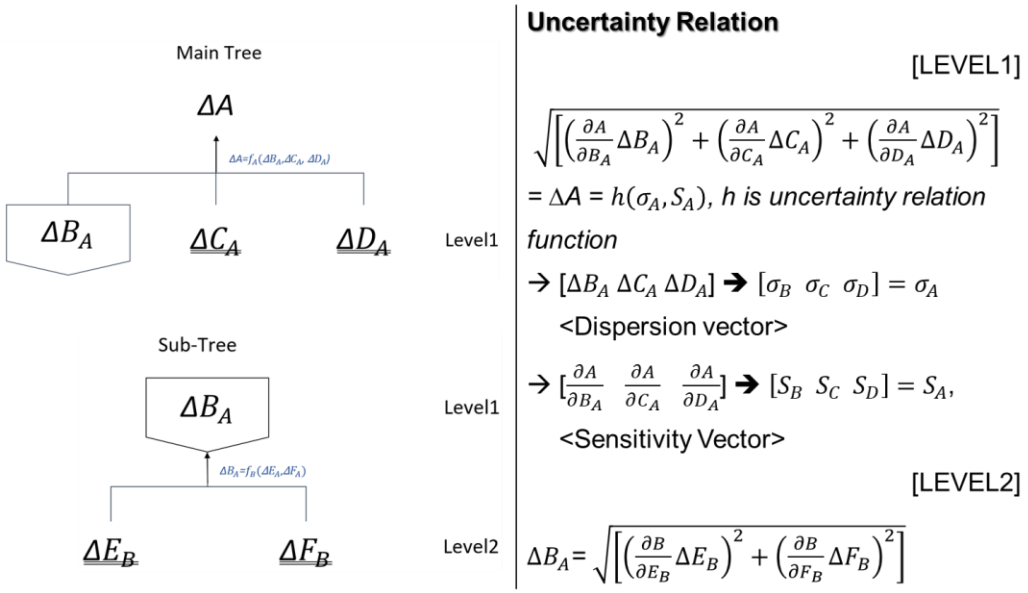

Figure 5.6 Example of the uncertainty tree and uncertainty relation equation

with the uncertainty relationship expressed in the prognosis metrics. In order to replicate an uncertainty tree, first, place the desired variable at the top of the tree. Below, list all uncertainty sources that contribute to the desired variable. Repeat this process until known variables with uncertainty are located at the end of each branch. The terminal variable should have a double underline to signify that it is terminated. Finally, desired uncertainty is determined simply by descending the tree one level at a time, until every branch of the tree is terminated with a variable of known uncertainty. In addition, each source of uncertainty within the same branch can be expressed by the uncertainty relation equation *(h),* which refers to a general law of uncertainty propagation [29] with the dispersion vector *(σ)* and the

gradient/sensitivity vector *(S)*. The MPP method derives from the gradient vector, based upon the dispersion and. Thus, propagated uncertainty can be written as:

$$\Delta A = \sqrt{\left[\left(\frac{\partial A}{\partial B_A}\frac{\partial B}{\partial E_B}\Delta E_B\right)^2 + \left(\frac{\partial A}{\partial B_A}\frac{\partial B}{\partial F_B}\Delta F_B\right)^2 + \left(\frac{\partial A}{\partial C_A}\Delta C_A\right)^2 + \left(\frac{\partial A}{\partial D_A}\Delta D_A\right)^2\right]} \quad (5.5)$$

Each branch shows the mathematical relationship, such as f_A and f_B in Figure 5.5.

5.6.2.2 Most Probable Point (MPP)

As previously mentioned, the MPP method is one of the most popular uncertainty or reliability analysis methods. In this method, fandom input variables are transformed into Gaussian variables, using a standard normal transformation. They are then linearized using Taylor's series expansion [164]. Figure 5.7 shows a general illustration of MPP estimation with both first- and second-order reliability. In this thesis, MPP is used for uncertainty propagation in the RUL prognostics. As mentioned, the goal of this stage is to compute uncertainty from the equation (5.1) based on output (Y) from input uncertainty (X). In other words, we compute the probability distribution function, or cumulative distribution, of the output (Y) with

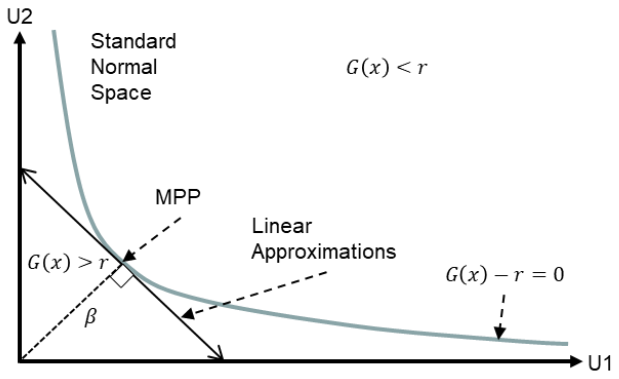

Figure 5.7 Illustration of the most probable point

respect to the probability distribution (X). In this computation, the propagation model (γ) cannot be linear; so, the MPP method is needed to compute the gradient vector of the uncertainty in (Y) in terms of the pdf of $f_Y(y)$ via transformation and linearization in the RUL prognosis [48]. The MPP method requires that the limited-state function $Z(x)$ be defined as greater or less than zero:

$$Z(x) = Y - c = \gamma(x) - c \tag{5.5}$$

Where c is constant, Y comes from equation (5.1), and X is the number of input variables $\{x_1, x_2, \cdots, x_n\}$. These input variables are transformed into the standard normal space $u = \{u_1, u_2, \cdots, u_n\}$ via the Rosenblatt equation:

$$u_i = \Phi^{-1}[F_i(x_i)], with\ (i = 1, \cdots, n) \tag{5.6}$$

Where Φ^{-1} refers to the inverse of the standard normal distribution function [165]. After this step, the limited-state function can be rewritten as u pace based as $Z(u) = \gamma(u) - c$ with a minimization equality constraint $\beta = \|u\|$. To summarize, compute the gradient vector while finding the shortest distance from the origin to the limited-state surface equation. Graphically speaking, the MPP is the tangential point of the surface of the limited state and the shortest-distance vector from the origin β in the normal (u) space. This tangential point overlaps with the gradient vector of the function $\Delta\gamma(u) = \left\{\frac{\partial\gamma}{\partial x_1}, \frac{\partial\gamma}{\partial x_2}, \cdots, \frac{\partial\gamma}{\partial x_n}\right\}$ [166]. This gradient vector becomes the key for comparison of the changing length of the CI with respect to a changing β on the CDF of Y. This gradient vector, in the form of a partial derivative, only results from a state-space model prognosis with physical

mathematical source variable handling. If data-driven methods are used for prognosis, use a gradient vector proportional to the CIS rate. At this stage, the problem with developing the uncertainty tree in the prognosis is that the dispersion and sensitivity vector equations described above cannot be implemented with pure numbers. Therefore, empirical data must be utilized to replace these variables via this MPP with the CI from the comparison of β based on a changing CDF.

These uncertainty propagation procedures can be applied to the RUL prognosis case in the following order. First, the identified and classified source of uncertainty can be used for input variables in equation (5.1) as follows:

$$\Delta RUL = \gamma_{RUL}(\Delta phys_{RUL}, \Delta data_{RUL}, \Delta model_{RUL}) \tag{5.7}$$

$$\Delta phys_{RUL} = \gamma_{phys}(\Delta load_{phys}) \tag{5.8}$$

$$\Delta load_{phys} = \gamma_{load}(\Delta ec_{load}, \Delta oc_{load}) \tag{5.9}$$

$$\Delta data_{RUL} = \gamma_{data}(\Delta sn_{data}, \Delta sd_{data}, \Delta me_{data}) \tag{5.10}$$

$$\Delta model_{RUL} = \gamma_{model}(\Delta mp_{model}, \Delta se_{model}, \Delta oc_{model}) \tag{5.11}$$

Where each $\Delta phys_{\Delta RUL}, \Delta data_{\Delta RUL}, and\ \Delta model_{\Delta RUL}$ refers to the total physical/system uncertainty, data uncertainty and model uncertainty on the RUL prognosis. ΔRUL is accumulated uncertainty after RUL prognosis in the engineering system as the output. Other uncertainty sources ($\Delta mp_{model}, \Delta se_{model}, \Delta oc_{model}, \Delta ec_{phys}, \Delta oc_{phys}, \Delta lo_{phys},$

$\Delta ec_{phys}, \Delta oc_{phys}, \Delta lo_{phys}$) refers to the input variables $(x_1, x_2, \cdots, x_n)$ in the equation (5.1). The ΔRUL can then be rewritten as:

$$\Delta\text{RUL} = \gamma_{RUL}\begin{pmatrix} \gamma_{phys}(\Delta ec_{phys}, \Delta oc_{phys}, \Delta lo_{phys}), \\ \gamma_{data}(\Delta sn_{data}, \Delta sd_{data}, \Delta me_{data}), \\ \gamma_{model}(\Delta mp_{model}, \Delta se_{model}, \Delta oc_{model}) \end{pmatrix} \quad (5.12)$$

The goal of the uncertainty propagation stage in the RUL prognosis is to compute the uncertainty of output Y in terms of $f_{RUL}(RUL)$ or $F_{RUL}(RUL)$ as the CDF, or to compute the uncertainty as the PDF output as follows:

$$f_{\text{RUL}}(\Delta\text{RUL}) = \int \gamma_{RUL}(\Delta\text{RUL}|\Delta phys_{\text{RUL}}, \Delta data_{\text{RUL}}, \Delta model_{\text{RUL}})\gamma_{RUL}(\Delta\text{RUL})\, dx \quad (5.13)$$

$$F_{\text{RUL}}(\Delta\text{RUL}) = \int_{\gamma(\Delta\text{RUL})<y} f_{\text{RUL}}(\Delta\text{RUL})\, dx \quad (5.14)$$

Based upon the above calculations, both the CDF and PDF of the RUL can be calculated from prognosis methods, such as via model-based methods, data-driven methods, or hybrid methods, as uncertainty bounds of the confidence interval. From this CDF, $F_{RUL}(RUL)$, the reference of β, $\beta_{reference}$, is estimated via the equation shown in Figure 5.6 of the MPP method. In addition, the gradient vectors, $\langle \frac{\partial RUL}{\partial phys_{RUL}}, \frac{\partial RUL}{\partial data_{\Delta RUL}}, \frac{\partial RUL}{\partial model_{RUL}}, \cdots \rangle$ also can be estimated while in transformation to the standard normal space. These gradient vectors adapt to the uncertainty relation equation in the uncertainty tree. Subsequently, the uncertainty tree of the RUL prognosis can be drawn as shown in Figure 5.6. This tree shows dependency and linkages between each source, and will be used at the management step for impactor estimation. The tree also shows the connected adjacent levels via functional relations as follows:

[1st level of main tree]

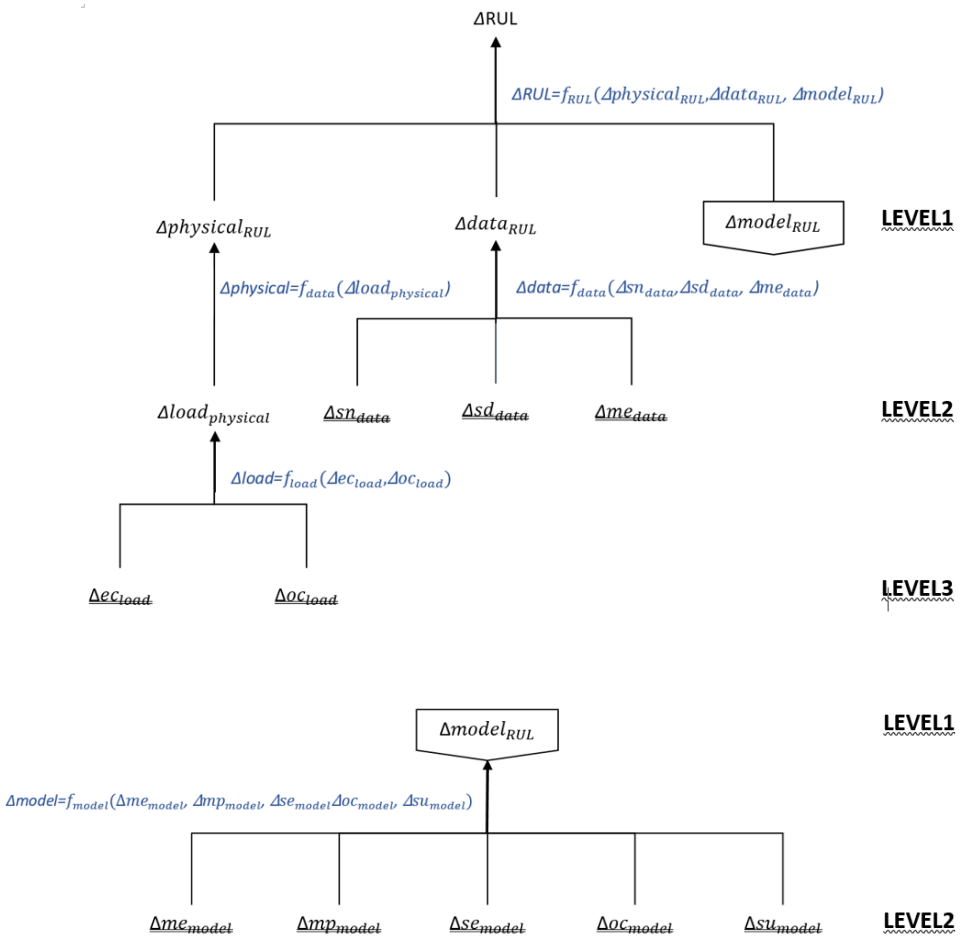

Figure 5.8 General schematics of the RUL uncertainty tree

$$\Delta RUL = \gamma_{RUL}(\Delta phys_{RUL}, \Delta data_{RUL}, \Delta model_{RUL})$$

$$= \left[\left(\frac{\partial RUL}{\partial phys_{RUL}}\Delta phys_{RUL}\right)^2 + \left(\frac{\partial RUL}{\partial data_{\Delta RUL}}\Delta data_{RUL}\right)^2 + \left(\frac{\partial RUL}{\partial model_{RUL}}\Delta model_{RUL}\right)^2\right]^{\frac{1}{2}}$$

[2nd level of main tree]

$$\Delta data_{RUL} = \gamma_{data}(\Delta sn_{data}, \Delta sd_{data}, \Delta me_{data})$$

$$= \left[\left(\frac{\partial data_{RUL}}{\partial sn_{data}}\Delta sn_{data}\right)^2 + \left(\frac{\partial data_{RUL}}{\partial sd_{data}}\Delta sd_{data}\right)^2 + \left(\frac{\partial data_{RUL}}{\partial me_{data}}\Delta me_{data}\right)^2\right]^{\frac{1}{2}}$$

$$\Delta phys_{RUL} = \gamma_{phys}(\Delta load_{phys}) = \frac{\partial phys_{RUL}}{\partial load_{phys}} \Delta load_{phys}$$

[2nd level of sub tree]

$$\Delta model_{RUL} = \gamma_{model}(\Delta mp_{model}, \Delta se_{model}, \Delta oc_{model})$$

$$= \left[\left(\frac{\partial model_{RUL}}{\partial mp_{model}} \Delta mp_{model} \right)^2 + \left(\frac{\partial model_{RUL}}{\partial se_{model}} \Delta se_{model} \right)^2 + \left(\frac{\partial model_{RUL}}{\partial oc_{model}} \Delta oc_{model} \right)^2 \right]^{\frac{1}{2}}$$

[3nd level of sub tree]

$$\Delta load_{phys} = \gamma_{load}(\Delta ec_{load}, \Delta oc_{load})$$

$$= \left[\left(\frac{\partial load_{phys}}{\partial ec_{load}} \Delta ec_{load} \right)^2 + \left(\frac{\partial load_{phys}}{\partial oc_{load}} \Delta oc_{load} \right)^2 \right]^{\frac{1}{2}}$$

At the end, the uncertainty relation equation can be re-written as:

$$\Delta RUL = \sqrt{\begin{bmatrix} \left(\frac{\partial RUL}{\partial physical_{RUL}} \frac{\partial physical}{\partial load_{physical}} \frac{\partial load}{\partial ec_{load}} \Delta ec_{load} \right)^2 + \left(\frac{\partial RUL}{\partial physical_{RUL}} \frac{\partial physical}{\partial load_{physical}} \frac{\partial load}{\partial oc_{load}} \Delta oc_{load} \right)^2 \\ + \left(\frac{\partial RUL}{\partial data_{RUL}} \frac{\partial data}{\partial sn_{data}} \Delta sn_{data} \right)^2 + \left(\frac{\partial RUL}{\partial data_{RUL}} \frac{\partial data}{\partial sd_{data}} \Delta sd_{data} \right)^2 + \left(\frac{\partial RUL}{\partial data_{RUL}} \frac{\partial data}{\partial me_{data}} \Delta me_{data} \right)^2 \\ + \left(\frac{\partial RUL}{\partial model_{RUL}} \frac{\partial model}{\partial me_{model}} \Delta me_{model} \right)^2 + \left(\frac{\partial RUL}{\partial model_{RUL}} \frac{\partial model}{\partial mp_{model}} \Delta mp_{model} \right)^2 \\ + \left(\frac{\partial RUL}{\partial model_{RUL}} \frac{\partial model}{\partial se_{model}} \Delta se_{model} \right)^2 + \left(\frac{\partial RUL}{\partial model_{RUL}} \frac{\partial model}{\partial oc_{model}} \Delta oc_{model} \right)^2 \\ + \left(\frac{\partial RUL}{\partial model_{RUL}} \frac{\partial model}{\partial su_{model}} \Delta su_{model} \right)^2 \end{bmatrix}}$$

In reality, it is only possible to determine the gradient vector of each source's variable when a physical-based system model is used for state estimatation, as opposed to

model-based prognosis methods. The gradient vector cannot exist with a form of the partial derivative; so, the confidence interval sensitivity (CIS) for the gradient vector will be:

$$\gamma(u) = \left\{\frac{CIS\gamma}{CISx_1}, \frac{CIS\gamma}{CISx_2}, \cdots, \frac{CIS\gamma}{CISx_n}\right\}$$

$$CI\gamma = \left(\hat{\gamma} - \alpha\sqrt{var(\gamma)}, \hat{\gamma} + \alpha\sqrt{var(\gamma)}\right); CIS\gamma = 2\alpha\sqrt{var(\gamma)}$$

This mathematical form will compare the gradient role in MPP to the CDF of γ and will calculate $\Delta\beta = \|\beta_i\| - \beta_{reference}$. It is impossible to determine each source's propagation with a single number via any mathematical formula; however, it is possible to show how each source of uncertainty affects all uncertainty at the end of propagation using the gradient and sensitivity vector probability. The MPP model advocates focusing on the CDF value to solve for the whole [167]. Finally, the uncertainty tree, the uncertainty relationship equation, the gradient/sensitivity vector, and β values are ready to proceed to the next stage through the suggested uncertainty propagation.

5.6.3 Uncertainty Management

The last step in this procedure is the uncertainty management stage. The key of this stage is to estimate the importance of the uncertainty sources in the prediction process via sensitivity analysis, then to simplify the uncertainty tree with high-impact sources only. This is referred to finding the 'source impactor' from the gradient vectors and $\Delta\beta$ comparisons via the sensitivity analysis from the propogation stage results. Next, regenerate the RUL prediction using the same prognosis methods that were used to estimate

the CDF and PDF of the RUL. A brief explanation follows; this stage is also depicted in Figure 5.9.

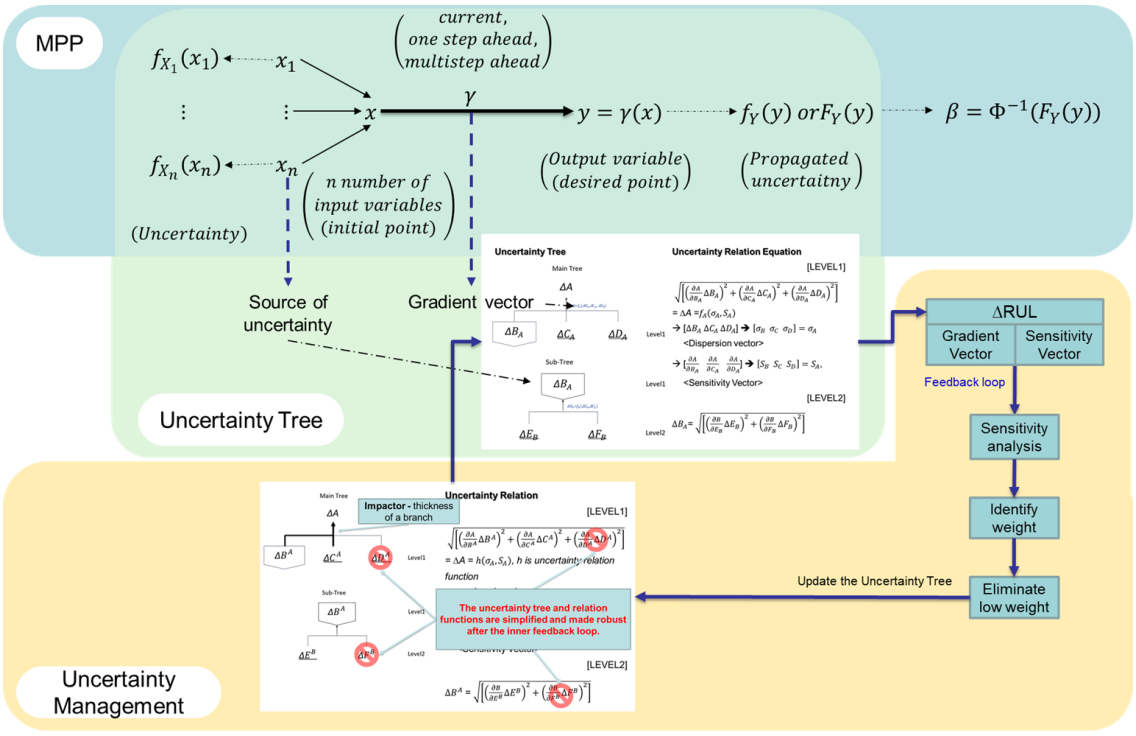

Figure 5.9 Illustration of the uncertainty management stage

5.6.3.1 Sensitivity Analysis

Generally, the sensitivity analysis represents how uncertainty in the output of the system can be apportioned to each source of uncertainty. It provides the theoretical framework and numerical tools to identify the contributions of uncertainty sources in the RUL prognosis. There are two types of sensitivity analysis methods commonly used: local sensitivity analysis and global sensitivity analysis. Global sensitivity analysis focuses on analyzing variability across the full factor space, whereas local sensitivity analysis focuses on analyzing sensitivity around some point in the factor space [98]. Generally, the global sensitivity methods, such as variance-based sensitivity [99], fit for nonlinear cases.

Otherwise, a linear case fitting the local sensitivity analysis method must be used, such as one-factor-at-a-time (OFAT). OFAT is a classical approach to deriving local sensitivity analysis. It consists of estimating, which characterizes the effect on the random value, $Y = f(X_1, X_2, \cdots, X_l)$, of perturbation on the input near the nominal value $\{X|X = (X_1, X_2, \cdots, X_l)\}$ as:

$$S_i = \frac{\partial y}{\partial X^{(i)}}\{X\} \tag{5.15}$$

This is the variable connected from the tangential point of the MPP, where it overlaps with the gradient vector of the function $\Delta\gamma(u) = \left\{\frac{\partial\gamma}{\partial x_1}, \frac{\partial\gamma}{\partial x_2}, \cdots, \frac{\partial\gamma}{\partial x_n}\right\}$. Then the sensitivity estimation can be re-written as $S_i = \Delta\gamma(u)\{X\}$ with $u_i = \Phi^{-1}[F_i(x_i)]$.

The variance-based method is another major sensitivity analysis method that decomposes output variance into parts attribution to both the input variable and the combination variables. This method was introduced by Dr. Sobol (1993); it is also referred to as the Sobol Method. The sensitivity of this method is estimated by the amount of variance in the output caused by the input [168]. Two effect estimations in this method are the first-order effect and total effects. The former estimates the contribution itself. The latter describes synthetical interaction among the input factors. These first-order sensitivity (S_{1_i}) and total effects sensitivity (S_{T_i}) estimations are written as:

$$S_{1_i} = \frac{V_i}{V} = \frac{var_{X_i}\left(E_{X_{\bar{i}}}(Y|X_i)\right)}{var(Y)} = \frac{var(X_i) - E(var(X_i|Y))}{var(Y)} \tag{5.16}$$

$$S_{T_i} = \sum_{k=i} S_k = 1 - \frac{var_{X_{\bar{i}}}\left(E_{X_i}(Y|X_{\bar{i}})\right)}{var(Y)} \tag{5.17}$$

Where $Var(Y)$ is the unconditional variance of the output, $X_{\underline{i}}$ is all factors except X_i, $Var_{X_i}\left(E_{X_{\bar{i}}}(Y|X_i)\right)$ is the variance of the conditional expectation, and $Var_{X_{\bar{i}}}\left(E_{X_i}(Y|X_{\bar{i}})\right)$is the first-order effect that does not correspond to X_i [169]. Each method has its own positive and negative properties. The indices in the Sobol method also have another attractive point than OFAT, because they quantify the effect of an input variable on the output [103]. Regardless, uncertainty sources as input variables are transformed into Gaussian variables using the standard normal transformation. They are then linearized using Taylor's series expansion via the MPP methods. In the end, the decision of which method is to be used is decided by the form of the gradient vector in the RUL prognosis.

The OFAT Method can adapt well to the RUL prognosis when the gradient vector has the mathematical form that the state model handles via model-based prognosis in the equation shown (5.15). In contrast, when the gradient vector consists of rate of confidence interval sensitivities, $\gamma(u) = \left\{\frac{CIS\gamma}{CISx_1}, \frac{CIS\gamma}{CISx_2}, \cdots, \frac{CIS\gamma}{CISx_n}\right\}$, the Sobol Method can be adapted for sensitivity estimation via CIS as:

$$CI\gamma = \left(\hat{\gamma} - \alpha\sqrt{var(\gamma)}, \hat{\gamma} + \alpha\sqrt{var(\gamma)}\right); CIS\gamma = 2\alpha\sqrt{var(\gamma)} \tag{5.18}$$

Each uncertainty source variables $(X_1, X_2, \cdots, X_l)$ are already assumed to be independent.

$$S_{1_i} = \frac{var_{X_i}\left(E_{X_{\bar{i}}}(\gamma|X_i)\right)}{var(\gamma)} = \frac{var(X_i) - E\left(var(X_i|\gamma)\right)}{var(\gamma)} = \frac{var(X_i)}{var(\gamma)} = \left(\frac{CISX_i}{CIS\gamma}\right)^2 \tag{5.19}$$

$$S_{T_i} = 1 - \frac{var_{X_{\bar{\imath}}}\left(E_{X_i}(Y|X_{\bar{\imath}})\right)}{var(Y)} = 1 - S_{1_{\bar{\imath}}} = \left(\frac{CISX_{\bar{\imath}}}{CIS\gamma}\right)^2 \quad (5.20)$$

For the resulting sensitivity estimation of both the OFAT and Sobol Methods, it is important that the sensitivity index, or first-order effect index, of a variable is high. If, instead, the total effects index of a variable is low, then that variable is of lesser consideration [83].

The results of sensitivity estimation show how uncertainty sources vary in their sensitivity in the output. The results of the sensitivity estimation are based on the percentage of each source's sensitivity and can be added to each source. This is used to simplify the uncertainty tree's focus to important sources of impact.

5.6.3.2 Updating the Uncertainty Tree

Uncertainty source variables are sorted by sensitivity after the sensitivity analysis. The key of the management stage is to focus on higher impact sources. To do so, the simplified uncertainty tree helps to make the process more intuitive. If the gap between the higher and lower sensitivity estimations is large, this thesis recommends using just higher sensitivity sources. If the gap is small, this thesis recommends choosing a higher random median or mean sensitivity estimation. Next, choose a weight based on source sensitivity. Weight can be added directly after the sensitivity estimation process but, it can be difficult to choose impact source factors from ranked numbers. Therefore, weight may be added directly after choosing impact sources based on the sensitivity estimation.

Updating the uncertainty tree is simple, as Figure 5.10 depicts. The chosen uncertainty sources that are ranked with higher impact remain in the tree and change the

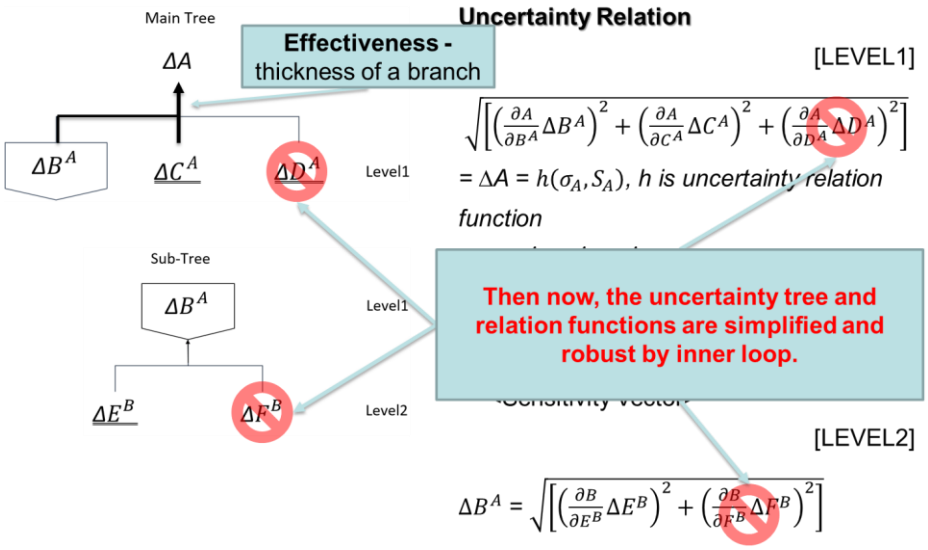

Figure 5.10 Updated Basic Uncertainty Tree

branch thicknesses. If the impact is remarkable, it is indicated by the thickest branches. In contrast, the disregarded uncertainty sources with lower impact ranking are removed from the tree and from the relational equation. Using this methodology ultimately accomplishes shrunk uncertainty bounds. Model-driven methods on prognosis therefore focus more on which model, model parameter, and state estimation variables reduce the modelling error. The weighted source variable in Matlab also can be used instead of zero or instead of the normally distributed variable that is generally used. The data-driven method on prognosis focuses more on sensitive reference data which has sensitive noise, operating conditions, and environmental conditions, than it uses a regression model to achieve shrinking uncertainty bounds. As discussed, the hybrid methods are the most beneficial, because they are based on data-driven methods with a physical model. Though uncertainty is significantly increased, it can be reduced in RUL prognosis. To paraphrase, this is similar

to having navigation guide your car: it helps you to reach your destination a little faster and to know which road to take when the familiar road is blocked through past experiences.

CHAPTER 6. CASE STUDY AND RESULT

This chapter validates uncertainty management by using an engineering system as a case study. Among many engineering systems, the energy storage system requires more precise RUL estimation in prognosis, and it is the hottest research component in the electric vehicle (EV). Nowadays, the EV is the market dominator for clean vehicles. More than half of new vehicles will likely be EVs instead of internal combustion engine vehicles by 2020 [18]. This thesis introduces this important topic through a general overview of EVs in terms of how they impact future vehicle technologies, the basic current understanding of the EV, and the life degradation of EVs. This thesis will finally discuss the RUL estimation of EV energy storage, with suggested adaptations for uncertainty handling methods via uncertainty representation, uncertainty propagation, and uncertainty management, to show sensitivity estimations of uncertainty sources. Lastly, this thesis will show shrunken uncertainty bounds in this case study to validate the theory.

6.1 About Electric Vehicles

Historically, the invention of the automobile gave immense contributions to human civilization. It increased social activity and interactions by allowing easier access to remote places; it increased economic growth and consumption; and it led to the advent of suburban society. Its many positive attributes have led the automobile to become the most popular and influential form of transportation in the world. During the past several decades, however, the automobile has also caused more negative effects than any other invention. Automobiles have led to dramatic increases in accidental death rates; air and noise pollution increases major traffic congestion and urban sprawl; and an increased use of non-

renewable fuels. Especially, scientists and consumers alike have begun to realize a connection between human-generated pollution and global warming. We have learned that the internal combustion engine (ICE) is one contributing factor. Yet, despite these shortcomings, society will not stop using ICE vehicles, because the positive effects in the short-term still outweigh the drawbacks in the long-term. Fortunately, both the automobile industry and academic researchers have been developing cars that can overcome the aforementioned drawbacks. Alternative fuel vehicles were invented as a result of these efforts. Electric, propane, methanol, and hydrogen are all used as alternative fuels that help to solve the pollution issue. Among them, the electric vehicle has become the most popular alternative fuel vehicle. Figure 6.1 shows the increase in the number of electric charging stations in 2017 since 2011. This thesis only discusses electric vehicles for the applied case study.

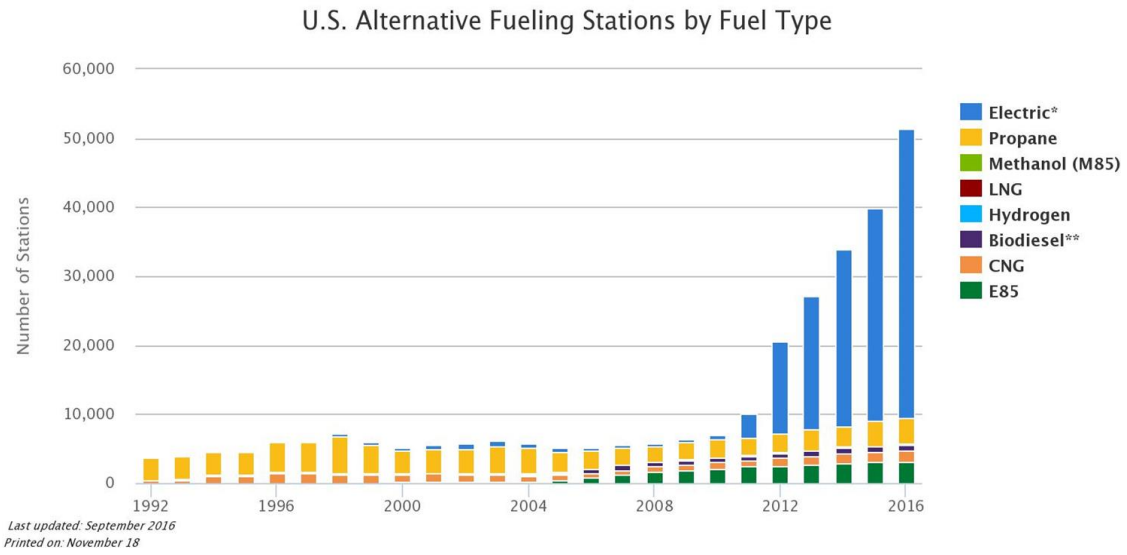

Figure 6.1 Alternative fueling station by fuel type (by U.S. Department of Energy)

The EV is a vehicle that does not use petroleum as the fuel. Rather, it uses an electric storage system and electric motors as its engines. The EV was, in fact, invented twelve

years prior to the ICE vehicle [126], but the battery is heavy, capacity is low, and the battery charging speed is slow. So, it has not been practically used until recently. More than 100 years have passed since the invention of the first electric vehicle. Researchers began to develop alternative fuel vehicles around the 1990s with better and better battery technologies Current EVs have attractive features such as no tailpipe air pollution, less

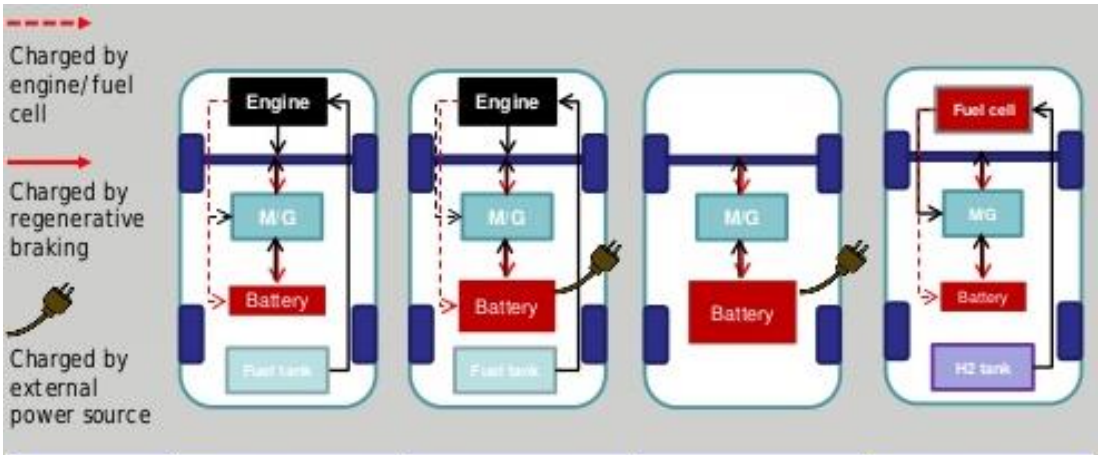

	HEV	PHEV	BEV	FCEV
Engine	Y	Y	N	Fuel cell
Regen. brake	Y	Y	Y	Y
External	N	Y	Y	N

Figure 6.2 Electric vehicle classification and overview

noise pollution than ICE vehicles, reduced carbon dioxide emissions, high-efficiency components, quiet and smooth operation due to fewer vibrating components, low recharge and maintenance costs, and government tax credits. In addition, one well-known electric vehicle company, Tesla Motors, is growing rapidly and receiving a constant media spotlight. These phenomena grab consumers' attention and accelerate the place of EVs in the market. However, the EV is not perfect yet. It has several negative properties such as a battery safety issue, an improved but still shorter driving range compared to ICE vehicles,

and a limited number of charging stations available. Fortunately, these negatives are well-known and solutions are under research. In addition, many governments have set goals to cut carbon dioxide emissions annually, and some are planning to ban sales and manufacturing of ICE vehicle in the near future. Commonly, EVs can be classified into hybrid electric vehicles (HEVs), plug-in hybrid electric vehicles (PHEVs), fuel cell electric vehicles (FCEVs), and (pure) battery electric vehicles (BEVs). HEVs are powered by an electric motor that uses energy stored in an energy storage system as well as an ICE. HEVs do not have a plug for battery charging because they are charged by an ICE or by regenerative braking. Therefore, battery packs do not need to be large. PHEVs are similar to HEVs because they also combine an electric tractive system with an ICE. The difference is that PHEVs can be plugged into the electric grid for charging. They can still be charged by an ICE or by regenerative braking, but their charging efficiency is lower than that of BEVs, which obtain their charge solely from the electric grid and are the purest form of EV. FSEVs in contrast, do not have an ICE or plugs for battery charging. However, they have a fuel cell system to generate electricity and thereby charge their battery packs. Generally, hydrogen is used for the fuel, and water is generated instead of carbon dioxide in the tailpipe. Therefore, FSEVs have zero emissions, long range, and short refueling time. However, a limited number of manufacturers are considering this vehicle, so the number of hydrogen charging stations are limited. In this paper, EVs only refer to the (pure) battery electric vehicles (BEVs).

6.2 EVES

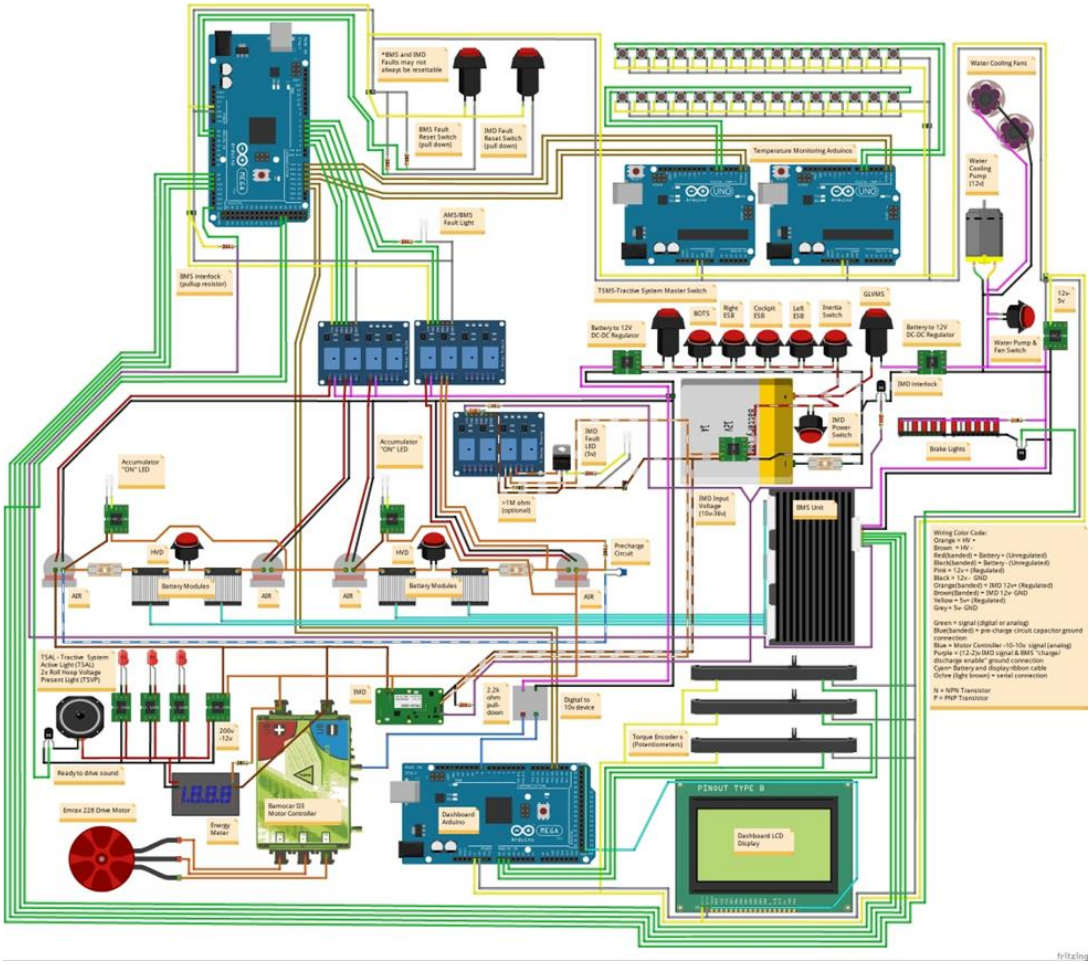

Figure 6.3 Example of EV configuration – academic level

The Electric Vehicle Energy System (EVES) architecture is illustrated in Figure 6.3, which was for academic purposes designed, built, and modified for a Formula SAE competition in 2015. As was mentioned previously, EVs comprise fewer parts than ICE vehicles. They have an electric control unit, an on/off board charger, a battery management system (BMS), a high-voltage energy storage system, batteries for low voltage, a DC converter, a power inverter, and a motor as the main components. Figure 6.4 shows both the high- and low-voltage systems. The high-voltage subsystem (also known as the tractive or energy system) and its components comprise a charger, an HV battery, a power inverter, and a motor. Voltages in the HV system increase with respect to the number of battery

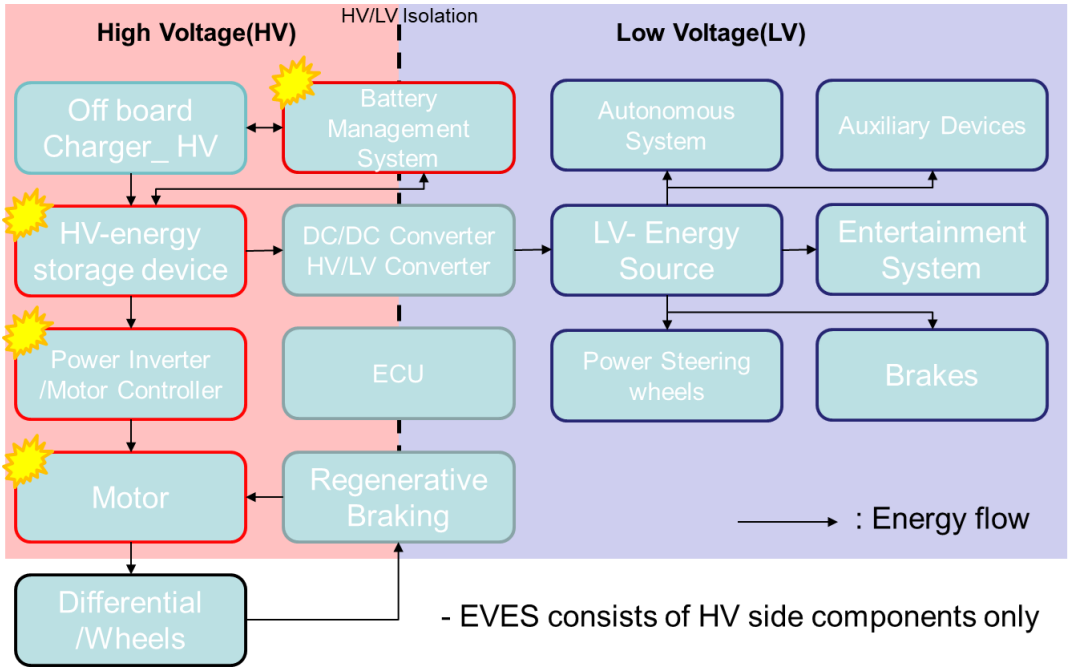

Figure 6.4 Electric systems in the electric vehicle (HV/LV)

packs, which typically start at 300V. For example, according to the Tesla Model-S datasheet, Tesla has nine bricks and 11 modules of NCR18650 battery cell in the Model S, so its high-voltage system covers around 356.4V from 9 $bricks * 3.6V * 11\ modules$. The low-voltage subsystem is similar to an ICE. It is generally 12 ~ 24 volts and handles any other electric devices, except tractive-related components. Among these subsystems and components, the energy system, motor controller/power inverter, and motor comprise

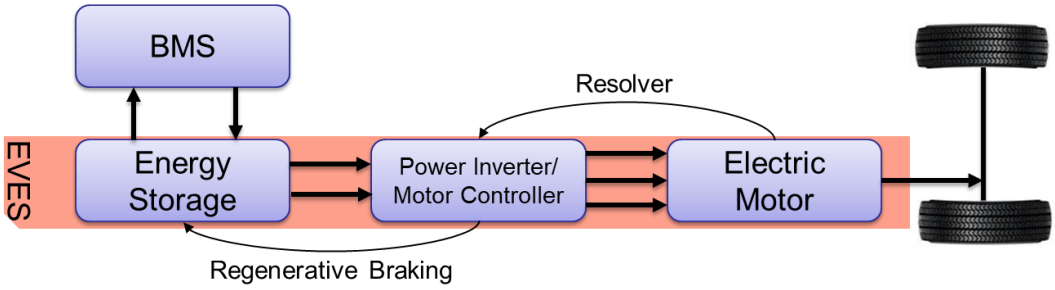

Figure 6.5 Electric Vehicle Energy System (EVES) configuration

the primary electric vehicle powertrain, which together is called the EVES as illustrated in Figure 6.5. This system does the same function as an engine in the ICE and is the most important part of propulsion.

6.3 Life Degradation of EVES

In the EVES subsystem, the motor components significantly degrade with time and operating stress. Electrical insulation weakens over time with exposure to the high temperature, voltage unbalance, over voltage, and voltage disturbance. The lubricant also weakens from high temperature and contamination. Dirt, moisture, and corrosive fumes also affect the motor's performance degradation. According to the United States Department of Energy, the life of the motor may last over 40,000 hours and it lasts much longer with a conscientious maintenance plan [127]. The motor controller and power inverter each have a similar life expectancy. Battery issues are mainly caused by chemical and/or mechanical problems. Many chemical degradation factors are only known from estimation or bias measurement results. For example, battery capacity can only be estimated via state-of-charge (SOC) that is defined as the available capacity and expressed as a percentage of its rated capacity. The depth of discharge (DOD) is the inverse of SOC.

$$SOC = \frac{C_{releasable}}{C_{rated}} * 100\%;\ DOD = \frac{C_{rated}}{C_{releasable}} * 100\%;$$

Where C_{rated} is rated capacity from the battery datasheet and $C_{releasable}$ is releasable capacity when the battery is completely discharged. In general, there are four methods to estimate SOC indirectly. Voltage methods convert battery voltage measurements to SOC using a discharge curve that determined from empirical data or open circuit voltage (OCV). Coulomb counting methods estimate SOC by integrating the measured battery current in time. The last method is the hybrid approach that estimates SOC via the combined voltage

method and current integration for better SOC estimation [130]. It is worth noting that chemical material more easily changes its property than metal which affects deterioration and failure. Therefore, the battery life degradation should be considered more thoroughly than any other part in the EVES.

In general, the battery case, performance and life deteriorate over time, whether the battery used or not. Degradation with usage is defined as 'cycle fade' and unused battery degradation is defined as 'calendar fade' [40,46], as shown in Figure 6.6. The former, battery cycle fade, is defined as the number of charging and discharging cycles completed until battery capacity reaches the soft failure threshold. According to K. Smith (2009) et al., typically time (t) and the number of charge-discharge cycles (N) are dependent, and often correlated log function with N by change of the depth of discharge (DOD) or log function of DOD, and the cycling fade is poorly understood by its wide condition factors [129]. Calendar fade is defined as the total elapsed period until battery capacity reaches the soft failure threshold, whether it is in active or inactive usage. In the inactive usage condition, temperature and time are the main factors and are mathematically dependent, as

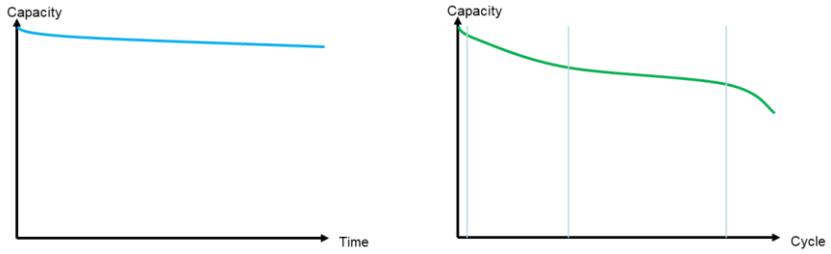

Figure 6.6 Calendar based (inactive) vs Cycle based (exercised) degradation

shown by K. Smith. Typically, this fade has $\sqrt{t}$ time dependency. This time dependency can be described by the Arrhenius relationship. It is described as the rate at which a chemical reaction proceeds and doubles for every degree increase in temperature. This

description can be applied to the rate at which the slow deterioration of active chemicals increases. In the active case, both calendar and cycling fades occurs but the impact of the former factor is almost negligible; therefore, many models only consider cycling degradation. However, the greatest accuracy in state estimation is achieved by considering both fades.There are several modes that cause degradation, such as a loss of active material, solid electrolyte interface (SEI) layer growth, internal resistance increase, capicity reduction, lithium plating, and elevated self-discharge [44,45].

Figure 3.8 compares EVES component life degredation. Each component's lifespan has a different degradation ratio; however, as shown in the graph, these can be divided into two major categories because the battery degradation plot has sharply decreased compared to others in deterioration degradation. Electrical and chemical properties degrade much more rapidly than mechanical properties. Therefore, energy storage components in EVES, especially the battery, can represent the entire system life degradation. Therefore, this

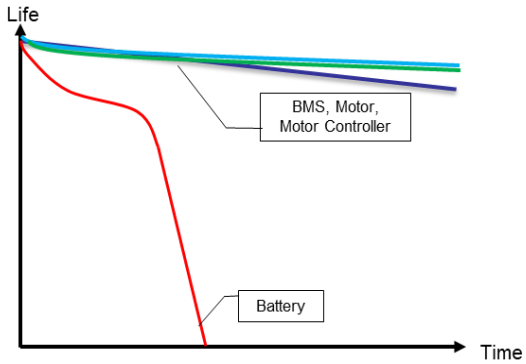

Figure 6.7 EVES component life degradation

thesis also assumes that since EVES degradation can be replaced by battery subsystem degradation, it will focus on this aspect for the RUL prognosis and uncertainty handling.

6.3.1 Battery Degradation Model

There are many types of battery degradation models. The most commonly used are the electrochemical model, the equivalent circuit model (ECM), and the exponential growth model. The electrochemical model is the most physically-based model. It attempts to represent the real battery system more precisely. The ECM model uses a simplified physically-based model, in which a capacitor and resistors are used to represent the diffusion process and internal impedance. The last model, the exponential growth model, is empirically-based [170]. Itl uses more simplified physically-based factors, and can therefore be viewed as a low-fidelity but high-efficiency model. At this point, there is no well-defined physical battery degradation model. In this thesis, the lack of full data regarding physically-based battery information, ECM, and the exponential growth model is adapted to uncertainty handling.

6.3.1.1 Equivalent Circuit Model (ECM)

The ECM model features extractions from the sensor data of voltage, power, resistance, frequency, temperature, and current to estimate the internal parameters. This method is commonly used in the BMS for SOC and SOH estimation. Moreover, the first-order resistor-capacitor (FORC) model and second-order resistor-capacitor (SORC) model are commonly used for ECM, as shown in Figure 6.9. It starts from the open circuit voltage (OCV) estimation of the cell which is $OCV = E_{cathode} - E_{anode}$. In the illustrations, R_O is the ohmic resistance of the battery, which describes the electrolyte and connection resistance of the battery, R_{PA} is polarization resistance, C_{PA} is polarization capacity, R_{PC} is nonlinear polarization resistance, and C_{PA} is nonlinear polarization capacity. With these

variables, the diffusion resistor current is $i_{PA,k+1}$, the hysteresis voltage is V_k, and the state of charge (SOC) z_{k+1} can be estimated as:

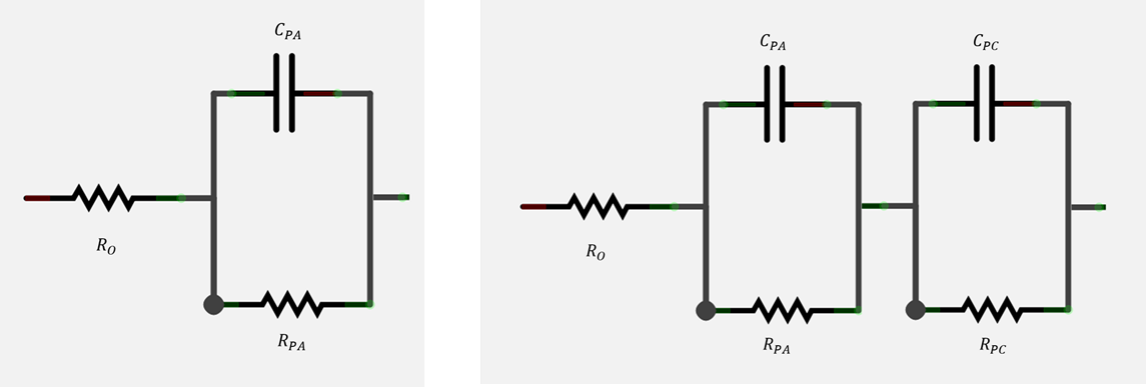

(a) (b)

Figure 6.8 The first-order RC ECM and second-order RC ECM

$$OCV = E_{cathode} - E_{anode} \tag{6.1}$$

$$i_{R_{PA},k+1} = exp\ \exp\left(\frac{-\Delta t}{R_{PA}C_{PA}}\right) i_{R_{PA},k} + \left(1 - exp\ exp\ \left(\frac{-\Delta t}{R_{PA}C_{PA}}\right)\right) i_k \tag{6.3}$$

$$V_{t,k} = OCV_k(SOC) - i_{R_{PA},k+1}R_{PA} - V_k \tag{6.4}$$

$$V_k = exp\ \exp\left(-\left|\frac{-\eta_k i_{k-1}\gamma\Delta t}{Q}\right|\right) V_k + \left(1 - exp\ exp\ \left(-\left|\frac{-\eta_k i_{k-1}\gamma\Delta t}{Q}\right|\right)\right) M \tag{6.5}$$

$$z_{k+1} = z_k - \frac{\eta_k i_k \Delta t}{Q} \tag{6.6}$$

$$SOC = \frac{\int \eta_k i_k \Delta t}{Q} \tag{6.7}$$

Where γ is a positive value that indicates the rate of decay, z_{k+1} is SOC at the $(k+1)th$ time step, η_k is charging and discharging efficiency, Q is rated capacity, and M is a polarization coefficient [171]. The second-order RC ECM comprises the following terms:

$$i_{\mathrm{R},k+1} = \begin{bmatrix} \exp\left(\frac{-\Delta t}{R_{PA}C_{PA}}\right) & 0 \\ 0 & \exp\left(\frac{-\Delta t}{R_{PA}C_{PA}}\right) \end{bmatrix} i_{\mathrm{R},k} + \begin{bmatrix} \left(1-\exp\left(\frac{-\Delta t}{R_{PA}C_{PA}}\right)\right) \\ \left(1-\exp\left(\frac{-\Delta t}{R_{PA}C_{PA}}\right)\right) \end{bmatrix} i_k \tag{6.8}$$

$$A_{\mathrm{RC}} = \begin{bmatrix} \exp\left(\frac{-\Delta t}{R_{PA}C_{PA}}\right) & 0 \\ 0 & \exp\left(\frac{-\Delta t}{R_{PC}C_{PC}}\right) \end{bmatrix}; B_{\mathrm{RC}} = \begin{bmatrix} \left(1-\exp\left(\frac{-\Delta t}{R_{PA}C_{PA}}\right)\right) \\ \left(1-\exp\left(\frac{-\Delta t}{R_{PC}C_{PC}}\right)\right) \end{bmatrix}$$

$$\begin{bmatrix} z_{k+1} \\ i_{\mathrm{R},k+1} \\ h_{k+1} \end{bmatrix} = \begin{bmatrix} 1 & 0 & 0 \\ 0 & A_{\mathrm{RC}} & 0 \\ 0 & 0 & \exp\left(-\frac{\eta_k i_k \Delta t}{\mathrm{Q}}\right) \end{bmatrix} \begin{bmatrix} z_{k+1} \\ i_{\mathrm{R},k+1} \\ h_{k+1} \end{bmatrix} + \begin{bmatrix} -\frac{\eta_k \Delta t}{\mathrm{Q}} & 0 \\ B_{\mathrm{RC}} & 0 \\ 0 & 1-\exp\left(-\frac{\eta_k i_k \Delta t}{\mathrm{Q}}\right) \end{bmatrix} \begin{bmatrix} i_k \\ M \end{bmatrix}$$

Next, these terms adapt to the state-space model as:

$$x_{k+1} = x_k - \frac{\eta_k i_k T}{Q} + w_k \tag{6.9}$$

$$y_k = \vartheta_{x_k} - i_k R + h_k + v_k + \delta(\cdot) \tag{6.10}$$

Where y_k is terminal voltage, ϑ_{x_k} is open circuit voltage at x_k, R is internal impedance, v_k is measurement noise, and $\delta(\cdot)$ stands for the uncertainty sources [172]. In addition to this state-space modeling, the modeling of degradation effect from side reaction such an solid electrolyte interphase (SEI) and deposit layer growth (R_{SEI}, R_{DL}), consumption of solvent of electrolyte (D_e), and isolation of certain anode particles due to SEI and deposits (ε_s) are following:

$$\eta_k = \varphi_s - \varphi_e - U_{eq} - \frac{R_{SEI}}{a_s} j^{Li} \tag{6.11}$$

$$V_k = \varphi_s - R_c i - R_{DL} \int j^{Li}(l) dl \tag{6.12}$$

$$\mathrm{Q} = (x_{max} - x_{min}) V_k \varepsilon_s c_s \mathrm{F} \tag{6.13}$$

$$\frac{\partial \varepsilon_s c_s}{\partial t} = \frac{\partial}{\partial l}\left(D_e \varepsilon_s \frac{\partial c_e}{\partial l}\right) + \frac{j^{Li}}{F} \tag{6.14}$$

Where $\varphi_s \; and \; \varphi_e$ are potential of anode and electrolyte, U_{eq} is equilibrium potential of anode, j^{Li} is reactive rate, a_s is ratio of electrode particle volume, $V_k$is terminal voltage, R_c is resistance of current collector, and ε_s is volume fraction of electrolyte [174].

6.3.1.2 Exponential Growth Model

The general shape for capacity vs. cycle numbers is plotted below. It has some features of each stage A to D in Figure 6.9. Region A has high capacity degradation

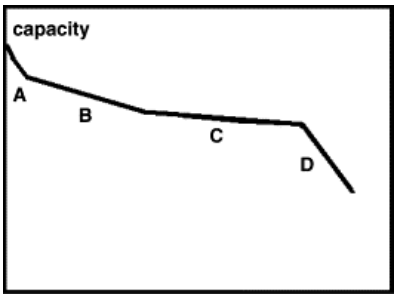

Figure 6.9 General shape for capacity versus cycle number plots [41]

initially, then it slows quickly at Region B, before slowing even more so at Region C. Degradation occurs rapidly at Region D. These rates are based on the mathematical and physically-based analyses. Furthermore, as previously mentioned, at around 70~80% of life degradation from the initial capacity, or SOH, it is recommended to replace the battery. This occurs at Regions B or C [41].

Unfortunately, the empirical graph does not follow the regional separated graph. The trend of degradation is similar to that shown by the exponential graph. Therefore, a simple form of the empirical degradation model is expressed by the exponential growth model as:

$$y = C\ exp\ \exp(-\lambda t) \tag{6.15}$$

Where y is the internal battery state, t is time or cycle, and C and λ are model parameters. Based on this approach, the battery state models are given as:

$$z_k = z_{k-1}\ exp\ \exp(-\Lambda_k) + w_k;\ with\ z_0 = C \tag{6.16}$$

$$\Lambda_k = \Lambda_{k-1} + v_k;\ with\ \Lambda_0 = \Lambda \tag{6.17}$$

$$x_k = [z_k; \Lambda_k] \tag{6.18}$$

$$y_k = z_k + v_k \tag{6.19}$$

Where the matrices $C\ and\ \Lambda$ contain decay parameters of C and λ, x_k is the state vector that combines with $\Lambda\ and\ Z$, and $v_k\ and\ w_k$ are noise, as in the ECM method.

6.4 About Data

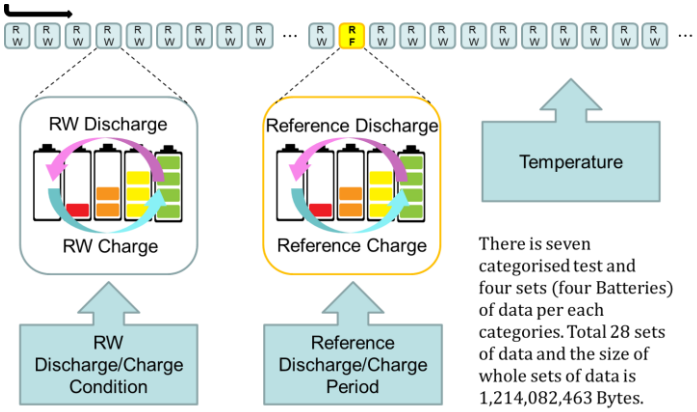

Figure 6.10 Data set - discharge / charge loop

Battery data is from NASA's Prognosis Center of Excellence. It was generated by Brian Bole, a NASA researcher and former fellow of Dr. Vachtsevanos.

Test-DATA Scheme

18650 Li-ion batteries in batches of four are run through three different operational profiles - charge, discharge and impedance - at ambient temperatures of 4, 24 and 44 °C. Charging was carried out in a constant current mode at 1.5A until the battery voltage reached 4.2V. It was then continued in a constant voltage mode until the charge current dropped to 20mA. Fixed and variable load currents at 1, 2, and 4 Amps were used and the

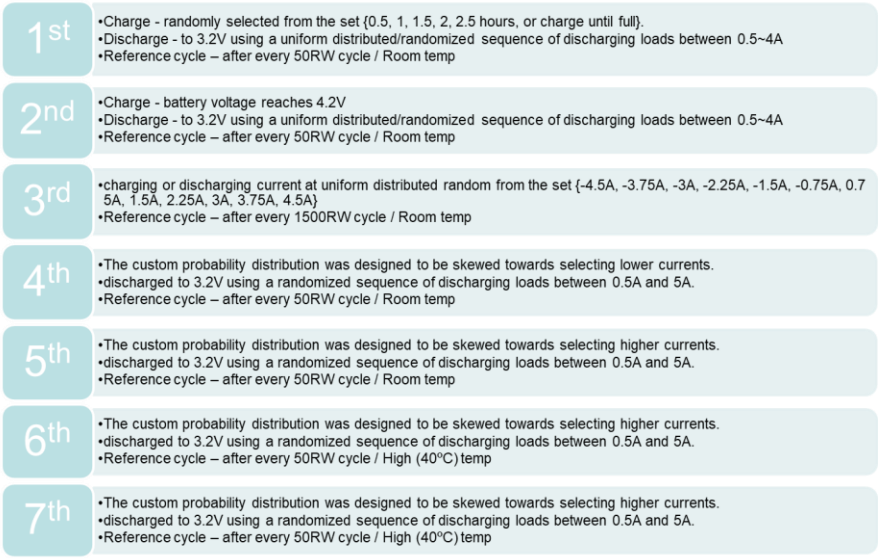

Figure 6.11 Figure Data set – Operating condition differences

discharge runs were stopped at 2V, 2.2V, 2.5V or 2.7V. The experiments were carried out until the capacity was reduced to at least 1.6Ahr (20% fade).

Reference charge and discharge cycle

1. Batteries are first charged at 2A (constant current), until they reach 4.2V, at which time the charging switches to a constant voltage mode and continues charging the batteries until the charging current falls below 0.01A.

2. Batteries are then discharged at 2A or 1A until the battery voltage crosses 3.2V.

Random Walk (RW) charge and discharge cycle

1. Charging the batteries to 4.2V. Batteries are charged at a 2A current until the battery voltage reaches 4.2V. When battery voltage reaches 4.2V then the system will switch to constant voltage charging. In this mode, the charging current will be regulated to maintain 4.2V at the battery output until the battery current drops below a lower threshold.

2. Batteries are discharged to 3.2V using a randomized sequence of discharging loads between 0.5A and 4A. Discharging periods last five minutes each.

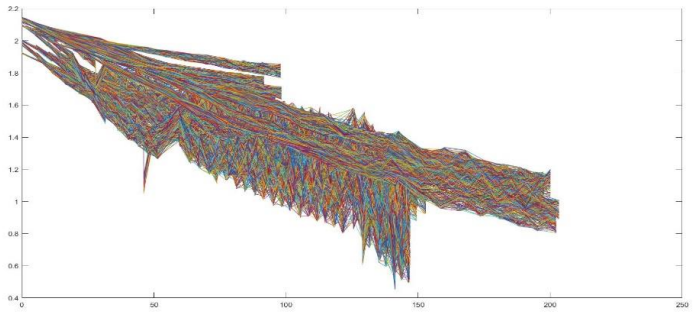

Figure 6.13 All data in one plot

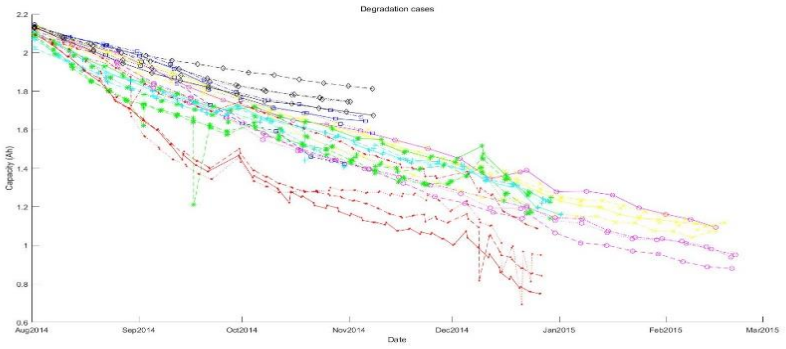

Figure 6.12 Reference data

As discussed, these data were collected under various operational and environmental conditions. An approximately 800mb-sized data plot with noise added is shown in Figure 6.12. Median reference data collected under the same conditions are shown in Figure 6.13.

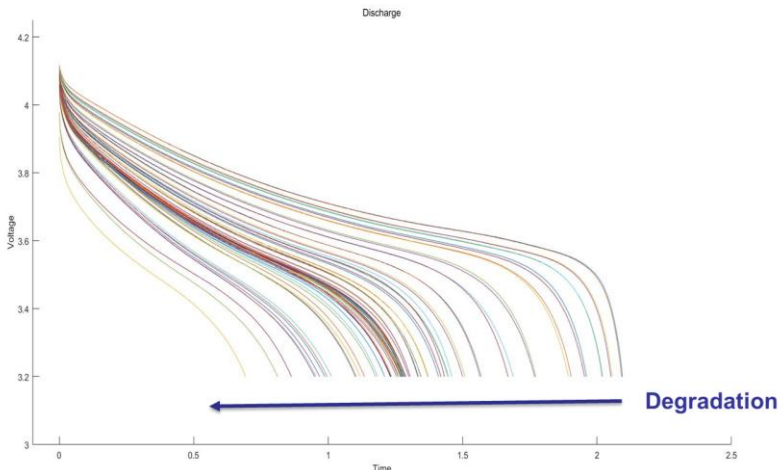

Figure 6.14 Li-ion battery discharge time decrasing by life degradation

The real battery life reduction is shown in Figure 6.14. This data is used to show and validate the RUL prognosis, as well as to indicate shrinking the prognosis uncertainty bounds.

6.5 RUL Prognosis via the data-driven, mode-based, and hybrid methods

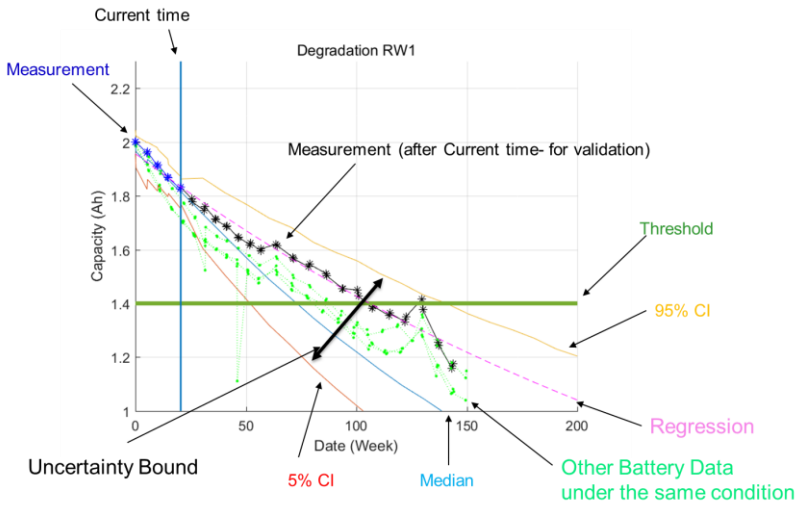

Figure 6.15 Plot explanation

The result of the prognosis of RUL estimation with empirical data via model-based, data-driven, and hybrid methods is shown as mentioned in Chapter 4. In the figure 6.15, the plot consists of measurement, threshold, upper and lower CIs, regression, median, current time, and the RUL probability distribution, also referred to as the uncertainty bound. The measurement is divided by the current time point. The measurement on the left side in blue used at a prognosis mechanism that only indicates as past and current data. The measurement on the right side is in black. These measurements are only used for validation of the RUL prognosis results, so the system and prediction mechanisms do not indicate the existence of those values. Figure 6.16 shows the result of prognosis via one of model-based

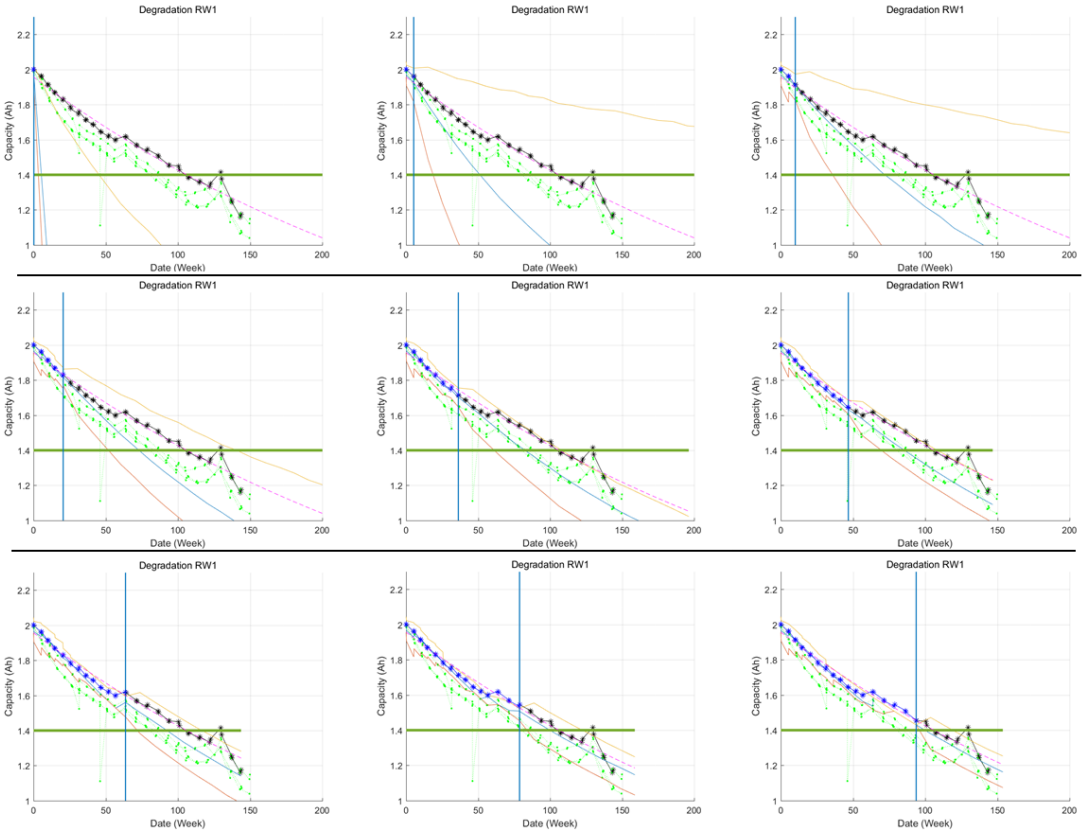

Figure 6.16 RUL prognosis via model-based method (PF)

prognosis that PF is used. The current timeline for the prediction point is at least the middle of the whole life degradation time. In addition, the uncertainty bound that is performed

from the right after the initial point has the widest result, and as such is meaningless for the prognosis. Thus, the RUL prognosis can be performed when the current point is located on greater than 10% and less than 60% of the total life period. Figure 6.17 shows the prognosis

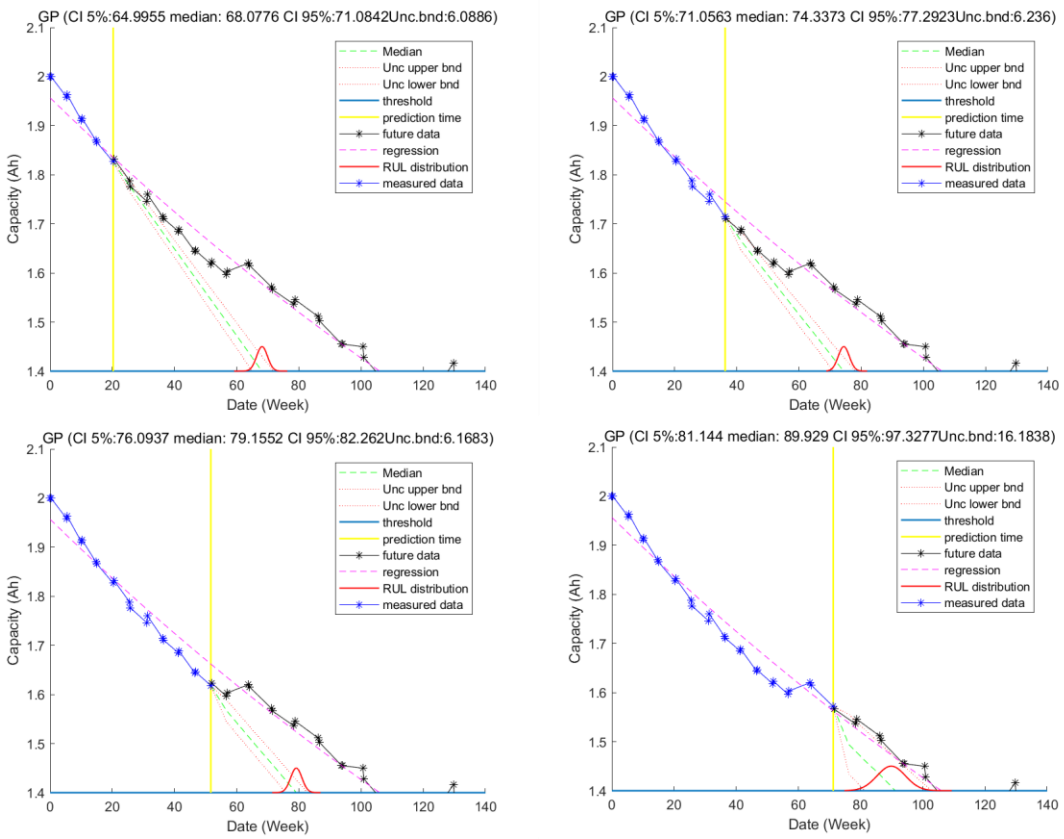

Figure 6.17 RUL prognosis result via data-driven (GP) method

result via the GP method as one of data-driven approaches using the empirical growth model. This method is based on data inference only, so if the data trend continues to decrease, then the prediction result will be high and thus have narrow uncertainty bounds. However, due to the unexpected occurrence of unpredictable events occurring in the 65th week, the prediction results have low accuracy. In other words, accuracy and precision

characteristics depends on the prognosis methods under the long-term and usage-based conditions. Often, the terms accuracy and precision are used interchangeably. However, they have totally different meanings in mathematics as Figure 6.18 shows. According to the ISO definition, accuracy is used to describe the closeness of true value. Precision is the closeness of data among a set of results [173]. Good results may have both high accuracy

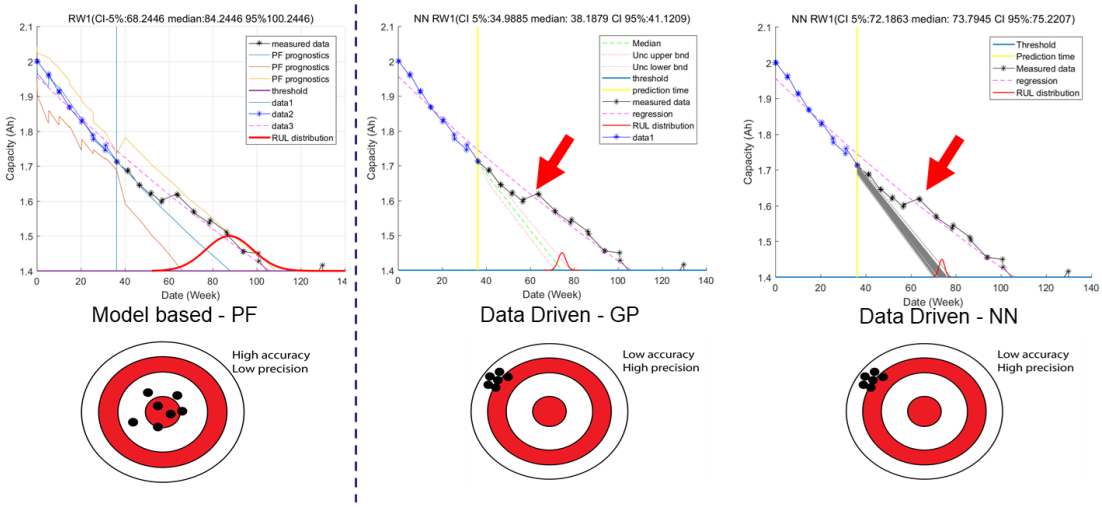

Figure 6.19 Accuracy and precision comparison under given condition

and high precision. Figure 6.19 shows this property classification via PF, GP, and the NN prognosis methods. Both data-driven methods are affected by irregular trends that should be accounted for, to achieve higher accuracy. In the battery case, the battery can self-charge right after discharge. If that phenomena occurs when the theoretical stage changes, this is

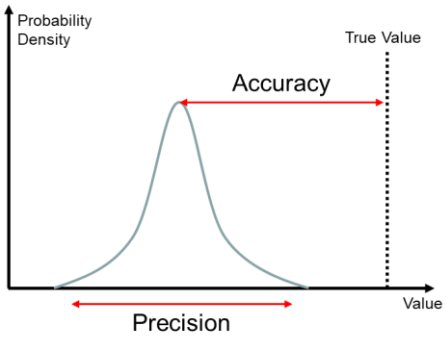

Figure 6.18 Accuracy and Precision

indicated as an arrow in Figure 6.19. The hybrid method, created by adding the surrogate model to the data-driven method, shows a better result in Figure 6.20.(b). The RUL

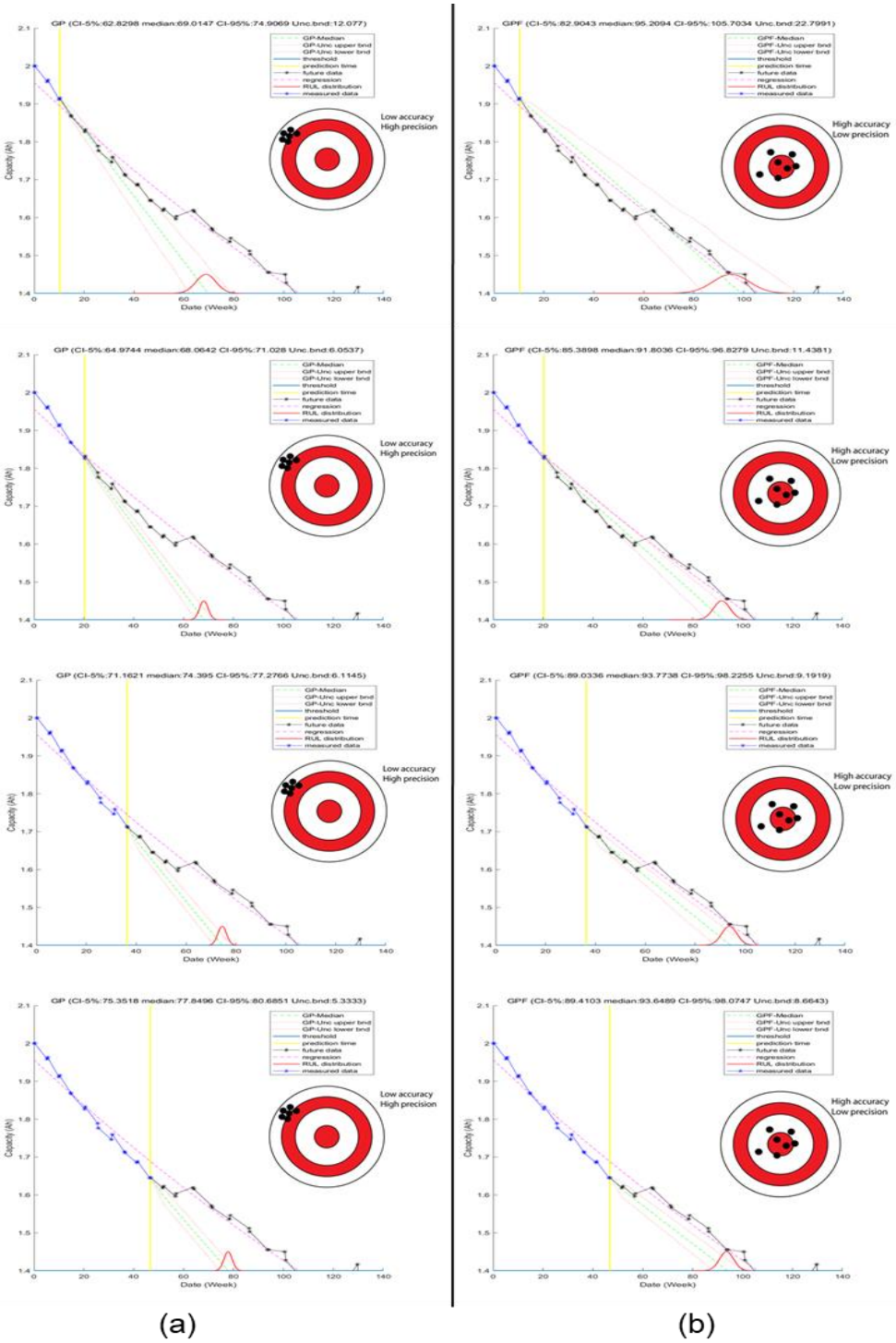

Figure 6.20 (a).Data-driven method VS (b).Hybrid Method

prognosis pdf covers expected validation points on the long-term prognosis using a physical model. Compared to data-driven methods in Figure 6.20(a), the hybrid method RUL prognosis result shows improved accuracy. However, as extra physical models are added, they show lower precision than in (a) plots. This can be handled through uncertainty management.

6.6 Uncertainty Management on the Long-term Prognosis of the 1860 Battery

6.6.1 Uncertainty Representation of the Li-ion RUL prediction

The first step, the uncertainty representation of the Li-ion RUL prediction, can be classified into three main types, as mentioned in the previous chapter: physical uncertainty, data uncertainty, and model uncertainty. Δ*temp* is uncertainty from operating temperature changes; Δ*D.O.D* is uncertainty from depth of discharge rate changes; Δ*S.O.C* is uncertainty from state of changes; Δc_rate is uncertainty from C-rate changes; $\Delta noise$ represents noises such as from a sensor or sparse; $\Delta meas$ is measurement error; Δs.*e.* is state estimation such an Δ*S.O.C or* Δ*S.O.H* at time t; and Δ*input* is the model inputs. There are three reliable Li-ion battery prognostics models: PF, GP, and GPF, which are used in this paper for better skewed lower and upper uncertainty bounds. Therefore, representation also deals with each model's uncertainty. $\Delta para\_pf$, $\Delta para\_gp, and\ \Delta para\_gpf$ are parameter uncertainties for each model; $\Delta m.e.pf, \Delta m.e.gp, and\ \Delta m.e.gpf$ are modeling errors for each model. At the end, the mathematical function with these uncertainty source variables and total uncertainties on the input can be expressed as;

$$Y = \gamma\begin{pmatrix} x_{sn_{data}}, x_{sd_{data}}, x_{me_{data}}, x_{me_{pf|gp|nn}}, x_{mp_{pf|gp|nn}}, x_{se_{pf|gp|nn}}, x_{oc_{pf|gp|nn}}, \\ x_{su_{pf|gp|nn}}, x_{temp_{load}}, x_{press_{load}}, x_{crate_{physical}}, x_{soh_{physical}}, x_{dod_{physical}} \end{pmatrix}$$

6.6.2 Uncertainty Propagation of Li-ion RUL prediction

The first step of uncertainty propagation of Li-ion RUL prediction is finding CDF of RUL via PF and GPF. The pdf graph already got from the RUL prognosis of chapter 6.5. From the estimated CDF, calculate β which shows the result of RUL bound on each present time setting on figure 6.21. These values got from at least 5,000 repeated prognosis

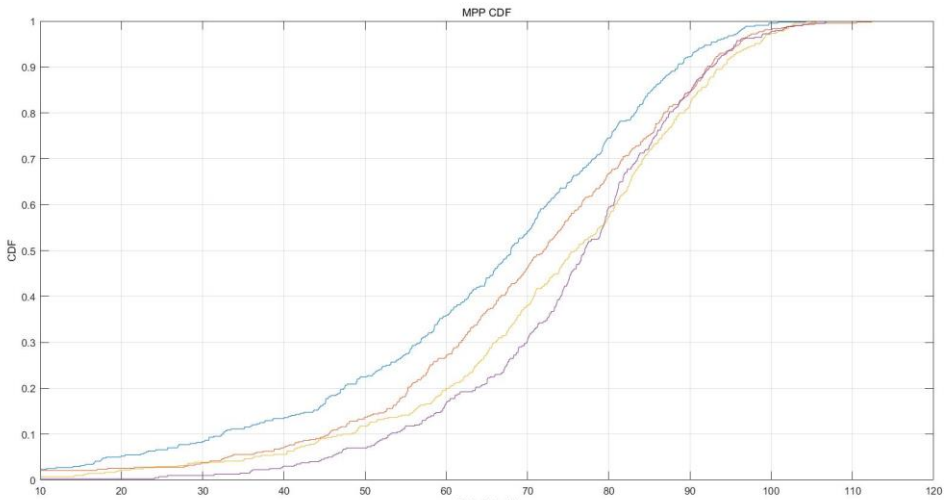

Figure 6.21 CDF plot on each time point

procedures to minimize uncertainty under the exact same condition. In addition, the earlier prognosis point doesn't have meaningful RUL prognosis result, it is neglect on long-term prognosis. After that, use MPP methods as forehead mention because this is one of prognosis methods via linear transformation and normalization while the process, gradient vector or each source is used. Therefore, find gradient vector using MPP methods via following algorithm using estimated β from PF and GP via following algorithm.

Table 6.1 CDF and β information via prognosis methods

time point	0.198056	5.376273	10.75583	16.19251	21.28657	26.2484	31.48904	36.60617
CDF bound	NULL	NULL	NULL	97.2468	81.5753	71.45686	62.75468	53.34656
Median time	NULL	NULL	NULL	45.4786	69.1264	75.74556	80.87341	81.74676
β	NULL	NULL	NULL	3.89	3.59	3.54	3.34	3.34

Algorithm 6.1 Most probable point

1: ***Procedure*** *MPP(t, u_i, β, g, t_{th})*
2: $k \leftarrow t - 1$
3: ***for*** *i=1 to* N_u ***do***
4: $u_i \leftarrow$ *uncertainty sources // from representation stage*
5: $\eta_k^{(i)} \leftarrow \frac{-\Phi(\beta_k)}{N_u}$
6: $i \leftarrow i + 1$
7: $\omega_0 \leftarrow \eta_k^{(1)}$ *//set initial weight via uniform distribution for optimization*
8: **end for**
9: $k \leftarrow t$
10: ***for*** *i=1 to* N_u ***do***
11: $\eta_k^{(i)} \leftarrow \frac{-\Phi(\beta_k)}{N_u}$
12: $\beta_k^{(i)} \leftarrow -\Phi^{-1}(\eta_k^{(i)} - \omega_0)$
13: $\beta_k \leftarrow \sqrt{\sum(\beta_k^{(i)})^2}$
14: $\omega_j \leftarrow \beta_k - \beta_{k-1}$
15: $i \leftarrow i + 1$
16: **end for**
17: $k \leftarrow t_{th}$
18: ***for*** *j=1 to* N_u ***do***
19: ***for*** *j=1 to k* ***do***
20: $\Phi_{jk} \leftarrow T_N(\omega_j)$
21: $\Phi_j \leftarrow \Phi_{jk}$
22: $\alpha_{jk} \leftarrow \frac{\partial g}{\partial \Phi_{jk}}$
23: $\alpha_j \leftarrow \alpha_{jk}$
24: **end for**
25: **return** α_j

After that, connect the gradient vector of each independent uncertainty sources via uncertainty tree. Using the uncertainty tree, uncertainty sources of the lithium ion battery's RUL prediction are constructed as shown in Figure 6.22. After that, the uncertainty relations and propagation are expressed as follows:

$$\Delta RUL = h(\sigma_{RUL}, s_{RUL});$$

$$\sigma_{RUL} = [\sigma_{physical}\ \sigma_{model}\ \ \sigma_{data}],\ s_{RUL} = [s_{physical}\ s_{model}\ \ s_{data}],$$

$$\sigma_{physical} = [\sigma_{c-rate}\ \sigma_{s.o.h.}\ \sigma_{d.o.d.}\ \sigma_{load}],\ s_{physical} = [s_{c-rate}\ s_{s.o.h.}\ s_{d.o.d.}\ s_{load}],$$

$$\sigma_{data} = [\sigma_{m.e.}\ \sigma_{s.d.}\ \sigma_{s.n.}],\ s_{data} = [s_{m.e.}\ s_{s.d.}\ s_{s.n.}],$$

$$\sigma_{pf|gp|nn} = [\sigma_{m.e.}\ \sigma_{m.p.}\ \sigma_{s.e.}\ \sigma_{o.c.}\ \sigma_{s.u.}],\ s_{pf|gp|nn} = [s_{m.e.}\ s_{m.p.}\ s_{s.e.}\ s_{o.c.}\ s_{s.u.}]$$

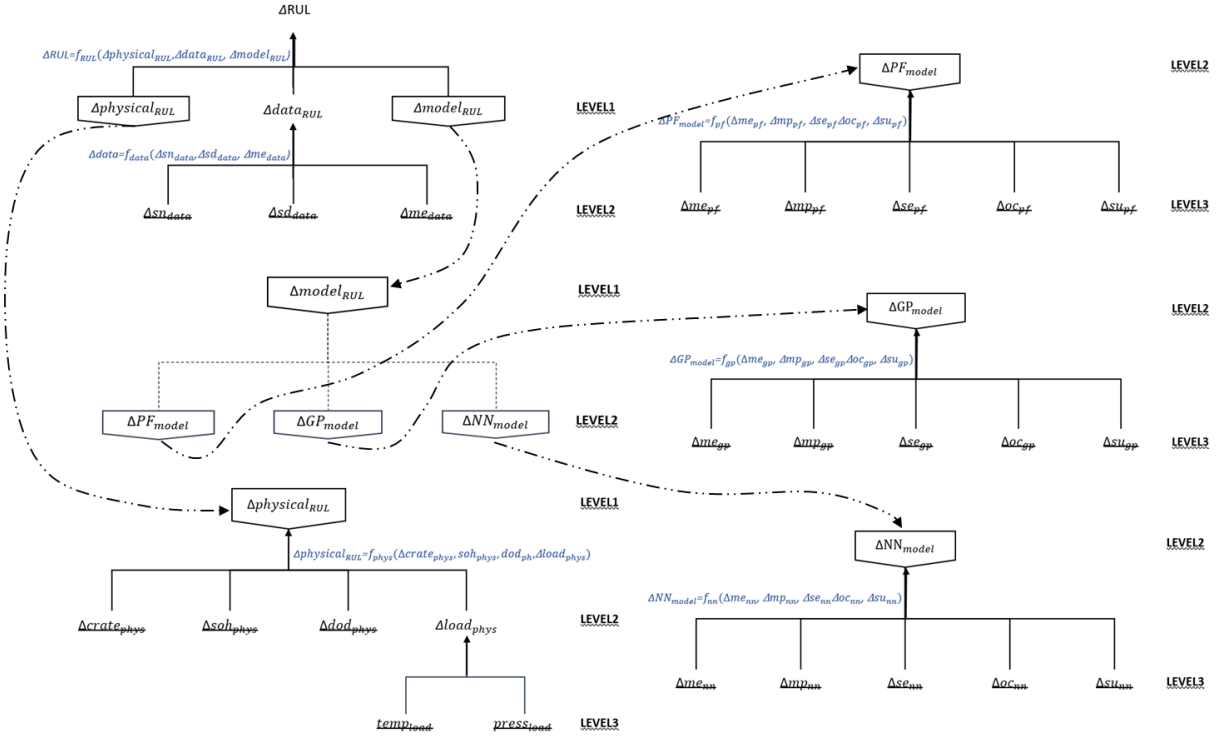

Figure 6.22 Uncertainty tree of lithium ion battery RUL estimation

$$= \sqrt{\left[\begin{array}{c}\left(\frac{\partial RUL}{\partial physical_{RUL}}\frac{\partial physical}{\partial load_{physical}}\frac{\partial load}{\partial temp_{load}}\Delta temp_{load}\right)^2+\left(\frac{\partial RUL}{\partial physical_{RUL}}\frac{\partial physical}{\partial load_{physical}}\frac{\partial load}{\partial press_{load}}\Delta press_{load}\right)^2 \\ +\left(\frac{\partial RUL}{\partial physical_{RUL}}\frac{\partial physical}{\partial crate_{physical}}\Delta crate_{load}\right)^2+\left(\frac{\partial RUL}{\partial physical_{RUL}}\frac{\partial physical}{\partial soh_{physical}}\Delta soh_{physical}\right)^2 \\ +\left(\frac{\partial RUL}{\partial physical_{RUL}}\frac{\partial physical}{\partial dod_{physical}}\Delta dod_{physical}\right)^2+\left(\frac{\partial RUL}{\partial data_{RUL}}\frac{\partial data}{\partial sn_{data}}\Delta sn_{data}\right)^2+\left(\frac{\partial RUL}{\partial data_{RUL}}\frac{\partial data}{\partial sd_{data}}\Delta sd_{data}\right)^2 \\ +\left(\frac{\partial RUL}{\partial data_{RUL}}\frac{\partial data}{\partial me_{data}}\Delta me_{data}\right)^2+\left(\frac{\partial RUL}{\partial model_{RUL}}\frac{\partial model}{\partial me_{pf|gp|nn}}\Delta me_{pf|gp|nnl}\right)^2 \\ +\left(\frac{\partial RUL}{\partial model_{RUL}}\frac{\partial model}{\partial mp_{pf|gp|nn}}\Delta mp_{pf|gp|nn}\right)^2+\left(\frac{\partial RUL}{\partial model_{RUL}}\frac{\partial model}{\partial se_{pf|gp|nn}}\Delta se_{pf|gp|nn}\right)^2 \\ +\left(\frac{\partial RUL}{\partial model_{RUL}}\frac{\partial model}{\partial oc_{pf|gp|nn}}\Delta oc_{pf|gp|nn}\right)^2+\left(\frac{\partial RUL}{\partial model_{RUL}}\frac{\partial model}{\partial su_{pf|gp|nn}}\Delta su_{pf|gp|nn}\right)^2\end{array}\right]}$$

6.6.3 Uncertainty Management of Lithium Ion RUL prediction

The last step of uncertainty handling of li-ion battery RUL prognosis is finding impact uncertainty sources via sensitivity analysis then simplify uncertainty tree to use impactor via prognosis procedure to shrink uncertainty bound. The 18650 li-ion battery

Table 6.2 first order and total effect index

	S_i	S_(T_i)		S_i	S_(T_i)
sn_data	8.3456683767E-08	8.3516015536E-08	me_gp	1.2951204497E-06	1.4860122327E-06
sd_data	9.1098139547E-08	8.9112248074E-08	mp_gp	7.9747212790E-10	7.7563624142E-10
me_data	1.3037561650E-07	1.4624928956E-07	se_gp	2.4944728331E-06	2.5994333357E-06
crate_phys	9.3850574983E-05	8.9808562812E-05	oc_gp	3.6096022651E-06	3.6828353440E-06
soh_phys	6.1962611113E-04	6.5823158739E-04	su_gp	N/A	N/A
dod_phys	9.9111021375E-05	9.6667722596E-05	me_nn	1.0137345706E-06	9.8127168420E-07
temp_phys	2.9381714566E-03	2.6038911503E-03	mp_nn	7.6236372740E-10	7.7653555241E-10
press_phys	N/A	N/A	se_nn	2.6843661396E-06	3.0163397969E-06
me_pf	9.5033019082E-03	9.4256847148E-03	oc_nn	4.3611982039E-06	4.3911143250E-06
mp_pf	9.6898294844E-02	9.7187633057E-02	su_nn	N/A	N/A
se_pf	6.8055443737E-05	7.0440051093E-05			
oc_pf	3.9504671712E-05	4.1290928042E-05			
su_pf	N/A	N/A			

case, estimated first and second order of sensitivity from gradient vector of MPP are shown on table 6.2. As shown by the indices, the researchers identified important sources of uncertainty and eliminated unimportant sources, while updating the uncertainty tree as shown in Figure 6.23. This updated uncertainty tree shows which source of uncertainty should focus on the shrinking uncertainty bounds. The lithium ion battery prognosis case,

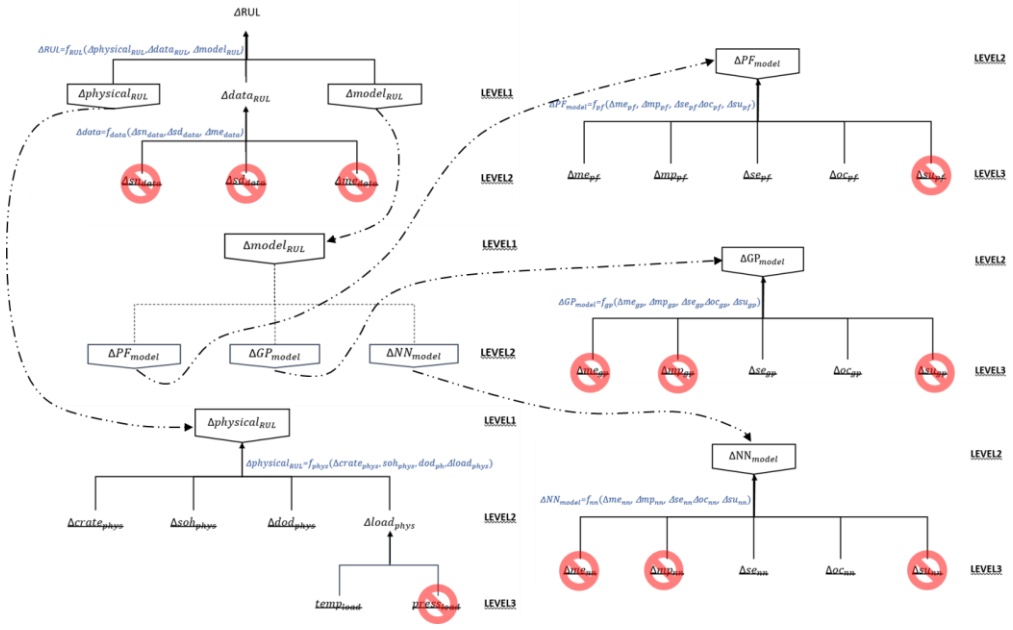

Figure 6.23 Updated uncertainty tree of Li-ion battery RUL estimation

the model parameter and temperature effects have higher first and total effects source of uncertainty on the model-based approach are indicated as the high impactor. Use the percentage of impactor weight in ω_j on MPP or adapt hyper parameter loop that Dr.Orchard suggested on 2008 as

$$var\{n(t+1)\} \coloneqq 0.95 * var\{n(t)\},\ if\ \frac{\|Pred_{error(t)}\|}{\|y(t)\|} < 0.1;$$

$$var\{n(t+1)\} \coloneqq 1.2 * var\{n(t)\},\ if\ \frac{\|Pred_{error(t)}\|}{\|y(t)\|} > 0.1$$

then RUL prognosis bound shows around 2 to 10% was shrunk as figure 6.24. In addition, this approach appears to have an excellent effect in securing the disadvantage of the hybrid method where physical modeling added on data-driven approach based on figure 6.25. As

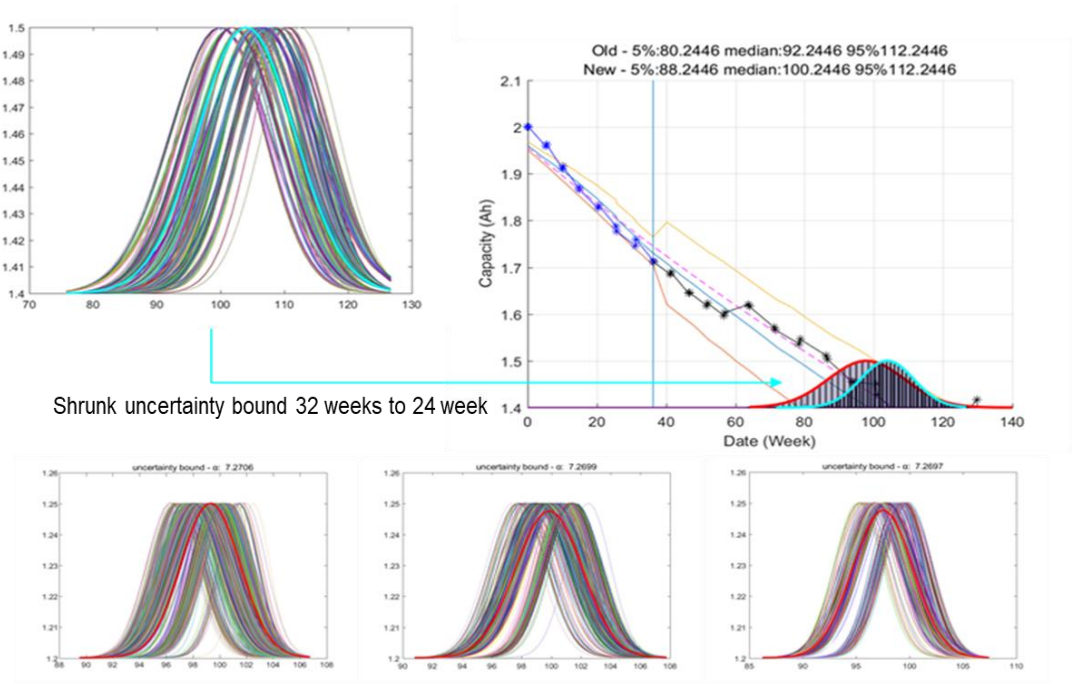

Figure 6.24 Shrunk uncertainty RUL bound

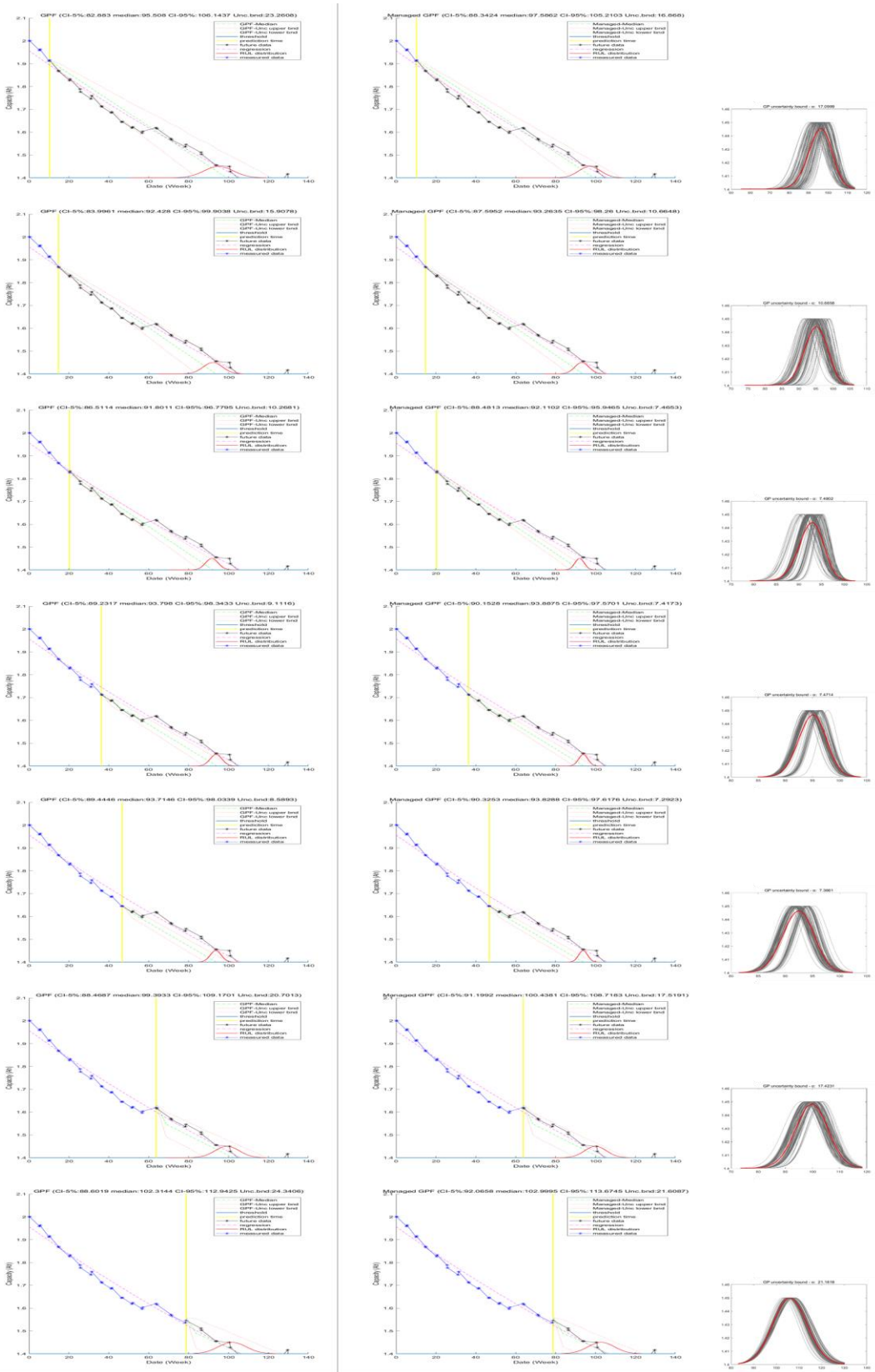

Figure 6.25 Original GPF (left) vs Uncertainty handled GPF(right)

a result, the RUL prognosis result via uncertainty handled GPF approach shows the most accurate and precision PDF graph among model-based and data-driven methods.

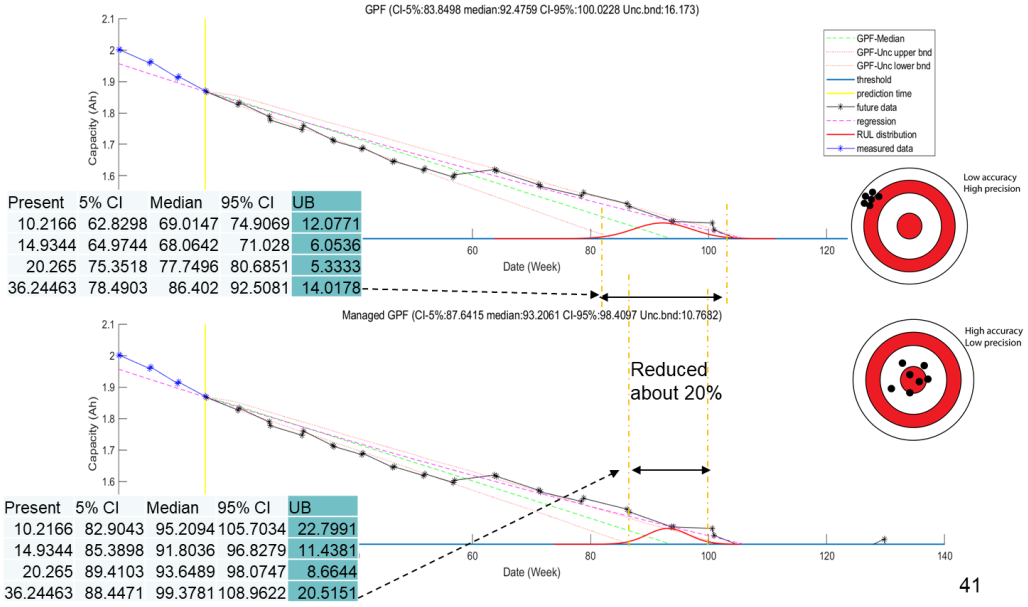

Figure 6.26 Shrunk uncertainty bound

6.7 Demonstration

6.7.1 Use Another Uncertainty Management for Demonstration

There are several literatures that suggest uncertainty managing [89-96]. Among them, Dr. Jing suggest battery performance and RUL estimation via parameter and model uncertainty quantification via ECM modeling [172]. First step did system model set up via ECM state space model as forehead mentioned. After that, parameter uncertainty quantification via mean and standard deviation (STD) of each parameter were calculated then ratio between mean and STD were computed. At the end, quantify the model uncertainty as a random process, construct GP for modelling the model uncertainty, and mean of the model uncertainty can be obtained from the GP on the last step. For the

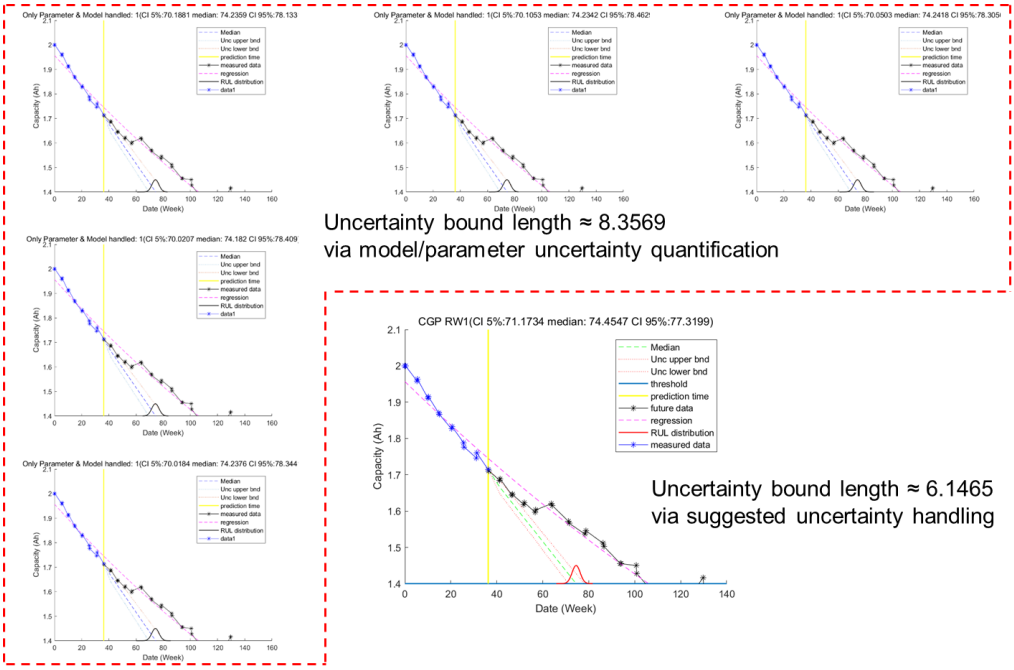

Figure 6.27 Uncertainty handling comparison

comparison, set up the same condition and do only GP with suggested uncertain handling then result shows on figure 6.26. There are much more uncertainty sources that effects to pdf and suggested approach could check more source via gradient vector then it shows more efficient RUL bound.

6.7.2 Simply apply to the 2nd Case Study – Bearing Crack Growth Case

Origin of CBM and RUL prognosis is invented for maintain the life of engineering system as longer as possible. Among many of engineering systems, this research is mostly demanded at aircraft engineering as mentioned on the background chapter. Engine or bearing crack growth was one of main concern on aircraft research field. Therefore, suggested uncertainty managing to shrink RUL uncertainty bound is also shown on this bearing crack growing case then compare the result from other older handling methods. First of all, the general state model of bearing crack growth model is following

$$x = \left[t * C \left(1 - \frac{m}{2} \right) (\Delta K)^m + {x_0}^{1-\frac{m}{2}} \right]^{\frac{2}{2-m}}$$

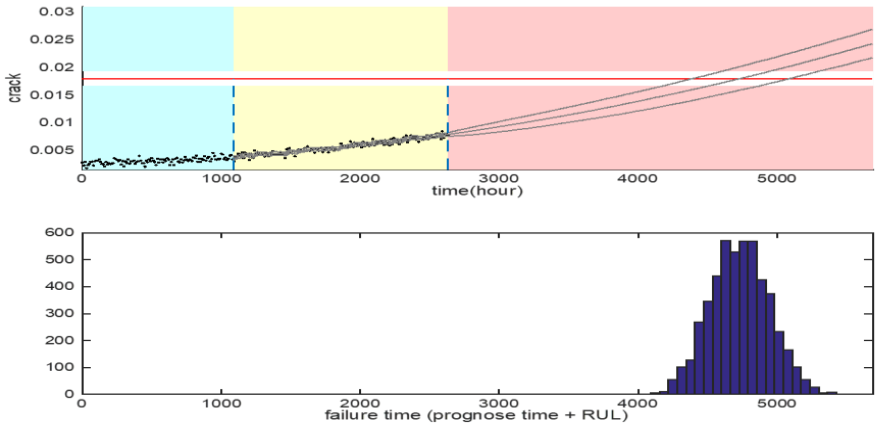

Figure 6.28 Bearing crack growth prognosis result [1102,1103]

Where x is a current crack length, x_0 is an initial crack size, ΔK is a stress factor that give main factor driving crack growth, and C and m is model parameter. The paper of Dr. C. Chen who is former student of Dr. Vachtsevanos researches about bearing crack growth using model-based and data-driven methods and prognosis result as figure [1102,1103]. Set same model, parameter, and data, then do the PF prognosis procedure as original researcher did. The RUL prognosis results on figure 6.28 and it is similar as original result

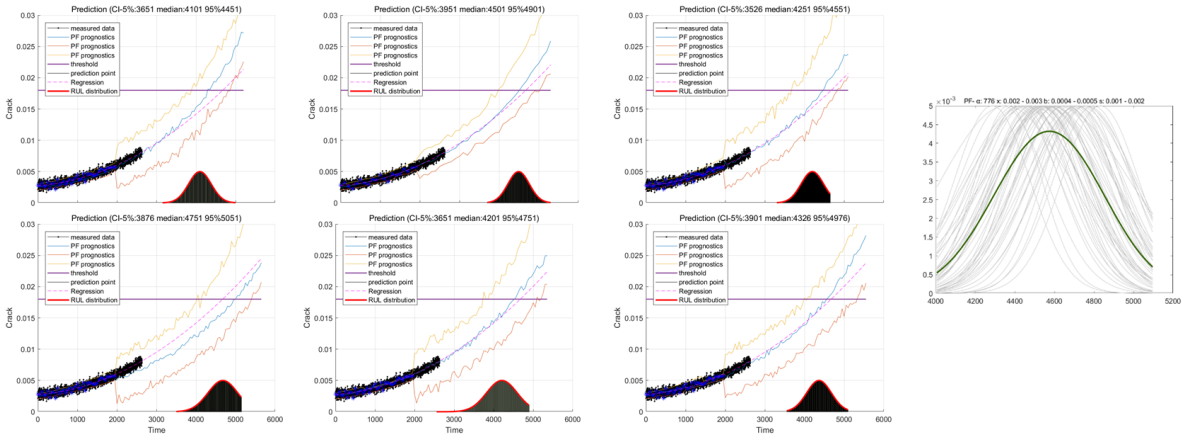

Figure 6.29 Bearing crack growth /w PF (original)

on 6.27. after that, adapt uncertainty handling methods via representation, propagation, and management step as suggested and the result shows on figure 6.29.

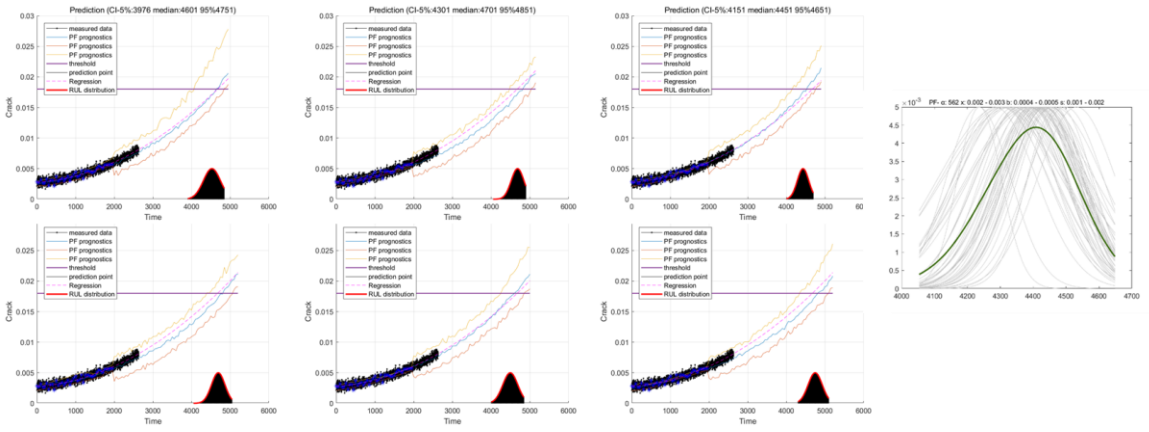

Figure 6.30 Figure 6.28 Bearing crack growth /w PF(uncertainty handled)

CHAPTER 7. CONCLUSION

On the conceptual front, the suggested research presented uncertainty handling procedure via model-based, data-driven, and hybrid prognosis methods to get more precise and accurate RUL prediction result by shrinking uncertainty bound. This research cannot show how each sources of uncertainty propagate exactly via mathematical equation but using idea from uncertainty tree, uncertainty relation, and gradient vector of MPP methods, estimating propagation of uncertainty sources via relation comparing between short-term propagation and long-term propagation.

7.1 Contribution

- Novel methodologies of prognoses of remaining useful life in usage-based conditions. Results of model-based methods such as the particle filter method and the Markov Chain Monte Carlo Method have high accuracy and low precision, whereas results of data-driven methods such as the Gaussian Process Method and the Neural Network Method have high precision and low accuracy under long-term and usage-based conditions.
- A general framework of characterization, representation, and classification of sources of uncertainty in the system. The general uncertainty management procedure of the prognostics system is frequently discussed from the representation, propagation, and management points of view. However, there are various interpretations of each procedure's terms and orders depending on the writer, so clarification here is helpful.

- The introduction and comparison of methodologies to estimate the propagation or impact ranking of uncertainty sources in the system. Generally, Monte Carlo simulation methods, probabilistic fuzzy approach, interval analysis, first- and second-order reliability methods (FORM; SORM), evidence approach methods, regression technique polynomial chaos expansions, and most probable point (MPP) methods are used for uncertainty propagation methods. Among these methods, some are not suitable for all types of uncertainty source handling, and some are difficult to classify in terms of the impact of sources. The rest of the methods have less accurate propagation; however, they have other positive aspects. Among the pros and cons of these methodologies, this thesis helps the reader to select the best methods for a given application via a thorough comparison.
- More accurate model-based methods results are shown via the uncertainty management procedure. The model-based methods have high accuracy and less precision, usually because the physical model is expected to catch most of the behavior or states via an outline of the model plot. However, the uncertainty management procedure has higher numbers of uncertainty sources than data-driven methods. It also affects uncertainty bounds on prediction points. For this reason, it has lower precision than data-driven methods. However, it can be improved via uncertainty management methods and results also show that the uncertainty bounds are shrunk.
- Data-driven methods, upgraded by adding a physical model, are introduced, with improved accuracy and precision results shown via adapted uncertainty handling methods. General Data-Driven (DD) methods only consider relationships between each data point, so the property of high accuracy does not always hold true when an

early phase prognosis is performed. In other words, DD methods do not catch later-occurring behavior in the system. Accuracy can be improved by adding a physical model to DD methods. However, in doing so, many additional uncertainty sources are added. At this point, expanded uncertainty bounds can be reduced by uncertainty management, thereby providing more accurate and precise results.

- The demonstration of the proposed framework in two case studies. The approaches presented in this thesis can be demonstrated using an 18650 li-ion battery, usually used in determining electric vehicle life degradation data, and also used in bearing crack growth data. Both data results indicated shrunk uncertainty bounds. Furthermore, this author's suggested approaches also are adaptable for comparison with other uncertainty management methods for demonstration.

7.2 Future Work

On the software side, whole code was Matlab based. Matlab is still used many engineering field but there definitely exists technical limitation and the modeling trend is moving to Python. Therefore, developing code that works on Python based. In addition, looking for more application that suggested uncertainty managing can be adapted to get more precision and accurate prognosis result. Furthermore, using R and Hadoop, adapt it to data analytical field. On application side, the author is going to jump in to the industry and adapt these suggested methods on different applications. As two of case study already shown that the uncertainty handling methods leads to shrink uncertainty bound on RUL prognosis for accuracy and precision result.

REFERENCES

[1] B. Peter and S. Mike, Asset Maintenance Management - The Path toward Defect Elimination, The masters of reliability and maintenance Conference, 1999

[2] W. Elghazel, J. Bahi, C. Guyeux, M. Hakem, K. Medjaher and N. Zerhouni, "Dependability of wireless sensor networks for industrial prognostics and health management", Computers in Industry, Vol. 68, 2015, pp. 1-15.

[3] JIN, X., SIEGEL, D., WEISS, B. A., GAMEL, E., WANG, W., LEE, J. & NI, J. 2016. "The Present Status and Future Growth of Maintenance in US Manufacturing: Results from a Pilot Survey", Manufacturing Review

[4] K. Goebel, G. Vachtsevanos, and M. Orchard, "Prognostics", IVHM: The Technology, Ed.: I. Jennions, SAE International, R-429, ISBN of 978-0-7680-7952-4, Chapter 4, 48-70, 2013

[5] R. Patrick, M.J. Smith, C. Byinton, G. Vachtsevanos, K. Tom, and C. Ly ,"Integrated Software Platform for Fleet Data Analysis, Enhanced Diagnostics, and Safe Transition to Prognostics for Helicopter Component CBM", Annual Conference of the Prognostics and Health Management Society, 2010

[6] Prognostic meaning of oxford dictionaries, Retrieved from https://en.oxforddictionaries.com/definition/us/prognostic

[7] A. Saxena, Prognostics (2010), Retrieved from https://www.phmsociety.org/sites/phmsociety.org/files/Saxena_Prognostics_TutorialPHM10.pdf

[8] Patrick, R., Smith, M.J., Zhang, B., Byington, C.S., Vachtsevanos, G.J., and Del Rosario, R., "Diagnostic Enhancements for Air Vehicle HUMS to Increase Prognostic System Effectiveness". IEEEAC paper #1608, IEEE, 2009

[9] K. Goebel, B. Saha, A. Saxena, J. R. Celaya, and J. Christophersen, "Prognostics in battery health management," IEEE Instrum. Meas. Mag., vol. 11, no. 4, pp. 33–40, Aug. 2008

[10] R. Sharda, ''Neural Network for the MS/OR Analyst: An Application Bibliography,'' Interfaces 24(2):116–130, 1994

[11] Rigamonti, M., Baraldi, P., Zio, E., Roychoudhury, I., Goebel, K., and Poll, S., (2016). Echo State Network for the Remaining Useful Life Prediction of a Turbofan Engine Under Variable Operating Conditions. In Proceedings of the Third European Conference of the Prognostics and Health Management Society 2016, Bilbao, Spain, July 2016.

[12] D. Brown, G. Georgoulas, B. Bole, H. Pei, M. Orchard, L. Tang, B. Saha, A. Saxena, K. Goebel, and G. Vachtsevanos, Prognostics Enhanced Reconfigurable Control of Electro-Mechanical Actuators, Annual Conference of the Prognostics and Health Management Society 2009

[13] J. Liu, A. Saxena, K. Goebel, B. Saha, and W. Wang, An Adaptive Recurrent Neural Network for Remaining Useful Life Prediction of Lithium-ion Batteries, International Conference on Prognostics and Health Management, 2010.

[14] K Javed, R Gouriveau, R Zemouri, N Zerhouni, Improving data-driven prognostics by assessing predictability of features, International Conference on Prognostics and Health Management, Portland, OR, October 2011
[15] J. Luo, K. R. Pattipati , L. Qiao , S. Chigusa, Model-Based Prognostic Techniques Applied to a Suspension System, IEEE Transactions on Systems, Man, and Cybernetics, Part A: Systems and Humans, v.38 n.5, p.1156-1168, September 2008
[16] J. C. Newman, FASTRAN-II: A Fatigue Crack Growth Structural Analysis Program, NASA Technical Memorandum, Langley Research Center, Hampton, VA. 1992
[17] M. Daigle, S. Sankararaman. Advanced methods for determining prediction uncertainty in model-based prognostics with application to planetary rovers. In the Proceedings of 2013 Annual Conference of the Prognostics and Health Management Society, New Orleans, LA, USA, Oct 14 - 17, 2013.
[18] Howell D, Annual progress report for energy storage R&D, Vehicle Technologies Program, Energy Efficiency and Renewable Energy. U.S. Department of Energy, Washington, DC, 2010
[19] L. Feng, H. Wang, X. Si, and H. Zou, A State-Space-Based Prognostic Model for Hidden and Age-Dependent Nonlinear Degradation Process, IEEE Transactions on Automation Science and Engineering, 1072–1086, 2013
[20] Jorgensen B., Lundbye C.S., Song PX-K et aI, A states pace model for multivariate longitudinal count data, Biometrika, vo1.86, no. 1. 1999, pp.169-181.
[21] Hashemi R., Jacqmin-Gadda H., and Commenges D., "A latent process model for join modeling of events and marker," Lifetime Data Analysis, vol 9, no A, 2003,pp.331-343.
[22] Argon Chen, and G. S. Wu, "Real-time health prognosis and dynamic preventive maintenance policy for equipment under ageing Markovian deterioration," International Journal of Production Research, vol.45 ,no.15,Aug. 2007, pp.3351-3379.
[23] M. Dubarry, C. Truchot, and B. Y. Liaw, Synthesize battery degradation modes via a diagnostic and prognostic model. Journal of Power Sources 219, 2012
[24] S. Sankararaman, K. Goebel. Uncertainty quantification in remaining useful life of aerospace components using state space models and inverse FORM. In the Proceedings of the 15th Structural Dynamics and Materials Conference, 2013.
[25] M. Daigle, A. Saxena, and K. Goebel, "An Efficient Deterministic Approach to Model-based Prediction Uncertainty Estimation," Annual Conference of the Prognostics and Health Management Society 2012, pp. 326-335, September 2012.
[26] William L. Oberkampf, Sharon M. Deland, Brian M. Rutherford, Kathleen V. Diegert, Kenneth F. Alvin, A New Methodology for the Estimation of Total Uncertainty in Computational Simulation, The 40th Structural Dynamics, and Materials Conference, 1999.
[27] S. Sankararaman, Y. Ling, S. Mahadevan, Fatigue Crack Growth Analysis and Damage Prognosis in Structures, Emerging Design Solutions in Structural Health Monitoring Systems, October, 2015

[28] Longtin, J., “The Uncertainty Tree: Reducing the Uncertainty of Uncertainty Analysis,” Review of Scientific Instruments, vol. 73, no. 10, pp. 3698-700, Oct, 2002.
[29] M. Drosg, Dealing with Uncertainties: A Guide to Error Analysis, Springer-Verlag. 2009.
[30] J. Anderson, The architecture of cognition, Harvard university, 1983
[31] W. Liu, J. C. Principe, and S. Haykin, Kernel Adaptive Filtering: A Comprehensive Introduction, Wiley Publishing, 2010
[32] Pola, D.; Guajardo, F.; Jofré, E.; Quintero, V.; Perez, A.; Acuña, D.; and Orchard, M., "Particle-Filtering-Based State-of-Health Estimation and End-of-Life Prognosis for Lithium-Ion Batteries at Operation Temperature," Annual Conference of the Prognostics and Health Management Society 2016 - PHM16, October 3rd-6th, 2016, Denver, CO, USA.
[33] M. Isard, A. Blake. Condensation – conditional density propagation for visual tracking. International Journal of Computer Vision, 29:5–28, 1998.
[34] B. Saha, K. Goebel, “Model adaptation for prognostics in a particle filtering framework,” International Journal of Prognostics and Health Management, vol. 2, no. 1, 2011.
[35] Y. Bagul, I. Zeid, and S. Kamarthi, Overview of Remaining Useful Life Methodologies, International Design Engineering Technical Conferences and Computers and Information in Engineering Conference, 2008
[36] L. Liao, F. Kottig, Review of Hybrid Prognostics Approaches for Remaining Useful Life Prediction of Engineered Systems, and an Application to Battery Life Prediction, Reliability, IEEE Transactions on, vol. 63, 2014
[37] J.V. White, S. Steingold, and C. Fournelle, Performance Metrics for Group-Detection Algorithms', Presented at Interface 2004, Baltimore, MD, May 29, 2004.
[38] A. Saxena, J. Celaya, and E. Balaban, A survey of metrics for performance evaluation of prognostics. Proceedings of International Conference on Prognostics and Health Management, 2008
[39] Roemer, M. J., Byington, C. S., Kacprzynski, G. J., Vachtsevanos, G. and Goebel, K. Prognostics, in System Health Management: With Aerospace Applications, John Wiley & Sons, Ltd, Chichester, UK. (2011)
[40] Gesell, T. F., Jones, M. F., de Planque, G. "The Role of Calibration Standards in Environmental Thermoluminescence Dosimetry" Proc. on Traceability for Ionizing Radiation Measurements, pg. 111, February, 1982
[41] R. Spotnitz, Simulation of capacity fade in lithium-ion batteries, Journal of Power Sources, Volume 113, 2003
[42] Nissan Leaf warranty information booklet (2016), Retrieved from https://owners.nissanusa.com/content/techpub/ManualsAndGuides/LEAF/2016/2016-LEAF-warranty-booklet.pdf
[43] Saxena, S., Le Floch, C., MacDonald, J., Moura, S.: Quantifying EV battery end-of-life through analysis of travel needs with vehicle powertrain models. J. Power Sources 282(15), 265–276, 2015

[44] K. Uddin, S. Perera, W.D. Widanage, L. Somerville, and J. Marco, Characterising lithium-ion battery degradation through the identification and tracking of electrochemical battery model parameters Batteries 2 (2), 13
[45] C. Schmitke, T. Dao, Developing Mathematical Models of Batteries in Modelica for Energy Storage Applications. Proceedings of 11th International Modelica Conference, pp. 469-477, 2015.
[46] M. Ecker, N. Nieto, S. Käbitz, J. Schmalstieg, H. Blanke, A. Warnecke, D.U. Sauer, Calendar and cycle life study of Li(NiMnCo)O2-based 18650 lithium-ion batteries, J. Power Sources 248, 839–851, 2014
[47] K. Smith, E. Wood, S. Santhanagopalan, G. Kim, J. Neubauer, A. Pesaran Models for battery reliability and lifetime Battery Congr. (April, 2013), pp. 15?16
[48] S. Sankararaman, K. Goebel, A novel computational methodology for uncertainty quantification in prognostics using the most probable point concept, in: Annual Conference of the Prognostics and Health Management Society, 2013.
[49] M. Daigle, S. Sankararaman, "Predicting Remaining Driving Time and Distance of a Planetary Rover under Uncertainty," ASCE-ASME Journal of Risk and Uncertainty in Engineering Systems, Part B: Mechanical Engineering, to appear
[50] K. Goebel, B. Saha, A. Saxena, J. R. Celaya, and J. Christophersen, "Prognostics in Battery Health Management", Instrumentation & Measurement Magazine, IEEE , vol.11, no.4, pp.33-40, August 2008.
[51] B. Saha and K. Goebel, "Uncertainty Management for Diagnostics and Prognostics of Batteries using Bayesian Techniques", Aerospace Conference, 2008 IEEE, pp.1-8, Big Sky, MT, March 2008.
[52] Hacking I (1975) The emergence of probability. Cambridge University Press, Cambridge
[53] Gillies D (2000) Philosophical theories of probability. Routledge, London
[54] Roy, C.J., Balch, M.S.: A holistic approach to uncertainty quantification with application to supersonic nozzle thrust. Int. J. Uncertain. Quantif. 2, 363–381, 2012
[55] Thunnissen D.P., "Uncertainty classification for the design and development of complex systems", Proceedings of the 3rd Annual Predictive Methods Conference, Veros Software, 2003
[56] McManus, H. and Hastings, D. (2005). A framework for understanding uncertainty and its mitigation and exploitation in complex systems. IEEE Engineering Management Review, 34(3):81– 94
[57] Walton, M. (2002). Managing uncertainty in space systems conceptual design using portfolio theory. PhD thesis, Massachusetts Institute of Technology
[58] Haimes, Y. Y. (2009). Risk Modeling Assessment and Management. In Risk Modeling Assessment and Management, chapter Six. Wiley, New York, third edition.
[59] Forrester, J. (1977). Industrial Dynamics. MIT Press, Cambridge, MA, ninth edition.
[60] de Neufville, R. (2004). Uncertainty Management for Engineering Systems Planning and Design. Technical report, Massachusetts Institute of Technology.
[61] de Neufville, R. and Scholtes, S. (2011). Flexibility in Engineering Design. MIT Press, Cambridge, MA

[62] McManus, H. and Hastings, D. (2005). A framework for understanding uncertainty and its mitigation and exploitation in complex systems. IEEE Engineering Management Review, 34(3):81– 94.
[63] Miller, R. and Lessard, D. (2000). The strategic management of large engineering projects - Shaping Institutions, Risks and Governance. MIT Press, Cambridge, MA.
[64] Walker, W. E., Rahman, S. A., and Cave, J. (2001). Adaptive policies, policy analysis, and policymaking. European Journal of Operational Research, 128:282–289.
[65] Erikstad, S. O. and Rehn, C. F. (2015). Handling Uncertainty in Marine Systems Design - State-ofthe-Art and Need for Research. 12th International Marine Design Conference 2015 Proceedings Volume 2 - 324 -, 2:324–342.
[66] Ross, A. M. and Rhodes, D. H. (2008b). Architecting Systems for Value Robustness : Research Motivations and Progress. IEEE International Systems Conference, 2008
[67] F. Hemez (2005) Uncertainty Quantification and the Verification and Validation of Computational Models. Chapter in Damage Prognosis for for Aerospace, Civil, and Mechanical Systems. Edited by D. J. Inman, C.R. Farrar, V. Lopes, and V. Steffen. 2005. ISBN 0-470- 86907-0. John Wiley & Sons Ltd
[68] D. Chelidze and J.P. Cusumano, A Dynamical Systems Approach to Systems Prognosis. J. Vib. Acoust. 126 (2). 2004. DOI. 10.1115/1.1640638.
[69] B. Saha and K. Goebel (2008) Uncertainty Management for Diagnostics and Prognostics of Batteries using Bayesian Techniques. 2008. Proceedings of the IEEE Aerospace Conference 2008. Big Sky, Montana. Mat 1 – Mar 8, 2008
[70] K. Medjaher, J. Y. Moya, and N. Zerhouni (2009) Failure Prognostic by Using Dynamic Bayes Networks. In the Proceedings of the 2nd IFAC Workshop on Dependable Control of Discrete Systems. DCDS 2009. July 1 – 8, Bari, Italy.
[71] S.W. Doebling, and F.M. Hemez, Overview of Uncertainty Assessment for Structural Health Monitoring. In the Proceedings of the 3rd International Workshop on Structural Health Monitoring, September 17-19, 2001
[72] C.R. Farrar, G. Park, F.M. Hemez, T.B. Tippetts, H. Sohn, J. Wait, D.W. Allen, and B.R. Nadler (2004). Damage Detection and Prediction for Composite Plates. J. of The Minerals, Metals and Materials Society, November 2004.
[73] M. Orchard, G. Kacprzynski, K. Goebel, B. Saha, and G. Vachtsevanos (2008) Advances in Uncertainty Representation and Management for Particle Filtering Applied to Prognostics. Annual Conference of the Prognostics and Health Management Society, 2008.
[74] Hammond, P.H., Theory of Self-adaptive Control Systems, Proceedings of the Second IFAC Symposium on the Theory of Self-Adaptive Control Systems September 14–17, 1965 National Physical Laboratory Teddington, England
[75] B. Sun, S. Liu, L. Tong, L. Shunli, and F. Qiang, “A cognitive framework for analysis and treatment of uncertainty in prognostics,” Chemical Engineering Transactions, vol. 33, pp. 187–192, 2013
[76] J. R. Celaya, A. Saxena, and K. Goebel, Uncertainty Representation And Interpretation In Model-Based Prognostics Algorithms Based On Kalman Filter Estimation, Conference of the Prognostics and Health Management Society, 2012

[77] M. E. Orchard, G. Kacprzynski, K. Goebel, B. Saha, and G. Vachtsevanos, Advances in Uncertainty Representation and Management for Particle Filtering Applied to Prognostics, Conference of the Prognostics and Health Management Society 2008
[78] Merrick J.R., Dinesh V, Singh A, . Propagation of uncertainty in a simulation-based maritime risk assessment model utilizing Bayesian simulation techniques. In: IEEE 2003 winter simulation conference, 7–10 December 2003
[79] B. Sun, S. Liu, L. Tong, L. Shunli, and F. Qiang, A cognitive framework for analysis and treatment of uncertainty in prognostics, Chemical Engineering Transactions, vol. 33, pp. 187–192, 2013
[80] Sankararaman, S. & Goebel, K., Remaining Useful Life Estimation in Prognosis: An Uncertainty Propagation Problem, in AIAA Infotech@Aerospace (I@A) Conference, 2013
[81] Pecht M.G., 2008, Prognostics and health management of electronics. Wiley-Interscience, New York, USA
[82] Saltelli A., Ratto M., Andres T., Campolongo F., Cariboni J., Gatelli D., 2008. Global Sensitivity Analysis: The Primer. John Wiley & Sons Ltd
[83] Sankararaman, S. & Goebel, K., Uncertainty in Prognostics and Systems Health Management, Annual Conference of the Prognostics and Health Management Society 2015
[84] Wang, H.-f. (2011, January) Decision of prognostics and health management under uncertainty. International Journal of Computer Applications, 13(4), 1–5. (Published by Foundation of Computer Science)
[85] Saha, B., & Goebel, K. (2009). Modeling li-ion battery capacity depletion in a particle filtering framework. In Proceedings of annual conference of the phm society.
[86] Saha, B., Goebel, K., Poll, S., & Christophersen, J. (2009, feb.). Prognostics methods for battery health monitoring using a bayesian framework. IEEE Transactions on Instrumentation and Measurement, 58(2), 291 -296. 2008
[87] G. Chowdhary, H. Kingravi, R.C. Grande, J.P. How, P. Vela, Bayesian nonparameteric model reference adaptive control using Gaussian processes, Conference on Guidance Navigation and Control, 2013
[88] H.A. Kingravi, G. Chowdhary, P.A. Vela, E.N. Johnson, Reproducing kernel Hilbert space approach for the online update of radial bases in neuro-adaptive control, IEEE transactions on neural networks and learning systems 23 (7), 1130-1141,2012
[89] Keil P., Schuster S. F., Wilhelm J., Travi J., Hauser A., Karl R. C., Jossen A., “Calendar Aging of Lithium-Ion Batteries,” J. Electrochem. Soc., 163, A1872 (2016)
[90] B Xu, Y Shi, DS Kirschen, B Zhang, Optimal Regulation Response of Batteries Under Cycle Aging Mechanisms
[91] X.Hu, S.Li and H.Peng, "A comperative study of equivalent circuit models for Li-ion batteries," Journal of Power Sources, no. 198, pp. 359-367, 2012.
[92] G. L.Plett, "Extended Kalman filtering for battery management systems of LiPBbased HEW battery Packs Part 2. Modeling and identification," Journal of Power Sources, no. 134, pp. 262-276, 2004.

[93] S.Cho, H.Jeong, C.Han, S.Jin, J.Lim and J.Oh, "State-of-charge estimation for lithium-ion batteries under various operating conditions using an equivalent circuit model," Computers and chemical engineering, no. 41, pp. 1-9, 2012.
[94] R.Klein, N.Chaturvedi, J.Christensen, J.Ahmed, R.Findeisen and A.Kojic, "State estimation of reduced electrochemical model of a lithium-ion battery," in American Control Conference, Baltimore, 2010.
[95] Y.Xie, J.Li and C.Yuan, "mathematical modeling of the electrochemical impedance spectroscopy in lithium ion battery," Electrochimica Acta, vol. 127, pp. 266-275, 2014.
[96] B Saha, K Goebel, S Poll, J Christophersen, Prognostics methods for battery health monitoring using a Bayesian framework, IEEE Transactions on instrumentation and measurement 58 (2), 291-296,2009
[97] NH Kim, D An, JH Choi,. Prognostics and Health Management of Engineering Systems: An Introduction, springer, 2016
[98] Jérôme Morio. Global and local sensitivity analysis methods for a physical system. European Journal of Physics, 2011.
[99] Saltelli, A., Ratto, M., Andres, T., Campolongo, F., Cariboni, J., Gatelli, D. Saisana, M., and Tarantola, S., 2008, Global Sensitivity Analysis. The Primer, John Wiley & Sons.
[100] Vachtsevanos, G., Lewis, F., Roemer, M., Hess, A. and Wu, B., Intelligent Fault Diagnosis and Prognosis for Engineering Systems, John Wiley & Sons, Inc. 2006
[101] Edwards, D., Orchard, M., Tang, L., Goebel, K., Vachtsevanos, G., "Impact of Input Uncertainty on Failure Prognostic Algorithms: Extending the Remaining Useful Life of Nonlinear Systems", Prognostics and Health Management Conference, 2010.
[102] Orchard, M. and Vachtsevanos, G., "A Particle Filtering Approach for On-Line Fault Diagnosis and Failure Prognosis," Transactions of the Institute of Measurement and Control, vol. 31, no. 3-4, pp. 221-246, June 2009.
[103] Orchard, M., Tobar, F., and Vachtsevanos, G., "Outer Feedback Correction Loops in Particle Filtering-based Prognostic Algorithms: Statistical Performance Comparison," Studies in Informatics and Control, Informatics and Control Publications, Volume 18, Issue 4, pp. 295-304, 2009.
[104] Know thyself. (2018, May 28). Retrieved from https://en.wikipedia.org/wiki/Know_thyself#cite_note-1
[105] Green, M. S. (2018). Know thyself: The value and limits of self-knowledge. New York: Routledge, Taylor & Francis Group.
[106] Know Thyself: The Impact of Portfolio Development on Adult Learning Judith O. Brown First Published May 1, 2002 Research Article
[107] The Art of War (2018, April 28). Retrieved from http://taggedwiki.zubiaga.org/new_content/e520eda54d25b02778c7c7df71fde9f1
[108] Dietz, T., Jianguo Liu, S.R. Carpenter, C. Folke, M. Alberti, C.L. Redman, S.H. Schneider, E. Ostrom, et al. 2007. "Complexity of coupled human and natural systems." Ambio, 36(8): 639-649.
[109] Brown, Judith. (2002). Know Thyself: The Impact of Portfolio Development on Adult Learning. Adult Education Quarterly - ADULT EDUC QUART. 52. 228-245. 10.1177/0741713602052003005.

[110] R. W. Henke, “Selbsterkenntnis,” in Handw¨orterbuch Philosophie,W. D. Rehfus, Ed. Stuttgart, Germany: UTB, 2003
[111] Smith, A., Hinchcliffe, G. 2004. RCM gateway to world class maintenance. Oxford: Elsevier Butterworth-Heinemann.
[112] SULLIVAN, G.P., PUGH, R., MELENDEZ, A.P., and HUNT, W.D., 2004. Operations and Maintenance Best Practices: A Guide to Achieving Operational Efficiency. Prepared by PNNL for the FEMP, U.S. DOE
[113] X Jin, D Siegel, BA Weiss, E Gamel, W Wang, J Lee, J Ni, The present status and future growth of maintenance in US manufacturing: results from a pilot survey
[114] K. Javed, “A robust & reliable Data-driven prognostics approach based on extreme learning machine and fuzzy clustering.,” Universite de Franche-Comte, 2014.
[115] Brahimi, Mehdi & Medjaher, Kamal & Leouatni, Mohammed & Zerhouni, Noureddine. (2016). Development of a prognostics and health management system for the railway infrastructure. Review and methodology. 1-8. 10.1109/PHM.2016.7819783.
[116] Weigend AS, Srivastava AN. Predicting conditional probability distributions: a connectionist approach. Int J Neural Syst. 1995 Jun;6(2):109-18.
[117] Joslyn S, Leclerc J. Decisions with uncertainty: the glass half full. Curr Dir Psychol Sci. 2013; 22: 308–315. doi
[118] Pecht, M., and Jaai, R. A prognostics and health management roadmap for information and electronics-rich systems. Microelectronics Reliability 50, 3 (2010),317–323
[119] Zio, Enrico. (2012). Prognostics and Health Management of Industrial Equipment. Diagnostics and Prognostics of Engineering Systems: Methods and Techniques. 10.4018/978-1-4666-2095-7.ch017.
[120] Chammas A., Sayed-Mouchaweh M., Duviella E., Lecoeuche S. (2012) Drift Detection and Characterization for Fault Diagnosis and Prognosis of Dynamical Systems. In: Hüllermeier E., Link S., Fober T., Seeger B. (eds) Scalable Uncertainty Management. SUM 2012. Lecture Notes in Computer Science, vol 7520. Springer, Berlin, Heidelberg
[121] W. Brogan, Modern Control Theory, Prentice Hall, Upper Saddle River, NJ, 07458, 1991.
[122] Luo, Jianhui & Namburu, M & Pattipati, Krishna & Qiao, Liu & Kawamoto, M & Chigusa, S. (2003). Model-based prognostic techniques [maintenance applications]. 330 - 340. 10.1109/AUTEST.2003.1243596.
[123] Daigle, Matthew & Saxena, Abhinav & Goebel, Kai. (2012). An Efficient Deterministic Approach to Model-based Prediction Uncertainty Estimation. 10.
[124] An, Dawn & Kim, Nam & Choi, Joo-Ho. (2015). Practical options for selecting data-driven or physics-based prognostics algorithms with reviews. Reliability Engineering & System Safety. 133. 223?236. 10.1016/j.ress.2014.09.014.
[125] Honglei Li. A framework for model-based diagnostics and prognostics of switched-mode power supplies, Annual Conference of the Prognostics and Health Management Society, September 2014

[126] Nissan-global, Evolution. (2013, July). Electric Cars Came First [Press release]. Retrieved from https://www.nissan-global.com/JP/TECHNOLOGY/FILES/2013/07/f51d2dd9e528d7.pdf
[127] "Extend the Operating Life of Your Motor," U.S. Department of Energy, September 2005.
[128] W. Meeker and L. Escobar, Statistical Methods for Reliability Data. John Wiley & Sons, New York, 1998.
[129] K. Smith, T. Markel, A. Pesaran, "PHEV Battery Trade-off Study and Standby Thermal Control," 26th International Battery Seminar & Exhibit, Fort Lauderdale, FL, March, 2009.
[130] M Murnane and Ghazel, A Closer Look at State of Charge (SOC) and State of Health (SOH) Estimation Techniques for Batteries, Technical Article, Analog Devices
[131] Fahrmeir L., Tutz G. (2001) State Space and Hidden Markov Models. In: Multivariate Statistical Modeling Based on Generalized Linear Models. Springer Series in Statistics. Springer, New York, NY
[132] M. Sanjeev Arulampalam, S. Maskell, and N. Gordon, "A Tutorial on Particle Filtering and Smoothing: Fifteen years later," Version 1.1, Dec. 2008
[133] Il-Won, J., Moradkhani, H. and Chang, H. (2012) Uncertainty assessment of climate change impacts for hydrologically distinct river basins. Journal of Hydrology: 73-87.
[134] T Wang, J Yu, D Siegel, J Lee,. (2008) A similarity-based prognostics approach for remaining useful life estimation of engineered systems. Prognostics and Health Management, 2008. PHM 2008.
[135] J. Melo, "Gaussian processes for regression: a tutorial", Technical Report, 2012.
[136] Rasmussen CE, Williams CKI. Gaussian processes for machine learning. Cambridge (MA): MIT Press; 2006.
[137] K. Goebel, N. Eklund, P. Bonanni Fusing competing prediction algorithms for prognostics IEEE Aerospace Conference, IEEE (2006), p. 10
[138] C. Chen, G. Vachtsevanos, M. Orchard Machine remaining useful life prediction: an integrated adaptive neuro-fuzzy and high-order particle filtering approach Mech. Syst. Signal Process., 28 (2011), pp. 597-607
[139] M.E. Orchard A Particle Filtering-Based Framework for On-Line Fault Diagnosis and Failure Prognosis Georgia Institute of Technology (2006)
[141] UNCERTAINTY | meaning in the Cambridge English Dictionary. (n.d.). Retrieved from https://dictionary.cambridge.org/dictionary/english/uncertainty
[142] Yen, B. and Ang, A. (1971). Risks analysis in design of hydraulic projects. In: C. Chiu (ed.), Stochastic Hydraulics, Proc. of First International Symposium, University of Pittsburgh, Pittburgh, PA, USA, pp. 694-709.
[143] Burges, S. and Lettenmaier, D. (1975). Probabilistic methods in stream quality management. Water Resources Bulletin, 11(1), pp. 115-130
[144] Klir, G. and Folger, T. (1988). Fuzzy sets, uncertainty, and information. Prentice Hall, Englewood Cliffs, NJ, USA.
[145] Frangopol, D. M., & Tsompanakis, Y. (Eds.). (2014). Maintenance and Safety of Aging Infrastructure, Structures & Infrastructures Book Series, Vol. 10. London: CRC Press / Balkema - Taylor & Francis Group, 746 p.

[146] M Bagheri, M Miri, N Shabakhty,. Modeling of epistemic uncertainty in reliability analysis of structures using a robust genetic algorithm, Iranian Journal of Fuzzy Systems 12 (2), 23-40
[147] Walley, P. 1991. Statistical Reasoning with Imprecise Probabilities. London: Chapman and Hall
[148] Moore, R.E. 1979. Methods and Applications of Interval Analysis. Philadelphia, PA: SAIM
[149] Kearfott, R.B. and V. Kreinovich, eds. 1996. Applications of Interval Computations. Boston, MA: Kluwer Academic Pub.
[150] Shafer, G. 1976. A Mathematical Theory of Evidence. Princeton, NJ: Princeton University Press
[151] Kohlas, J. and P.-A. Monney. 1995. A Mathematical Theory of Hints - An Approach to the Dempster-Shafer Theory of Evidence. Berlin: Springer
[152] Dubois, D. and H. Prade. 1986. Possibility Theory: An Approach to Computerized Processing of Uncertainty. New York: Plenum Press
[153] Cooman, G., D. Ruan, and E.E. Kerre, eds. 1995. Foundations and Applications of Possibility Theory, ed. K. Hirota, et al Singapore: World Scientific Publishing Co
[154] Klir, GJ. and T.A. Folger. 1988. Fuzzy Sets, Uncertainty, and Information. 1st ed. Englewood Cliffs, NJ: Prentice Hall.
[155] Ross, TJ. 1995. Fuzzy Logic with Engineering Applications. New York, NY: McGraw-Hill, Inc
[156] Johnson, Jay Dean, Helton, Jon Craig, Oberkampf, William Louis, & Sallaberry, Cedric J. (Aug 2008). Representation of analysis results involving aleatory and epistemic uncertainty (SAND--2008-4379). United States
[157] E. Zio and N. Pedroni, "Literature review of methods for representing uncertainty," Cahiers de la Sécurité Industrielle, Toulouse, 2013.
[158] Dempster, A. P. (1967). Upper and lower probabilities induced by a multivalued mapping. The Annals of Mathematical Statistics, 38(2):325–339
[159] Shafer, G. (1976). A Mathematical Theory of Evidence. Princeton University Press, Princeton, NJ. isbn: 978-0691081755, 297 pages
[160] J.C. Helton, J.D. Johnson, W.L. Oberkampf, et al. Representation of analysis results involving aleatory and epistemic uncertainty Int. J. Gen. Syst., 39 (6) (2010), pp. 605-646
[161] E. Zio and N. Pedroni, Literature review of methods for representing uncertainty. FonCSI, 2013.
[162] Motra, H.B., A. Dimmig-Osburg and J. Hildebrand, 2013. Influence of measurement uncertainties on results of creep prediction of concrete under cyclic loading. Proceedings of the 8th International Conference on Fracture Mechanics of Concrete and Concrete Structures, March 10-14, 2013, Toledo, Spain, pp: 805-814.
[163] N. Pedroni, E. Zio, “Uncertainty analysis in fault tree models with dependent basic events”, Risk Analysis, Volume 33, Issue 6, pages 1146–1173, June 2013, ISSN 0272-4332

[164] Hasofer, A.M. and Lind, N.C., 1974, “Exact and Invariant Second-Moment Code Format,” Journal of the Engineering Mechanics Division, ASCE, Vol. 100, pp. 111-121.
[165] Rosenblatt, M., 1952, “Remarks on a Multivariate Transformation,” Annal of Mathematical Statistic, Vol. 23, pp. 470-472
[166] Du, X. and Chen, W., 2001a, A Most Probable Point Based Method for Uncertainty Analysis. Journal of Design and Manufacturing Automation, 4:47-66.
[167] H. MILLWATER and Y. WU. "GLOBAL/LOCAL METHODS FOR PROBABILISTIC STRUCTURAL ANALYSIS", 34th Structures, Structural Dynamics and Materials Conference, Structures, Structural Dynamics, and Materials and Co-located Conferences
[168] Sobol’, I. M. Sensitivity estimates for nonlinear mathematical models. Mathematical Modelling and Computational Experiment 1, 407–414. 1993
[169] Saltelli, A., P. Annoni, I. Azzini, F. Campolongo, M. Ratto, and S. Tarantola, 2010: Variance based sensitivity analysis of model output: Design and estimator for the total sensitivity index. Comput. Phys. Commun., 181, 259–270, doi:10.1016/j.cpc.2009.09.018
[170] B. Saha, K. Goebel and J. Christophersen, “Comparison of prognostic algorithms for estimating remaining useful life of batteries”, Transactions of the Institute of Measurement & Control, vol. 31, no. 3-4, 2009, pp. 293-308.
[171] Liaw, B.Y. R.G. Jungst, A. Urbina, T.L. Paez, Modeling of Battery Life, I. The Equivalent Circuit Model (ECM) Approach,” EESAT 2003
[172] Z Xi, R Jing, C Lee, M Hayrapetyan,.Recent Research on Battery Diagnostics, Prognostics, and Uncertainty Management,Advances in Battery Manufacturing, Service, and Management Systems, 175, 2016
[173] BS ISO 5725-1: "Accuracy (trueness and precision) of measurement methods and results - Part 1: General principles and definitions.", p.1 (1994)
[174] R Fu, SY Choe, V Agubra, J Fergus,."Development of a physics-based degradation model for lithium ion polymer batteries considering side reactions",Journal of Power Sources 278, 506-521